A study of the sorption characteristics at the solution-solid interface, and the hydrogen bonding characteristics of a series of para-substituted phenols

Bernard Joel Hawley

A STUDY OF THE SORPTION CHARACTERISTICS AT THE SOLUTION-SOLID INTERFACE, AND THE HYDROGEN BONDING CHARACTERISTICS OF A SERIES OF PARA-SUBSTITUTED PHENOLS

by

Bernard Joel Hawley

THESIS SUBMITTED FOR THE DEGREE OF

MASTER OF SCIENCE

IN THE UNIVERSITY OF DURHAM

DERBY AND DISTRICT COLLEGE OF TECHNOLOGY

MAY 1968

ABSTRACT

A characterisation of the activated alumina used in the sorption studies has been attempted from results obtained by X-ray diffraction techniques, low temperature nitrogen sorptions and sorptions from the liquid phase.

The sorption characteristics at an alumina-dioxan interface of a series of 4-substituted phenols (phenol, 4-methyl-, 4-t-butyl-, 4-chloro-, 4-nitro-, and 4-cyano-phenols) have been determined at 35°C.; solubilities in dioxan measured at 35°C.; experimental adsorption isotherms constructed and sorption saturation values estimated.

In order to compare the sorptive affinity of the alumina surface for the phenols an index of sorption has been defined as "the number of moles of phenol sorbed at constant relative mole fraction of phenol in the mobile phase", and it has been demonstrated that this index can be related logarithmically to the Hammett sigma constant for the appropriate 4-substituent.

The effects of 4-substitution on properties of the OH bond which reflect its hydrogen bonding tendency have been examined, such as association to dioxan in solution. Absorbance measurements in the near ultra-violet have enabled association constants in solution for the process

$$\text{substituted phenol} + \text{dioxan} \rightleftharpoons \text{complex}$$

to be determined at 25°C. and 35°C.

Comparisons have been made with other relevant characteristics of the OH bond, for example acidity, polarity and near infra red stretching frequency, again showing (as with the hydrogen bonding association constants) good correlation with the Hammett structural parameter.

The results obtained suggest that in the sorption of 4-substituted phenols from dioxan solution onto an activated alumina the forces on the surface are the dominant ones, since the phenols are not adsorbed as complexes but as discreet molecules. Interaction with the surface appears to be through the mechanism of hydrogen bonding and the phenol molecules probably assume a vertical orientation on localised sorption sites.

ACKNOWLEDGEMENTS

I would like to thank the Governors of the Derby and District College of Technology for their award of a Research Assistantship and Mr. M.S.J. Twiselton for the use of the research facilities in the Chemistry Department.

I am indebted to Dr. G. Kohnstam, my Supervisor in Durham, for his interest in the work, his painstaking study of the Manuscript and his valuable comments.

Finally, I would like to express my gratitude to my Director of Research in Derby, Dr. D.A. Ibbitson, for his suggestion of the topic, for his patient and assiduous supervision during the course of the investigation and for the benefit of his invaluable experience in presenting this thesis.

DERBY. B.J. HAWLEY

MAY, 1968.

CONTENTS

INTRODUCTION

A - SORPTION OF NON-ELECTROLYTES AT THE SOLUTION-SOLID INTERFACE

The Sorption Process

Many early workers record the ability of charcoal to adsorb gases (C.W. Scheele 1773, Abbe F. Fontana 1777) and to remove coloured solutes from solution (T. Lowitz 1785); many later observations have demonstrated the property of fine powders to take up substances from solution.

The term "adsorption" (Kayser 1881) strictly refers to the existence of a higher concentration of any particular component at the surface of a liquid or solid phase than is present in the bulk, as opposed to "absorption" which implies more or less uniform penetration. As these two effects frequently overlap the more general term "sorption" is employed.

The nature of the sorption process may be regarded thus: the units of a crystal lattice may be considered as being surrounded by a field of force and although there is but little residual attraction within the crystal, where each unit is situated symmetrically with respect to the electrical forces of cohesion, the unsaturated character or the intensity of this field assumes large values in the space adjacent to the crystal surface. The surface of a crystal may thus be regarded as unsaturated and the existence of a definite surface energy is due to this unsaturation.

Since the surface of a crystal consists of a regular lattice of orderly distributed units (i.e. ions or atoms) the surface adhesional forces may be regarded as being distributed over the centres of these lattice units, although in all probability these points represent maxima in a continuous

field. Owing to the solid possessing a residual field of force there will be a tendency for the thermodynamic free energy of any surface to decrease and it is this tendency which is ultimately responsible for the phenomenon of sorption. In addition to the diminution in free energy of the system when sorption occurs it is natural to suppose that as a result of the enhanced configurational restriction imposed on the molecule sorbed on the solid surface a decrease in entropy will result. By application to the sorption process of the thermodynamic equation

$$\Delta G = \Delta H - T.\Delta S$$

in which ΔG, ΔS and ΔH represent the change in free energy, entropy and heat content respectively associated with a change of state of a system at temperature T, it can be seen that since ΔG and ΔS are both negative then ΔH will also be negative, i.e. the process of sorption is exothermic.

VARIABLES IN THE SORPTION PROCESS

The nature and extent of sorption of a solute in solution onto a solid sorbent surface depend upon:-

(a) concentration of the solution,

(b) nature of the solvent,

(c) nature of the solute,

(d) nature of the sorbent surface, and

(e) temperature.

(a) Concentration of the Solution

In the experimental determination of the sorption isotherm it is usual to bring a known weight of solution of chosen concentration into contact

with a known weight of sorbent and allow equilibrium to be reached. The equilibrium concentration of the solution is then determined - usually by a convenient physical method - and the extent of the sorption of the solid solute calculated. This procedure is repeated with a series of solutions of different initial concentrations and the isotherm so constructed.

The shapes of the curves obtained are a function of adsorption mechanism and the physical nature of the solute and sorbent surface; Giles et al.[1] have described a system of classification of all solution adsorption isotherms. The initial slopes of the isotherms are used to classify the curves into four main groups (S, L, H and C isotherms) and the upper portions to divide the main groups into a number of sub-groups (see Fig. 1).

The initial direction of curvature of the S curve shows that adsorption becomes easier as concentration rises. This type of isotherm may be anticipated when molecules of solvent are strongly held on the surface, effectively competing with the solute for adsorption sites, and when considerable intermolecular attraction exists between solute molecules, so aiding further adsorption after a small preliminary up-take. Moreover, for these intermolecular forces to be maximally operative the solute molecules must be packed perpendicularly to the surface and for this to be likely the solute molecule must have one localised point of attachment only. Thus mono-hydric phenols sorbed from a polar solvent (e.g. water or ethanol)

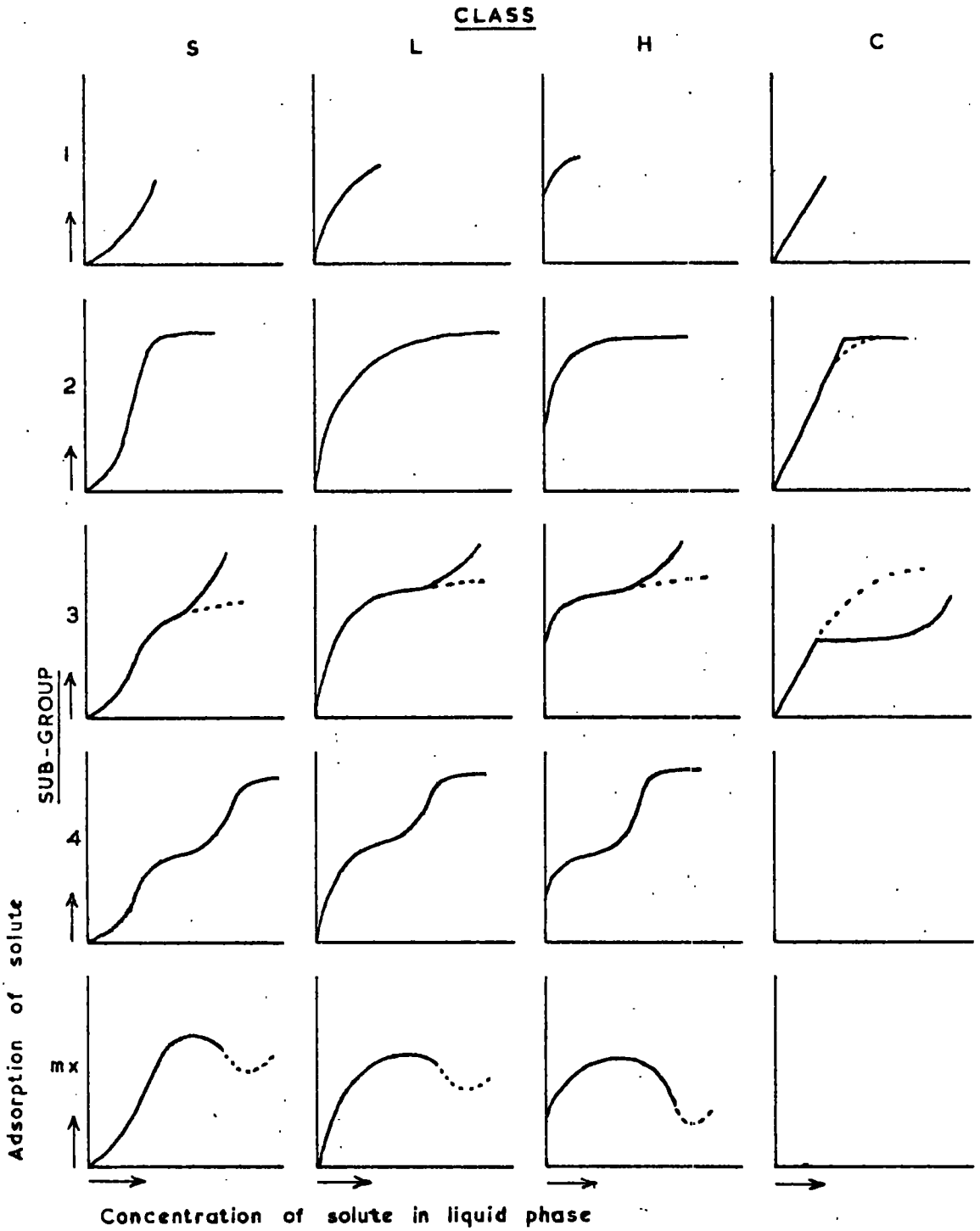

SYSTEM OF CLASSIFICATION OF ISOTHERMS

Fig. 1

onto a polar substrate (e.g. alumina) give an S isotherm, but not when sorbed from a non-polar solvent such as cyclohexane.

The L curves are those most frequently encountered: L2 in particular occurs in the majority of sorptions from solution and indeed all the isotherms obtained in this investigation were of this type. Here, as more sites in the substrate are filled it becomes increasingly difficult for a bombarding solute molecule to find a vacant site available. Either the sorptive molecules are not vertically orientated or the solvent does not compete effectively for surface sites. Thus, while resorcinol, terephthaldehyde and phenol give L curves, the two former compounds are horizontally aligned to the surface and the latter vertically orientated when sorbed from a non-polar and therefore non-competing solvent such as pentane, cyclohexane or benzene.

Should such high affinity exist between the solute and substrate surface that in dilute solution no measurable amount of solute remains in solution after sorption then the H type isotherm is produced in which the initial part is vertical. The adsorbed species are often large units, e.g. ionic micelles or polymeric molecules, but sometimes they are apparently single ions which exchange with others of much lower affinity for the surface, e.g. sulphonated dye ions which exchange with chloride ions on alumina.

The C type isotherm is characterised by a constant partition of solute between solution and substrate right up to the maximum possible adsorption

when an abrupt change to an horizontal plateau occurs. The linearity shows that as more solute is adsorbed more sites must be created so that the number of sites for adsorption remain constant, i.e. the substrate surface can be penetrated by solute molecules. C curves are characteristic of synthetic polymer and wool fibre substrates.

The type of adsorption isotherm most frequently encountered for the process of sorption of a solid from solution is shown in Fig. 2. An equation of the form originally much used by Freundlich usually fits an isotherm of this shape at low concentration

$$\frac{n}{m} = k.c^{\frac{1}{a}}$$

where n denotes the number of moles of sorptive taken up by m g. of solid,

c denotes equilibrium concentration of the solution (moles $l.^{-1}$)

k and a are constants for the given system and temperature.

However, it is usually found that at higher concentrations the curve asymptotically approaches a limiting value of sorption not predicted by the Freundlich equation.

A much more satisfactory fitting of experimental points is given by the empirical Jowett[2] equation:-

$$\frac{n}{m} = A - (A - a)e^{-Bc}$$

where n moles of solute are taken up by m g. of adsorbate,

A is a constant: the limiting sorption value,

a and B are constants,

c is the equilibrium concentration.

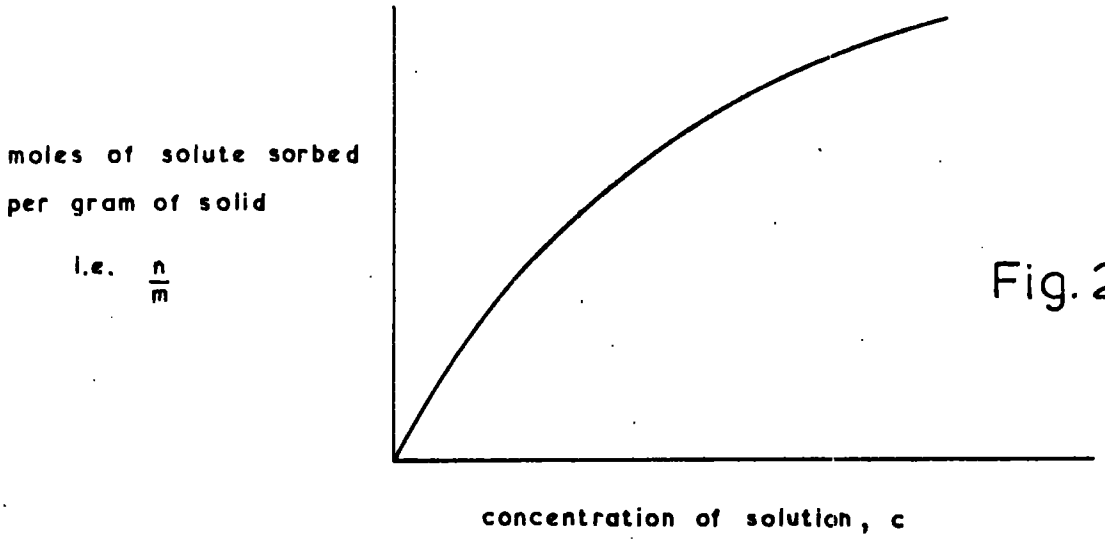

Fig. 2

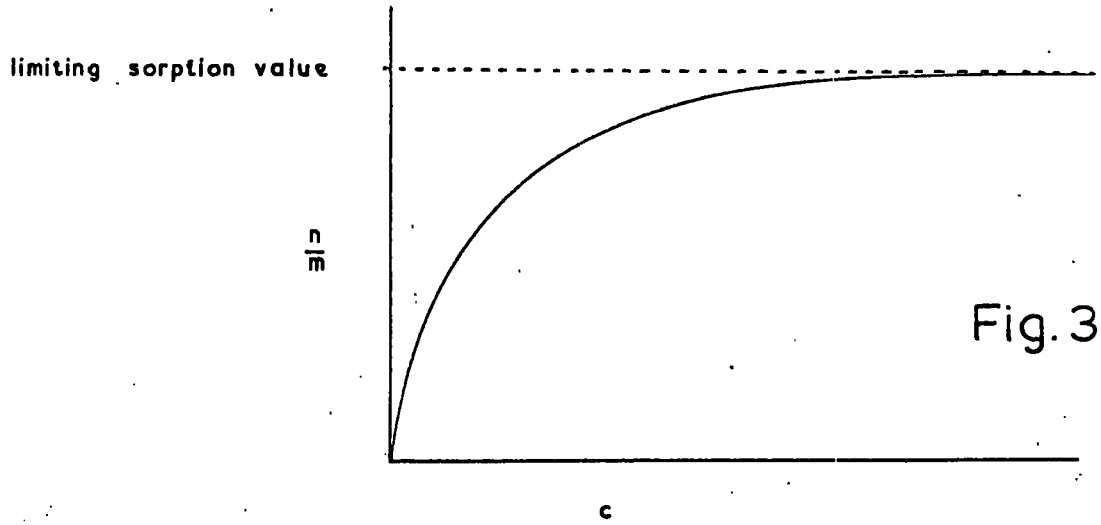

Fig. 3

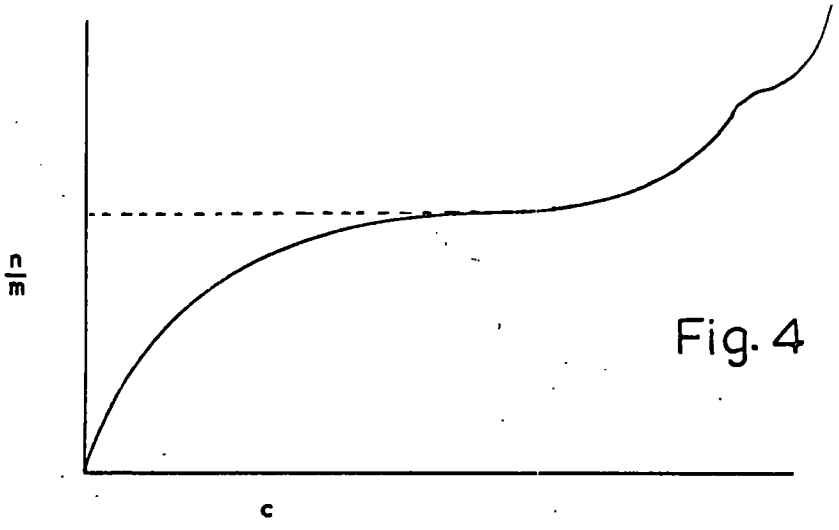

Fig. 4

In suggesting this equation no mechanism of sorption is inferred and in fact the curve need not pass through the origin. Application of this equation gives very reasonable results for limiting sorption values (see Fig. 3).

In the experimental determination of the sorption isotherm the equilibrium concentration measured reflects the sorption of both solute and solvent and as such the isotherm is better designated "an isotherm of concentration change" or "composite isotherm". In such an isotherm the plateau probably represents the completion of a monolayer on the sorbent surface, although great caution must be exercised in ascribing a physical significance to a feature displayed on an isotherm. Nevertheless, as the equilibrium concentration rises the curve often continues in a stepwise manner pointing to the formation of further layers (Fig. 4).

Assuming that the limiting sorption value corresponds to monolayer coverage, equilibrium constants for real sorption processes can be estimated but here again they are of doubtful worth owing to the difficulty of calculating activity coefficients for sorbed species.

Everett[3] has attempted to establish an ideal or perfect model for sorption at the solid-liquid interface and to use it as a reference system against which to measure the deviations from ideality of real systems. He pictures the solution as an array of plane lattices stacked together with their planes parallel to the sorbent surface. Adsorption in this pseudo-crystalline model is supposed to be monomolecular so that the average

mole fractions of the components are constant in all lattice planes except that immediately adjacent to the solid surface, where variation is caused by selective adsorption of one or more of the solution components. This plane is the "adsorbed phase", s, and consists of N^s identical adsorption sites. A binary mixture is considered of components 1 and 2 of the same molecular size so that each molecule occupies one lattice point. In the adsorbed phase there are N_1^s molecules of component 1 and N_2^s of component 2, similarly in the liquid phase there are N_1^ℓ and N_2^ℓ molecules of 1 and 2 respectively.

Then $N_1^s + N_2^s = N^s$

and $N_1^\ell + N_2^\ell = N^\ell$, the total number of lattice points in the liquid phase.

On this model the adsorbed phase could be referred to as "a perfect adsorbed monolayer" and the concept has been used by other workers[4, 5, 6, 7].

If Ω^s and Ω^ℓ are the number of ways of arranging the molecules in the surface and in the solution respectively, the total number of arrangements Ω of the system is

$$\Omega = \Omega^s \times \Omega^\ell = \frac{N^s!}{N_1^s!\, N_2^s!} \times \frac{N^\ell!}{N_1^\ell!\, N_2^\ell!} \quad \ldots\ldots\ldots (1)$$

Now configurational entropy, $S^{config.} = k \ln \Omega$

$$\therefore S^{config.} = k(\ln N^s! + \ln N^\ell! - \ln N_1^s! - \ln N_2^s! - \ln N_1^\ell! - \ln N_2^\ell!)$$

But $\ln X! = X\ln X - X$ by Stirlings theorem.

$$\therefore S^{config.} = k(N^s \ln N^s + N^\ell \ln N^\ell - N_1^s \ln N_1^s - N_2^s \ln N_2^s - N_1^\ell \ln N_1^\ell - N_2^\ell \ln N_2^\ell)$$

Converting to molar quantities (n), where N_m is Avogadro's number, then $k \times N_m = R$, and

$$S^{config.} = R(n^s \ln n^s - n_1^s \ln n_1^s - n_2^s \ln n_2^s + n^\ell \ln n^\ell - n_1^\ell \ln n_1^\ell - n_2^\ell \ln n_2^\ell) \quad \ldots\ldots\ldots (2)$$

The total entropy expression must include contributions from the vibrational and rotational entropy (thermal entropy) of the molecules. The molar thermal entropies are denoted by S_1^{*s}, S_2^{*s}, $S_1^{*\ell}$, $S_2^{*\ell}$ and are assumed to be independent of the composition of both surface and solution. The thermal entropy of the system is then

$$S^{therm.} = n_1^s S_1^{*s} + n_2^s S_2^{*s} + n_1^\ell S_1^{*\ell} + n_2^\ell S_2^{*\ell} \quad \ldots\ldots\ldots (3)$$

Furthermore, since the solution is assumed to be perfect and all adsorption sites to have identical properties, the energy of the system (U) is

$$U = n_1^s u_1^{*s} + n_2^s u_2^s + n_1^\ell u_1^\ell + n_2^\ell u_2^\ell, \quad \ldots\ldots\ldots (4)$$

where u_1^s, u_2^s, u_1^ℓ, u_2^ℓ are the molar energies of molecules of the two kinds in the adsorbed and liquid phases respectively: these again are independent of composition.

The free energy, F, of the whole system is

$$F = U - T(S^{config.} + S^{therm.})$$

The equilibrium state is that for which $\left(\frac{\partial F}{\partial n_i}\right)_{T,V} = 0$, $i = 1,2$. for a process in which at constant temperature (T) and volume (V), dn moles of component 1 are transferred from the solution, i.e. the number of surface molecules (and hence the area of contact between solution and solid) remains constant. In effect we seek the equilibrium constant of

the phase-exchange reaction

$$(1)^s + (2)^\ell \rightleftharpoons (1)^\ell + (2)^s$$

This leads to the condition

$$\ln\left[\frac{n_2^\ell}{n_1^\ell}\right] - \ln\left[\frac{n_2^s}{n_1^s}\right] = \frac{\Delta_a u_2 - \Delta_a u_1}{RT} - \frac{\Delta_a S_2^* - \Delta_a S_1^*}{R}$$

where $\Delta_a u$, and $\Delta_a S_i^*$ are the changes of energy and of the thermal part of the entropy on adsorption:-

$$\Delta_a u_i = u_i^s - u_i^l; \quad \Delta_a S_i^* = S_i^{*s} - S_i^{*l}; \quad i = 1, 2.$$

Thus $$\frac{n_2^\ell \times n_1^s}{n_1^\ell \times n_2^s} = \exp.\left[-\frac{\Delta_a u_1 - \Delta_a u_2}{RT} + \frac{\Delta_a S_1^* - \Delta_a S_2^*}{R}\right]$$

or, in terms of mole fraction, x, ($n_1^s = n^s x_1^s$ etc.)

$$\frac{x_1^s \cdot x_2^\ell}{x_2^s \cdot x_1^\ell} = K \qquad \ldots\ldots\ldots\ldots (5)$$

Equation (5) can be regarded as the "Langmuir equation" for adsorption from solution, and its close analogy with the Langmuir adsorption isotherm for a gas-solid interface is seen by writing (5) as

$$\frac{x_1^s}{(1-x_1^s)} = \frac{K x_1^\ell}{x_2^\ell}$$

and comparing with the Langmuir isotherm written in the form:

$$\frac{\theta}{(1-\theta)} = K_L . p.$$

Nonetheless, equation (5) has been derived from first principles rather

than by analogy from the gas-solid interface.

The next step is to formulate an expression involving a linear relationship enabling K to be calculated from experimental data. From equation (5)

$$K = \frac{x_1^s (1 - x_1^\ell)}{x_1^\ell (1 - x_1^s)}$$

$$\therefore x_1^s = \frac{K.x_1^\ell}{1 + x_1^\ell(K-1)}$$

But $x_1^s = n_1^s/n^s$ $\quad \therefore n_1^s = \dfrac{n^s.K.x_1^\ell}{1 + x_1^\ell (K-1)}$ ..... (6)

and $n_2^s = n^s - n_1^s = n^s \left[1 - \dfrac{K.x_1^\ell}{1 + x_1^\ell(K-1)} \right]$

or $\quad n_2^s = \dfrac{n^s (1 - x_1^\ell)}{1 + x_1^\ell(K-1)}$ ..... (7)

Now suppose that n^o moles of mixture of components 1 and 2 are brought into contact with m g. of solid sorbent, let n_1^s and n_2^s be moles sorbed by 1 g. of solid whilst n_1^ℓ and n_2^ℓ moles remain in the mobile phase at equilibrium, i.e.

$$n^o = n_1^\ell + n_2^\ell + mn_1^s + mn_2^s$$

Initial mole fraction of component 1 in liquid phase, x_1^o

$$= \frac{n_1^\ell + mn_1^S}{n^o}$$

Equilibrium mole fraction of component 1 in liquid phase, x_1^{ℓ}

$$= \frac{n_1^{\ell}}{n_1^{\ell} + n_2^{\ell}}$$

Change in mole fraction in liquid phase, $\Delta x_1^{\ell} = x_1^{o} - x_1^{\ell}$

$$= \frac{n_1^{\ell} + mn_1^{s}}{n_1^{\ell} + n_2^{\ell} + mn_1^{s} + mn_2^{s}} - \frac{n_1^{\ell}}{n_1^{\ell} + n_2^{\ell}}$$

$$\therefore \Delta x_1^{\ell} = \frac{mn_1^{s}n_2^{\ell} - mn_2^{s}n_1^{\ell}}{(n_1^{\ell} + n_2^{\ell})(n_1^{\ell} + n_2^{\ell} + mn_1^{s} + mn_2^{s})}$$

$$\therefore \frac{n^{o}\Delta x_1^{\ell}}{m} = x_2^{\ell}n_1^{s} - x_1^{\ell}n_2^{s}$$

or $$\frac{n^{o}\Delta x_1^{\ell}}{m} = n_1^{s}(1 - x_1^{\ell}) - n_2^{s}x_1^{\ell} \qquad \ldots\ldots\ldots (8)$$

Substituting equations (6) and (7) into equation (8):

$$\frac{n^{o}\Delta x_1^{\ell}}{m} = \frac{n^{s}Kx_1^{\ell}(1 - x_1^{\ell})}{1 + x_1^{\ell}(K-1)} - \frac{x_1^{\ell}n^{s}(1 - x_1^{\ell})}{1 + x_1^{\ell}(K - 1)}$$

$$= \frac{n^{s}x_1^{\ell}(1 - x_1^{\ell})(K - 1)}{1 + x_1^{\ell}(K - 1)}$$

$$\therefore \frac{x_1^{\ell}(1 - x_1^{\ell})}{n^{o}\Delta x_1^{\ell}/m} = \frac{1}{n^{s}}\left[x_1^{\ell} + \frac{1}{(K \mp 1)}\right] \qquad \ldots\ldots\ldots (9)$$

For a perfect system, therefore, the left hand side of equation (9) plotted against x_1^{ℓ} should give a linear graph of slope $1/n^{s}$ and intercept

when $x_1^{\ell} = 0$ of $1/n^s$ $(K - 1)$ enabling both n^s (the total number of moles which can be accommodated in the sorbed phase per gram of solid) and K to be determined from experimental composite isotherm data. Provided the assumptions of the model are justifiable, and if the areas occupied by the two kinds of molecule do not differ significantly, then by assuming an area per molecule the specific surface area of the solid can be calculated.

The determination of the individual isotherms is not possible by any direct method, but use can be made of equation (8). On condition that the sorbed layer is monomolecular, then, as shown by Kipling and Tester[8]

$$\frac{n_1^s}{(n_1^s)_m} + \frac{n_2^s}{(n_2^s)_m} = 1 \qquad \ldots\ldots\ldots\ldots (10)$$

where $(n_1^s)_m$ and $(n_2^s)_m$ are the numbers of moles of the individual components, respectively, required to cover the surface of unit mass of solid completely. Sorption of the individual vapours of the pure components and application of the Langmuir or B.E.T. equation to the isotherms yields values for $(n_1^s)_m$ and $(n_2^s)_m$ provided that the orientations of the molecules are the same whether sorbed from the vapour phase or from a liquid mixture. For a solid solute resort has to be made to accepted bond lengths and angles for the crystal or from an assumed packing of the molecules to calculate $(n_1^s)_m$. Thus the individual isotherms can be constructed by application of equations (8) and (10) to the experimental values of Δx and x_1^{ℓ} permitting n_1^s and n_2^s to be calculated.

Examples of calculated individual isotherms are shown in Figs. 5 and 6,

one being for an aqueous and the other for a non-aqueous system[9]. In both instances the sorption of the solvent is very high for dilute solutions because the solvent molecules are considerably smaller than those of the solute and a greater number of moles is required to cover a given area.

In Fig. 5 it is seen that the individual isotherm for the sorption of the solute lies close to the composite isotherm. For many systems there is even less separation, the reason lying in the form of equation (8). As the limiting solubility usually occurs at a low value of the mole fraction all realisable values of x_1^{ℓ} are small. Consequently, even if n_2^s is large, $n_2^s x_1^{\ell}$ is usually small compared to $\frac{n^o \Delta x_1^{\ell}}{m}$. Moreover, because $(1 - x_1^{\ell})$ is very nearly unity, then

$$\frac{n^o \Delta x_1^{\ell}}{m} \simeq n_1^s \qquad \ldots\ldots\ldots\ldots (11)$$

The composite isotherm therefore gives an acceptable representation of the individual isotherm for sorption of the solute, even if there is considerable sorption of the solvent.

In Fig. 6 the composite and individual isotherms for malonic acid diverge markedly as the mole fraction of acid increases, the principal cause being the relatively high value of n_2^s at high values of x_1^{ℓ}.

(b) Nature of the Solvent

Dispersion forces, dipole interactions and hydrogen-bonding are key factors in governing the influence of a solvent upon a sorption process.

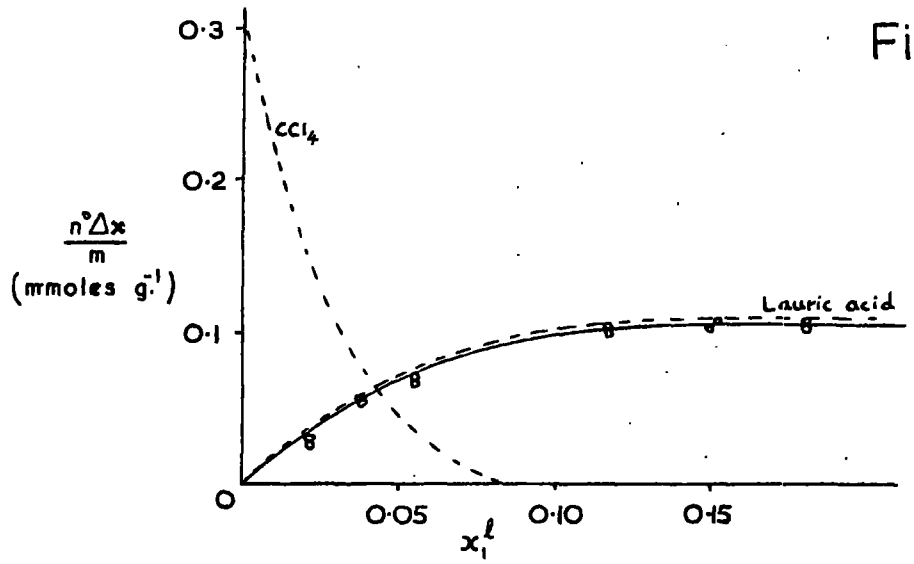

Fig. 5

Lauric acid in CCl_4

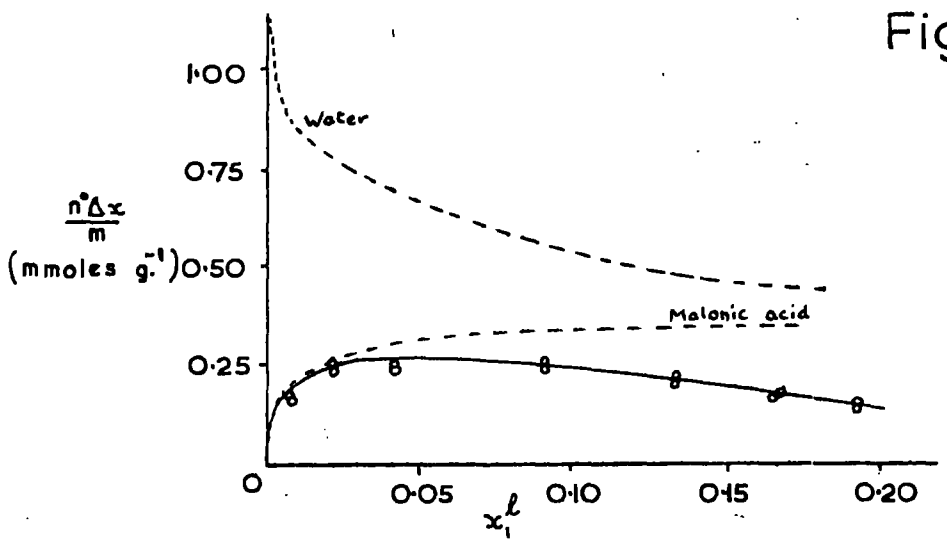

Fig. 6

Malonic acid in water

COMPOSITE ISOTHERMS (FULL LINES) AND INDIVIDUAL ISOTHERMS (BROKEN LINES) FOR ABSORPTION ON GRAPHON

Van de Waals dispersion forces are weak (less than 5 Kcals. per mole) but act between all molecules and are responsible for adsorption of inert gases onto neutral surfaces. Dipole interactions are stronger and may be important even though the solvent molecule has no resultant dipole moment, e.g. the dipole moments of a series of n-alcohols were found to be greater in carbon tetrachloride than in cyclohexane as a result of solute-solvent interaction between the polar O - H bond in the alcohols and the C - Cl dipoles in the solvent.[10]

Hydrogen bonds are stronger interactions than either of the previously mentioned effects as the work of Ibbitson and Moore[10] shows. They discovered that dipole moments and near-infrared spectra of n-alcohols in dioxan solution differed significantly from values in benzene and suggest that the alcohol molecules hydrogen-bond to dioxan and that the observed dielectric behaviour and infrared absorption are properties of the complex formed. That the dipole moments in dioxan are greater than those in benzene is also indicative of the greater solute-solvent interaction in dioxan. The mechanism of hydrogen bonding can enable the solvent to compete effectively with the solute for surface sites when the isotherm may be the S type instead of the more generally observed L type, as illustrated by phenol sorption onto alumina from water[11] (S type) and cyclohexane[12] (L type).

For solvents not so widely different in polarity as water and cyclohexane, the plateau of the isotherm assumes significance. Kipling and Wright[9] investigated the sorption on carbon blacks of stearic acid from

cyclohexane, ethanol, carbon tetrachloride and benzene. In the sorption on graphon, the isotherms come to a plateau whose height was almost the same for sorption from the four solvents (Fig. 7). This might, therefore, represent complete coverage of the surface by stearic acid molecules. Knowing the surface area of the graphon and the height of the plateau, then the area available to each mono meric stearic acid molecule is calculated to be 114$\mathring{A}^2$. If the molecules were sorbed with the long axis parallel to the surface, and close packed, as shown in Fig. 8, each monomeric molecule would occupy 114$\mathring{A}^2$: it is reasonable to suppose that such an orientation would be adopted on a graphon surface.

From the molecular area of 114$\mathring{A}^2$ the sorption on Spheron 6 corresponding to a complete monolayer of stearic acid was calculated. This proved to be higher than the level reached by any of the isotherms (see Fig. 9) and it was concluded that the surface of Spheron 6 is sufficiently polar to attract solvent molecules appreciably but not sufficiently polar to bring about disruption of the dimeric stearic acid molecules and their subsequent orientation perpendicular to the surface.

That the solvent can have profound effects on sorption characteristics was reported by Freundlich who found that adsorption of benzoic acid by charcoal was, for the same concentrations, ten times less from solution in diethyl ether than from aqueous solution[13]. A similar discovery was made in this study in the sorption of phenol onto the alumina surface:-

Fig.7

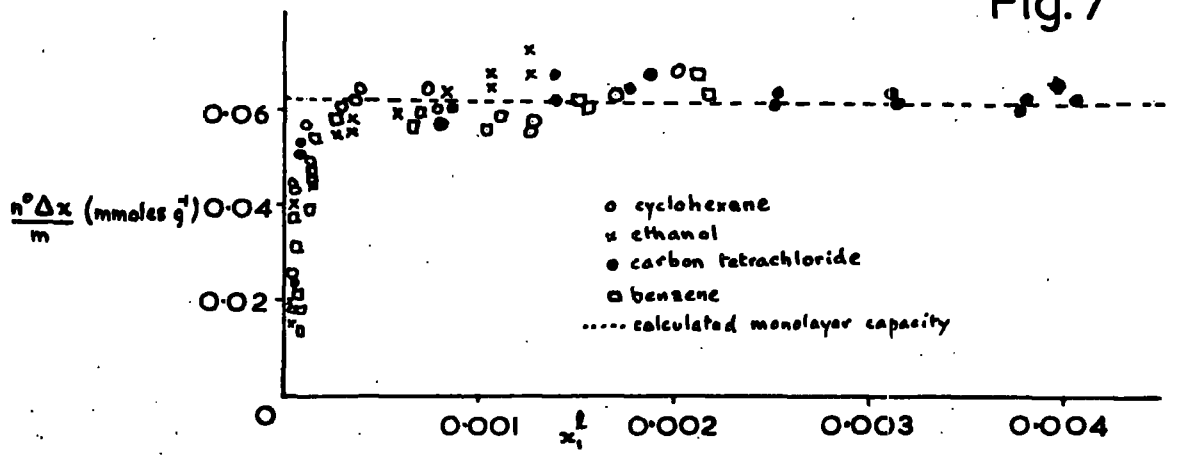

Adsorption of stearic acid on Graphon

Fig.8

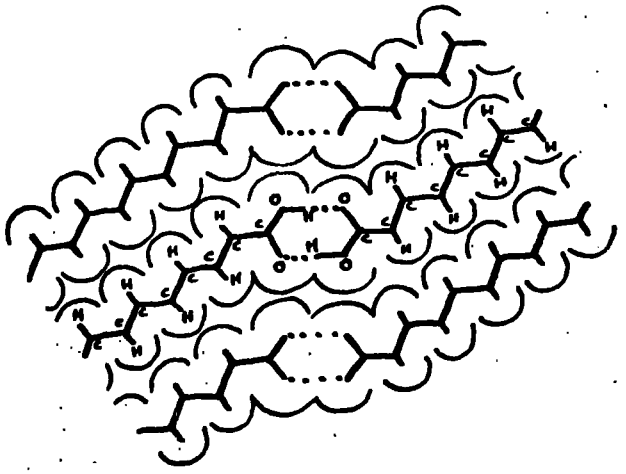

Monolayer of stearic acid molecules on Graphon

Fig.9

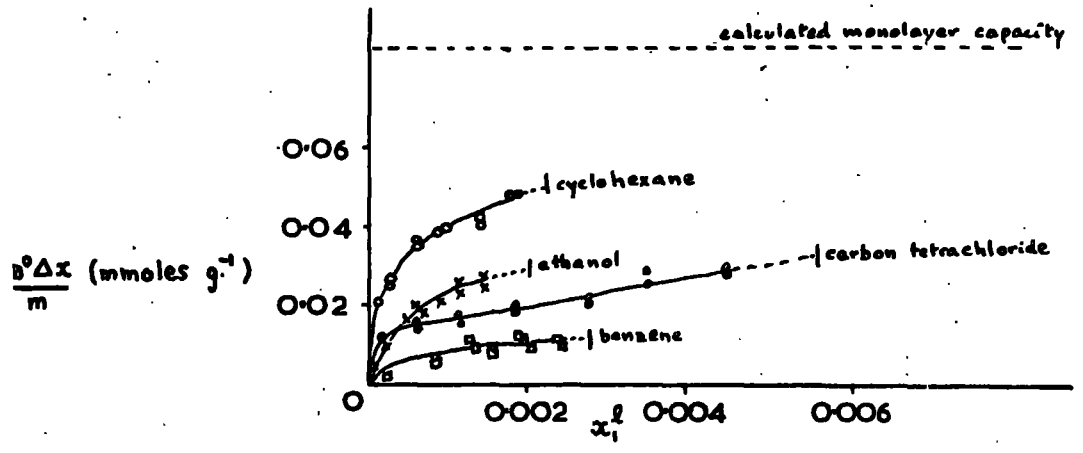

Adsorption of stearic acid on Spheron 6

Solvent	Limiting sorption value per gram of alumina
heptane	0.632 mmoles[14]
cyclohexane	0.651 mmoles
dioxan	0.168 mmoles

and again for p-nitrophenol:

benzene	0.605 mmoles
dioxan	0.212 mmoles

The limiting sorption values from heptane and cyclohexane probably represent monolayer coverage by phenol molecules only but from dioxan the uptake is much reduced. This indicates that dioxan is strongly attracted to the hydroxylated surface of the alumina and in fact more dioxan is adsorbed than phenol, although here the isotherm type remains unchanged (see Figs. 10 and 11).

Nature of the Sorptive

(a) Homology and Traube's Rule

In comparing the sorption properties of different sorptives, it is essential that the study be made using the same solvent and sorbent surface. Even under these conditions differences in orientation of the sorptive molecules at the sorbent surface can lead to erroneous conclusions regarding sorption affinity. In fact, for a complete interpretation of sorption characteristics, sorptive orientation must be known.

It becomes of interest, then, to compare the extents of sorption of members of an homologous series, and in this connection there has been a tendency for any progressive change to be regarded as an example of Traube's

Fig. 10

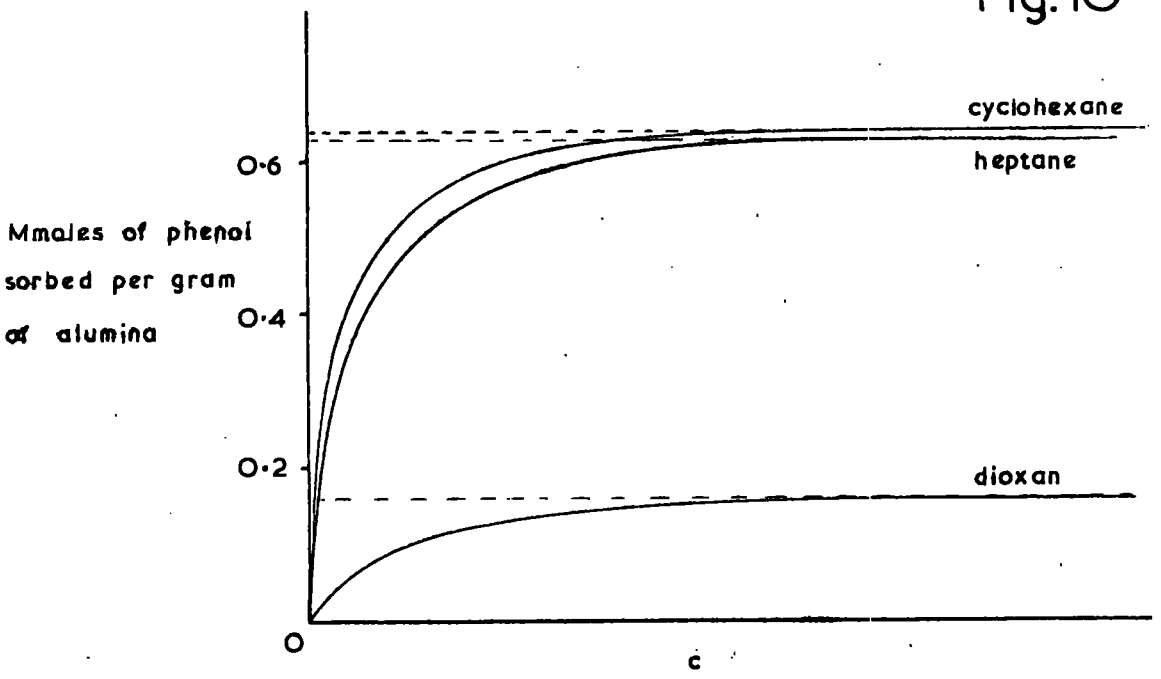
cyclohexane
heptane
dioxan
0·6
0·4
0·2
0
c
Mmoles of phenol sorbed per gram of alumina

Fig. 11

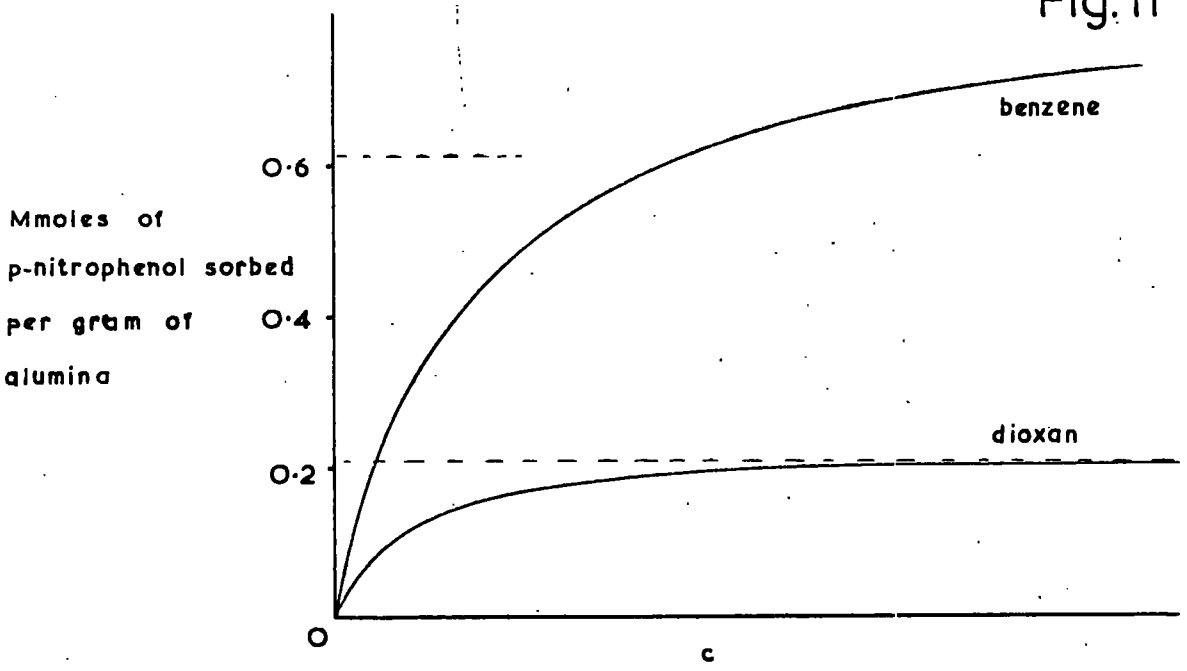
benzene
dioxan
0·6
0·4
0·2
0
c
Mmoles of p-nitrophenol sorbed per gram of alumina

rule[15] (or as an inversion of it). Traube observed a regularity in the lowering of the surface tension of water by members of the three homologous series of fatty acids, alcohols and esters at low concentrations. He stated that in an homologous series of surface-active substances there is a constant ratio between the molar concentrations of two successive homologues giving rise to the same very small surface tension lowering in aqueous solutions. This is true only in the limiting case of extreme dilution at which adsorbed films are considered to be in a state comparable with that of a two dimensional ideal gas.

Traube found that surface activity increased strongly and regularly as any series was ascended. Because surface activity is related to sorption at an interface, Traube's rule has been expressed in terms of the regular increase in the strength of sorption of successive members, as measured by the work required to remove one mole from the surface layer to the bulk of the solution. Traube's original concept of a comparison of the decreasing concentration required to produce a given degree of surface activity (or sorption) as the series ascended has been supplemented by the concept of comparison of increasing extent of sorption at constant concentration. When making this latter comparison, however, it should not be ignored that Traube's rule should strictly be regarded as a limiting case applied to infinitely dilute solution.

Freundlich's early work on sorption of the lower fatty acids from aqueous solution by charcoal[13] showed increasing sorption with increasing chain length (Fig. 12). From decimolar solution the molar ratios of acid

sorbed per gram of charcoal were

acetic	: formic	1.26
propionic	: acetic	1.55
n-butyric	: propionic	1.56

It is suggested that the molecules of acid are sorbed with the major axis parallel to the surface, each CH_2 group contributing an equal amount to the energy of sorption.

Other systems to which Traube's rule applies include solutions of paraffin wax in benzene, with charcoal as sorbent[16] and acidified aqueous solutions of aliphatic aldehydes with charcoal.[17]

Whereas the extent of Traube's rule to the solid-solution interface is obeyed for the sorption of fatty acids from water, Nekrassow[18] has found that no general increase in sorption on charcoal from the less polar organic solvents (benzene, carbon tetrachloride, carbon disulphide) occurs as the chain length of the acid increases. Sorption from the oxygen containing solvents passed through a minimum in the region C_3 - C_6. Recent sorption studies by Kipling and Wright[19] on carbon black from solutions of mono-carboxylic acids in organic solvents show a complex pattern of behaviour. The acids can be classified into a group of solids, a group of liquids completely miscible with the solvents, and the single member, formic acid, which is a liquid only partially miscible with the solvents. The solids are readily sorbed at low concentrations on graphon, forming a complete monolayer if the sorbent does not attract the solvent strongly (Fig. 13). The higher the molecular weight of the acid the more strongly it is sorbed

Fig. 12

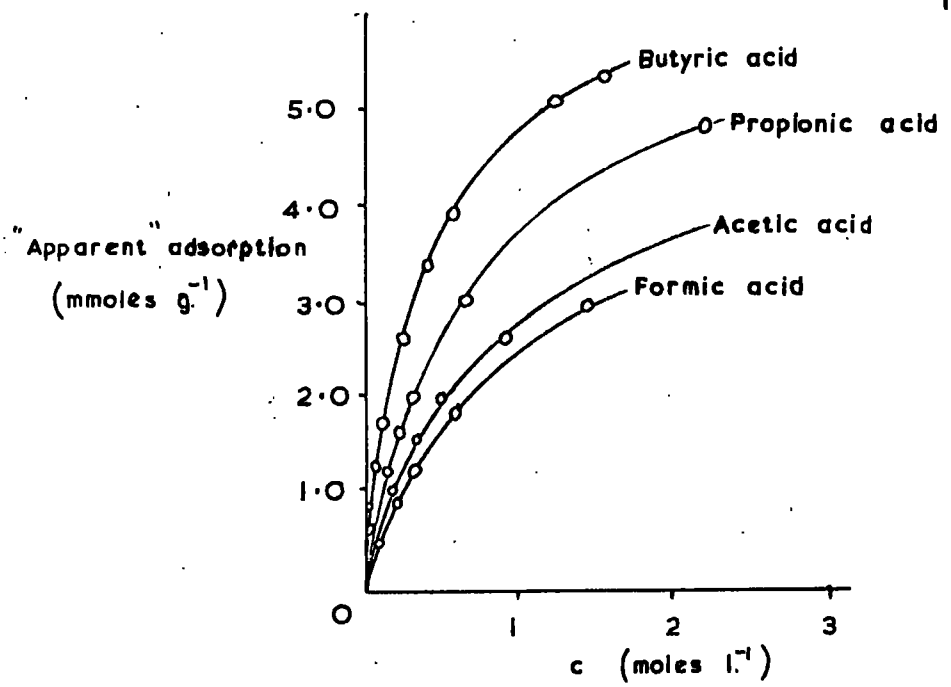

ADSORPTION BY CHARCOAL FROM DILUTE AQUEOUS SOLUTIONS OF THE LOWER FATTY ACIDS

Fig. 13

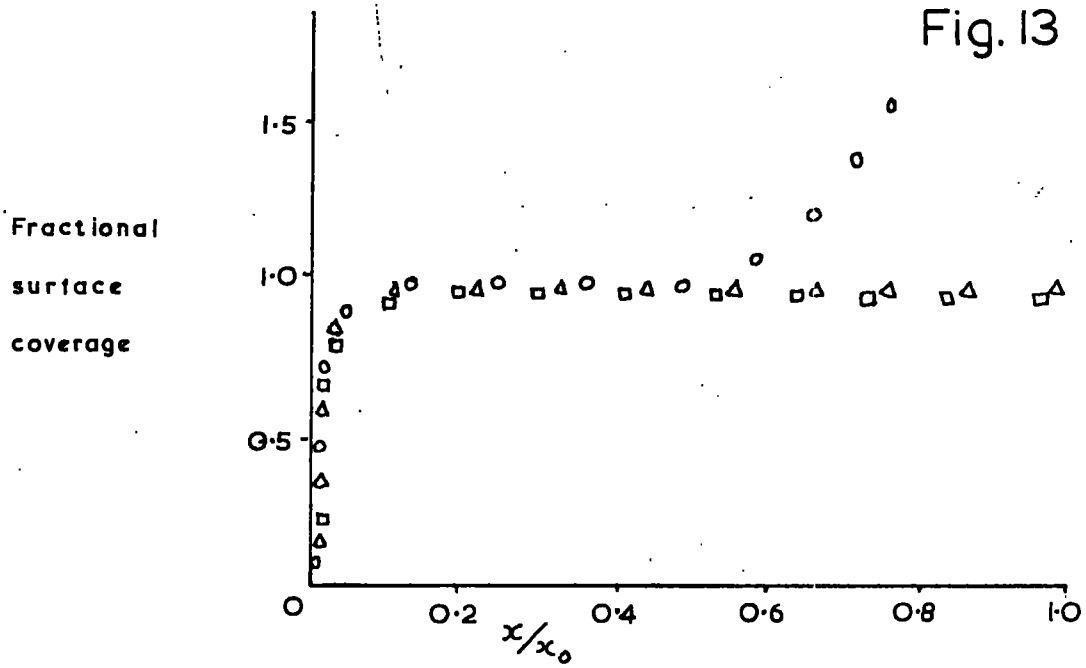

SURFACE COVERAGE OF GRAPHON IN ADSORPTION OF C_{16} ACID FROM o CARBON TETRACHLORIDE, △ CYCLOHEXANE, □ BENZENE

at low concentrations, and this is in accord with Traube's rule. Acids completely miscible with the second component form a complete monolayer only at a mole fraction of unity (Fig. 14) and there is some evidence that the lower members of this group are more strongly sorbed than the higher members. The former compounds being relatively more polar, produce solutions undergoing more positive deviations from ideal behaviour and are thus more strongly sorbed. Acid-surface and acid-solvent interactions are particularly important in these cases and explain deviations from Traube's rule. The gradual rise in the individual isotherm for sorption of formic acid from carbon tetrachloride by graphon (Fig. 15) may prove to be typical of the sorption of highly polar substances by relatively non-polar solids. An extreme case is the sorption of water vapour by graphon.[20]

Conformity to the extension of Traube's rule is thus probably found only when there is a combination of favourable circumstances. In the sorption of fatty acids from aqueous solutions by charcoal observed by Nekrassow[18] and others[21, 22, 23] the interaction between water and charcoal is weak, the interaction between the acid and the charcoal increases with increasing chain length, whereas the interaction between the acid and water becomes proportionately less as the ratio of polar to non-polar section of the molecules decreases. The combination of trends would lead to an increase in sorption with increasing chain-lengths. In a recent comparison of the sorption behaviour of aqueous solutions of dicarboxylic acids on graphon Wright[24] observes that the plots of $n_1^s/(n_1^s)_m$ against x for the systems show that sorption of the acids increases in a regular order with increasing chain length (Fig. 16).

Fig. 14

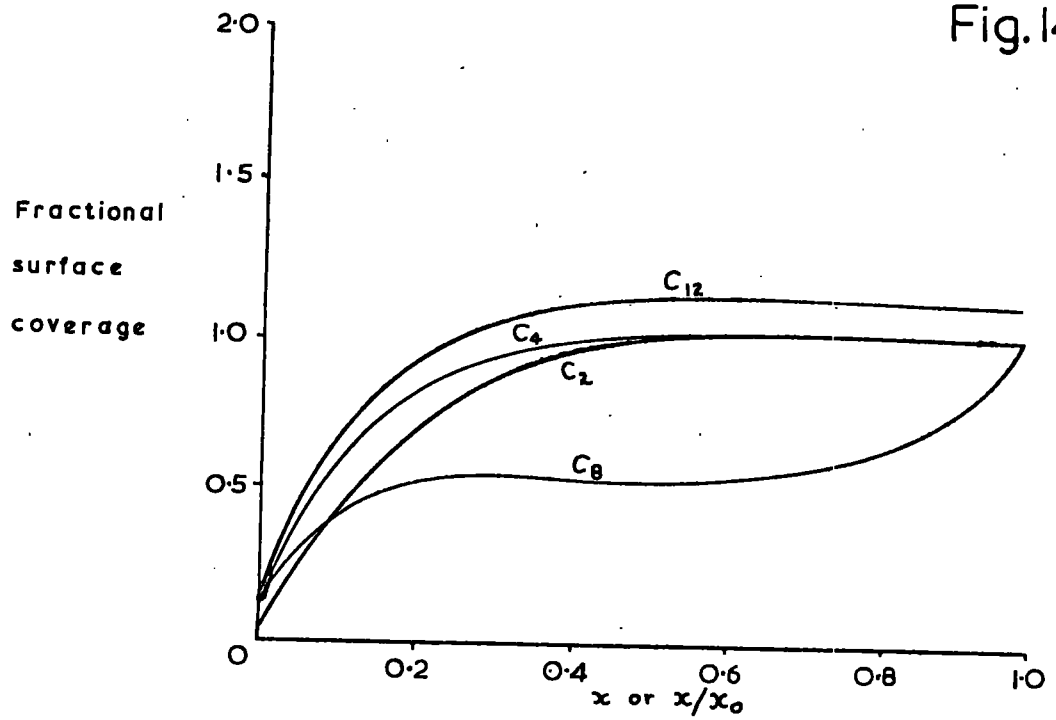

SURFACE COVERAGE OF GRAPHON IN ADSORPTION OF FATTY ACIDS FROM CCl_4. (ABSCISSÆ x/x_o FOR C_{12})

Fig. 15

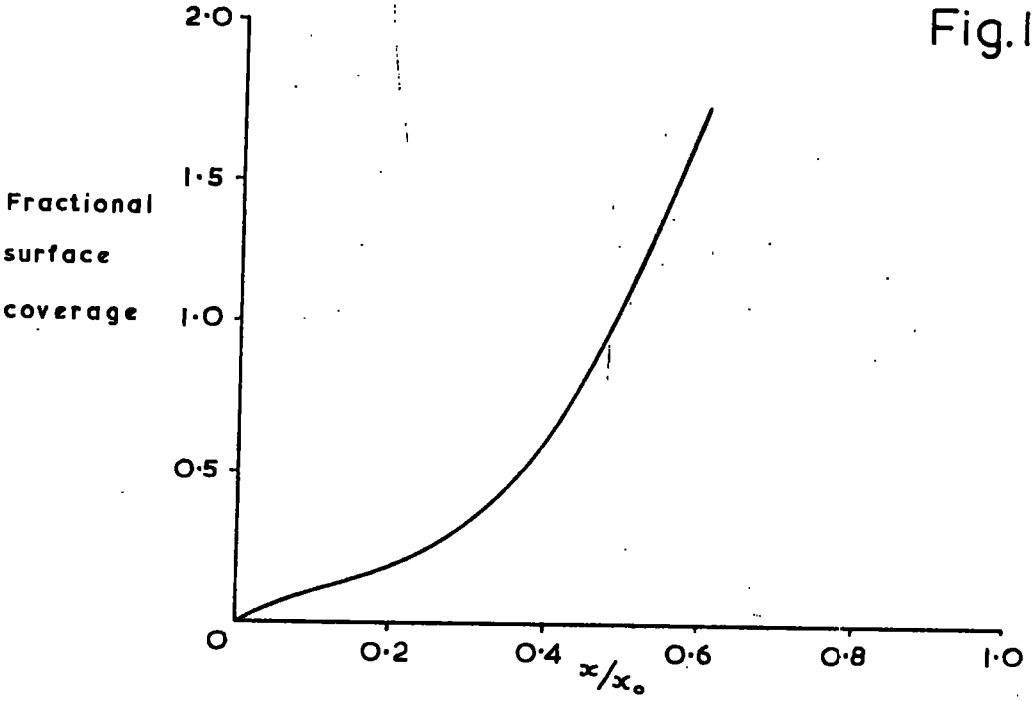

SURFACE COVERAGE OF GRAPHON IN ADSORPTION OF FORMIC ACID FROM CCl_4.

The sorption behaviour thus seems to conform, at least qualitatively, with the expectation of Traube's rule in conformity with the results for sorption of fatty acids on charcoals from dilute aqueous solutions,[18] but unlike the behaviour of fatty acids sorbed on carbon blacks from organic solvents.[19]

The discussion of the effect of the nature of the sorptive on sorption at the solid-solution interface has so far been restricted to sorption of homologous series of compounds. Other structural features and properties of the sorptive molecule will now be briefly considered.

(b) Effects of Substitution

Linner and Gortner[25] examined the sorption of substituted fatty acids from aqueous solution onto Norit charcoal and concluded that whereas the introduction of an OH group into the molecule reduced the extent of sorption, the presence of an NH_2 group caused an even greater reduction. In explanation it was suggested that the additional group increases the extent of the interaction between sorptive and solvent and so reduced the escaping tendency of the sorptive molecule to the solution-solid interface. Although the introduction of a second OH group caused a further decrease in the extent of sorption, the decrease was less than the primary effect.

With regard to the sorption of aromatic carboxylic acids from aqueous solution onto animal charcoal, Sata[26] found the order of sorption to be para - < meta - < ortho-hydrobenzoic acids; illustrating the importance of the position of substitution in the aromatic nucleus.

Bartell and Scheffler[27] sorbed saturated mono-basic alcohols from

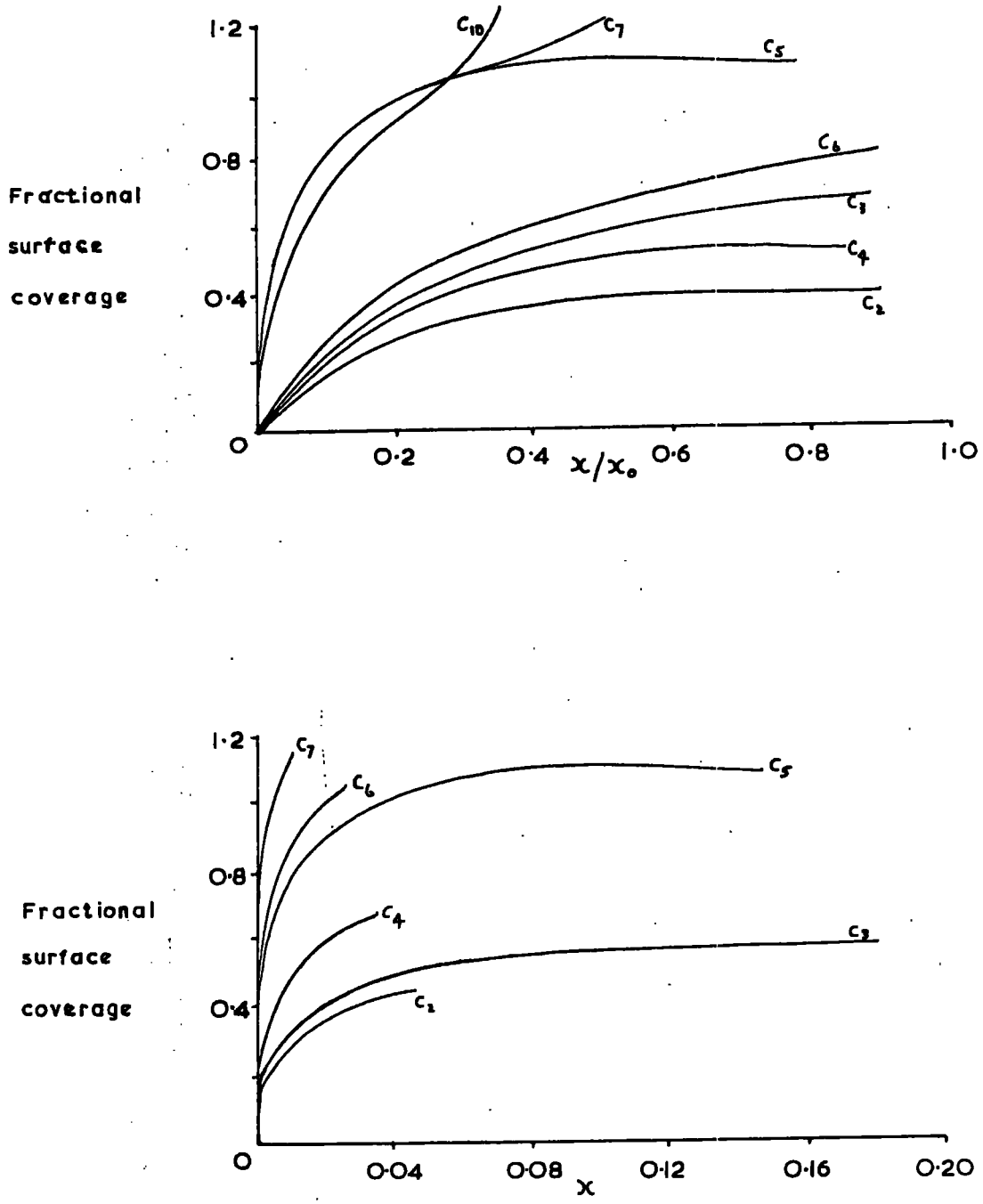

SURFACE COVERAGE OF GRAPHON IN ADSORPTION FROM AQUEOUS SOLUTIONS OF DICARBOXYLIC ACIDS

Fig. 16

benzene onto ash-free blood charcoal. The isotherms showed that the sorption decreased with rise in molecular weight, and also that sorption of the solvent was important. Increasing solubility of the higher alcohols in benzene is obviously an important factor in determining order of sorption in this case. The reversal of Traube's rule is again noted and identified with the process of sorption on charcoal from an organic solvent. In fact from aqueous solution Amiot[28] found the order of increasing sorption onto Merck animal charcoal to be methyl < ethyl < isopropyl < propyl < isobutyl < butyl < isoamyl alcohol.

The sorption of hydrocarbons from mixtures onto silica gel was examined by Moir and Forziate[29] who found that for compounds of approximately equal molecular weights the order of increasing sorption is paraffins, naphthenes, monolefins, diolefins and one, two, three and four-ring aromatic hydrocarbons, subject to certain limitations on the type and configuration of the aromatic rings.

(c) Melting Point of Sorptive

When the sorption of two similar compounds under identical conditions is compared, it would be expected that the compound of lower melting point, being more soluble in the solvent, would be sorbed to the lesser extent. This is known to occur in sorption from relatively non-polar solvents onto relatively non-polar surfaces, and the following examples of the sorption of diphenylpolyenes supports the view:-

Compound	m.p.	Solubility in gram/litre in benzene	in chloroform
$C_6H_5-CH = CH-C_6H_5$	124°C.	102.12	153.2
$C_6H_5-(CH = CH)_2-C_6H_5$	152.5°C.	66.15	97.8

This relationship is, however, of limited application as can be seen from the relative sorbabilities of cis and trans azobenzenes, which follow the rule in non-polar but not in polar solvents.

Compound	m.p.	Solubilities in millimoles per litre Pet. ether at 0°C.	Water at 25°C.	Methanol at 0°C.
Trans-azobenzene	68°C.	192	0.02	164
Cis-azobenzene	71.4°C.	49.4	0.65	410

Cis-azobenzene is sorbed to a greater extent from petroleum ether onto alumina than the trans compound, the reverse order being obtained on sorption from water or methanol onto Norit charcoal.

(d) Extent of Association of Sorptive

Bakr and McBain[30] examined the sorption of acetic acid and tolvene onto sugar charcoal and animal charcoal. They found that at high temperatures little acetic acid but considerable tolvene was sorbed, and they related this to the dissociation of acetic acid dimers at high temperature.

Heymann and Boye[31] examined the sorption of benzoic acid from nitrobenzene, acetone and nitromethane onto charcoal and concluded that sorption was greatest from nitrobenzene since benzoic acid was strongly associated in this compound. This increase in sorption with association

may well be due to the decrease in polarity of the solute molecules on association, the polymers having a greater affinity for the non-polar charcoal.

(e) Polarity of Sorptive

From general considerations it would be anticipated that the influence of polarity of sorptive molecule on the extent of sorption would only become distinguishable in certain restricted sorption systems. For example, it may be considered that in the case of the sorption of a polar solute from a non-polar solvent, which is only weakly interacting with the sorbent, then the polarity of the solute may have an important influence on the order of sorption. It would be necessary that the sorbent be essentially ionic, i.e. alumina or silica gel, or other metal oxide type, and that the solvent be preferably cyclohexane, heptane, hexane or even pentane.

In order to establish any relationship between extent of sorption and polarity, it is necessary to attach quantitative significance to the property of the sorptive which has been termed polarity. Since the dipole moment of the molecule is a measure of polarity it becomes of interest to assess its influence upon sorption affinity. This assessment has, unfortunately, been beset with difficulties. For example, in the case of sorption of n-alcohols from cyclohexane onto alumina Eric[32] found that whereas the equilibrium constant for the sorption process showed a progressive increase with increasing length of hydrocarbon chain from methanol to n-octanol, dipole moments in cyclohexane showed little change

from ethanol to n-octanol. Heymann and Boye's[33] study of the influence of polarity of sorptive upon the sorption of fatty acids from chloroform, benzene, ethanol, acetone and water, was inconclusive. Arnold's[34] attempt to relate the order of sorption in chromatography with dipole moment was beset with exceptions.

Summarising, it would appear that only when sorption occurs via a strongly polar group should the above correlation be attempted. Even then, the functional group moment would be more fundamental than the dipole moment of the molecule as a whole. If, of course, polar groups are plentiful in the rest of the sorptive molecule, then solvent-solute interactions may appreciably weaken the main surface sorption force, and so the sorption affinity may well be unrelated to the dipole moment of the functional group itself.

For a study of this relationship, therefore, it is essential that a very careful choice of sorption system be made.

A comparison of sorptive polarisability with sorbability has proved more successful. The molar polarisation is made up of two terms, an atom polarisation P_a and an electron polarisation P_e. The latter can be calculated from the refractive index of the substance for visible light and usually constitutes the greater part of the molar polarisation. Arnold[34] concluded that where no permanent dipoles exist in the sorptive molecules those with higher polarisabilities were more strongly sorbed on alumina. Bhatnager[35] also found some correlation between the polarisability of solute and solvent and the sorption onto polar and non-polar types of

phenol-formaldehyde and amine-formaldehyde resins.

Generally it may be supposed that if the molecule possesses no permanent polarity, then if sorption occurs from a non-polar solvent onto a polar sorbent, the greater the molecular polarisability of the sorptive, the greater the degree of sorption.

(f) Hydrogen-bonding ability of Sorptive

Hydrogen bonding of the sorptive with the solvent would be expected to result in increased solubility of the solute and decreased sorbability, whereas hydrogen bonding with the sorbent would tend to increase the extent of sorption.

Much evidence exists that hydrogen bonding is responsible for the sorption of non-ionic solutes from non-polar solvents onto activated alumina[11, 36]. Ibbitson, Jackson, McCarthy and Stone[37] concluded that hydrogen bonding plays a significant role in the sorption of simple substituted azo compounds from benzene solution onto alumina. If the hydrogen atom of the hydroxyl group in 4-hydroxy-azobenzene is replaced by a methyl group, then sorption becomes negligible. Also if the hydrogen atoms of the amino group in 4-aminoazobenzene are both replaced by methyl groups, the resulting compound shows little affinity for the alumina surface. Eric, Goode and Ibbitson[12] studied the sorption of para-substituted phenols from cyclohexane onto alumina. They found that the surface saturation values corresponded to a surface area requirement of 24 $\mathring{A}^2$ per phenol molecule, in accord with "edge-on" orientation at the sorbent surface and a likely hydrogen bonding sorption mechanism. Sandall[38] studied the

sorption of phenol from cyclohexane, dioxan and cyclohexane/dioxan mixtures. The isotherms of Fig. 17 clearly illustrate the effect of hydrogen bonding between sorptive and solvent on the extent of sorption on alumina.

It is concluded that if hydrogen bonding is possible at the solution-solid interface it will be a preferred mechanism of sorption, provided steric effects are absent.

Nature of the Sorbent

Competitive adsorption at the liquid-solid interface from binary mixtures is influenced by the nature of the interactions between the solid and each component on the surface, by the porosity of the surface and by its heterogeneity.

(a) Chemical Nature of the Surface

In amorphous solids the physical properties are the same in all directions, unlike crystalline solids in which properties may have different values in different directions, thus a crystal will sometimes sorb one dye on one set of faces and another on a second set, no sorption of the first dye occurring on the second set of faces or vice versa (lead nitrate sorbs methylene blue on the '110' faces, another set of faces sorbing none of this dye but easily sorbing picric acid).

Although crystals are usually classified according to the type of geometric lattice, a classification based on the nature of the surface force associated with a given solid is often more instructive in sorption problems. The chemical nature of the surface is of prime importance.

Fig. 17

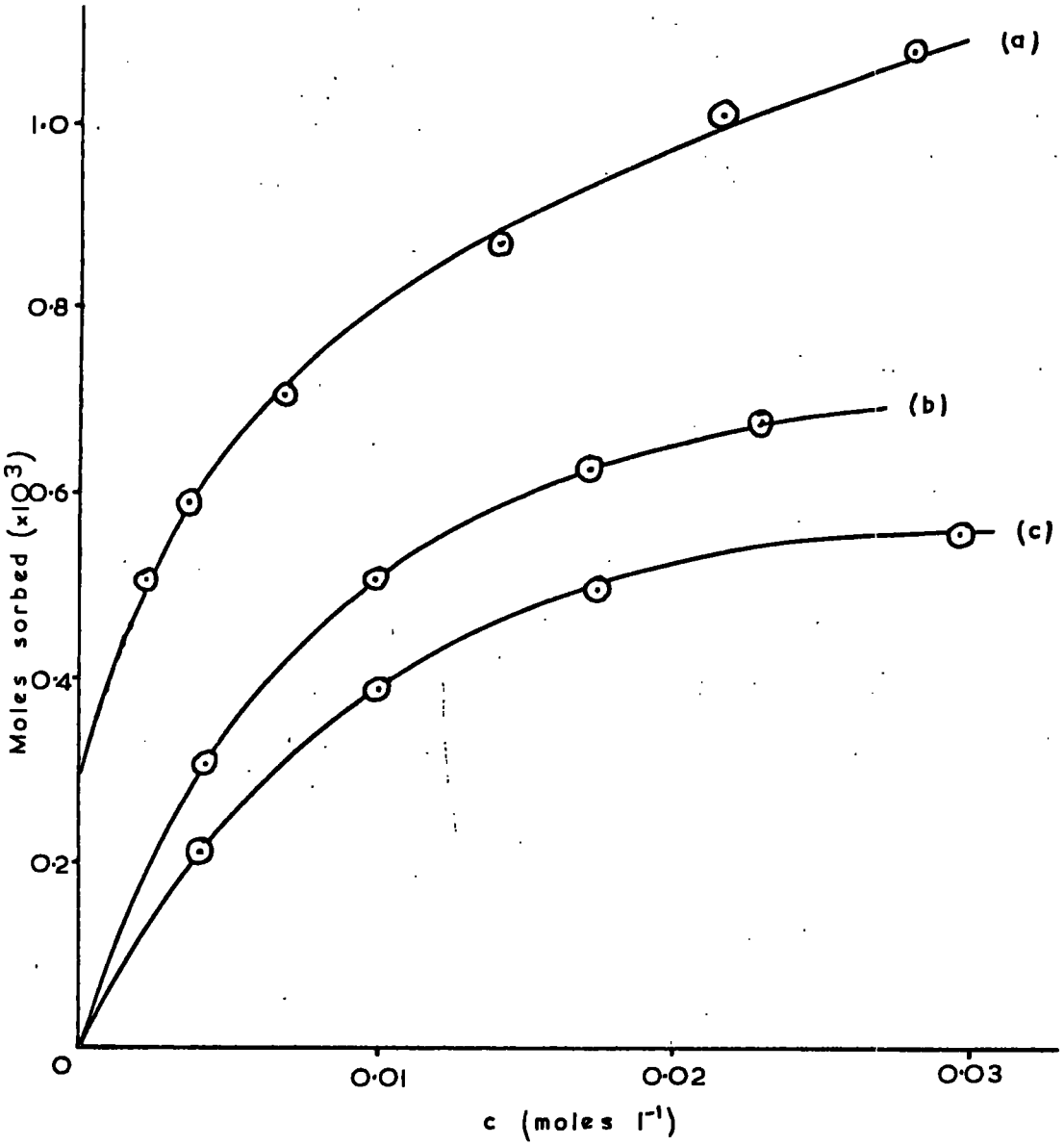

ADSORPTION OF p-ISOPROPYLPHENOL ON ALUMINA FROM (a) 100:5 CYCLOHEXANE:DIOXAN, (b) 50:50 CYCLOHEXANE:DIOXAN, (c) DIOXAN

Its force field is such that preferential adsorption by a solid is appreciably greater than that which occurs at other interfaces, but the extent, and even the sign, of the selectivity varies considerably. This is most clearly evident when adsorption takes place from a mixture of a polar and a non-polar (or relatively non-polar) liquid. Silica gel adsorbs alcohols in preference to iso-octane[39] and in preference to benzene[27], whereas charcoals usually adsorb benzene in preference to alcohols[40] (see Fig. 18). These preferences may be ascribed to the highly polar nature of the silica gel surface and the relatively non-polar nature of the charcoal surface. Other gels (alumina, titania etc.) resemble silica gel in this respect[41].

On such adsorbents, hydrogen-bonding may be responsible for the preferential adsorption of one component. The relative affinities of silica gel for a series of nitro and nitroso derivatives of diphenylamine and N-ethylaniline dissolved in simple solvents depends on the strengths of hydrogen bond which can be formed between adsorbent and adsorbate[42]. The strong preferential adsorption of phenol from cyclohexane by charcoal is probably largely due to hydrogen bonding as the adsorption is drastically reduced by substitution of t-butyl groups in the two ortho positions. The effect of these substituent groups is mainly steric (which alone points to the importance of the hydroxyl group as a centre of adsorption), but indirectly they also weaken the hydrogen bond (methyl groups produce a much smaller reduction in adsorption[43]). Again, hydrogen bonding accounts for the tenacity with which dioxan molecules are attached to an

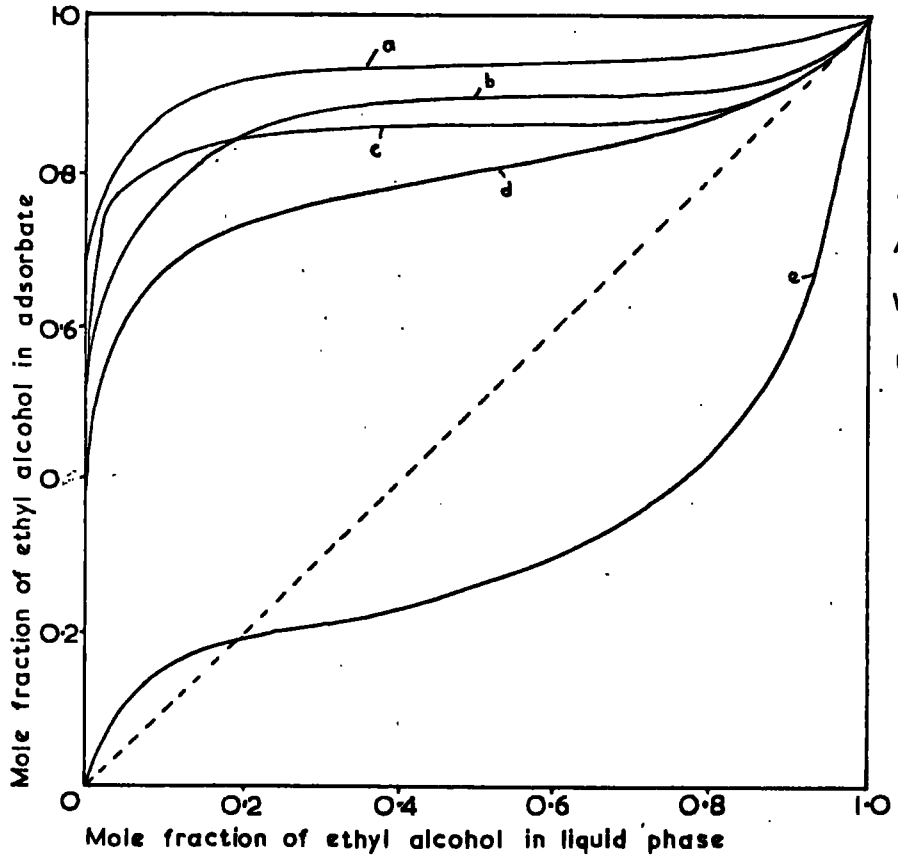

Fig. 18

ADSORPTION OF ETHYL ALCOHOL FROM MIXTURES WITH BENZENE ON

(a) GIBBSITE

(b) SILICA GEL

(c) BOEHMITE

(d) γ-ALUMINA

(e) CHARCOAL

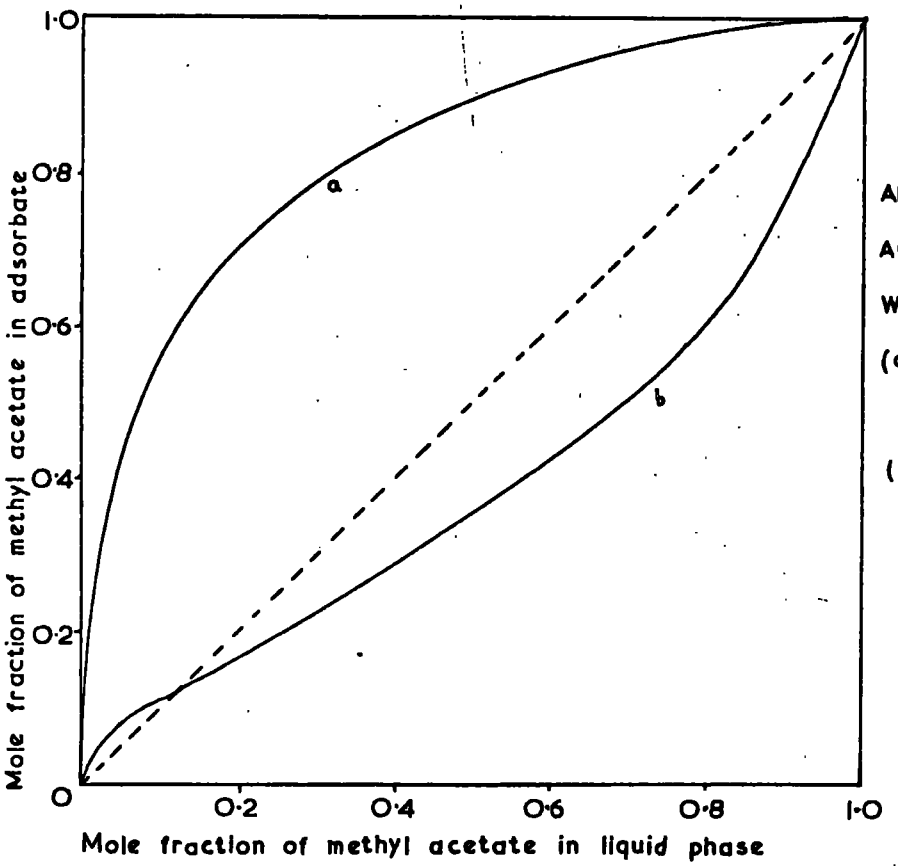

Fig. 19

ADSORPTION OF METHYL ACETATE FROM MIXTURES WITH BENZENE ON

(a) SILICA GEL OR BOEHMITE

(b) CHARCOAL

hydroxylated alumina surface.

Charcoals are generally of less definite composition, especially with respect to surface groups[44, 45], than oxide or hydroxide gels. Moreover, the surface can readily be altered by treatment with oxidising or reducing gases. If a charcoal is very strongly oxidised, its preference for ethyl alcohol relative to benzene increases with oxidation until it approaches that shown by silica gel[46] (see Fig. 18). Conversely, preferential sorption of alcohol can, to some extent, be reduced by removal of the oxygen groups from the surface[47].

Again, the effects of the chemical nature of the surface can be seen in the system methyl acetate-benzene[40] (Fig. 19). The ester is prefentially adsorbed by silica gel and by alumina, and this can be attributed to specific interaction of the polar centre of the ester molecule with the polar groups which cover the surface of the solid. On charcoal, on the other hand, methyl acetate is preferentially adsorbed only at low mole fractions, and over most of the concentration range benzene is preferentially adsorbed. This corresponds to a relatively low concentration of polar groups on the surface of charcoal.

(b) Porosity of the Surface

The surface of a solid sorbent may be completely non-porous or may have cavities described as macro, intermediate or micro pores and in the limiting case molecular sieves in which the entry to the pores is so small the larger component is completely excluded though the smaller is admitted, adding a degree of preferential adsorption irrespective of the

competitive adsorption due to other factors.

Porosity of the sorbent surface is revealed by hysteresis loops in gas adsorption isotherms. Fig. 20 shows a type II isotherm which might be obtained by low temperature (-195°C.) nitrogen adsorption on an oxide such as alumina[48]. ABCD represents the sorption isotherm and DEB the desorption isotherm: repeated sorption and desorption ("cycling") enables the same loop to be travelled many times. That a finite area is enclosed between the sorption and desorption curve indicates porosity and by applying Kelvin's analysis, derived from the capillary condensation theory, estimates of pore size and distribution can be made. Fig. 21 displays a typical result.

The effect of porosity is best seen with adsorbents capable of being prepared with varying degrees of surface porosity, e.g. charcoals by varying the degree of activation[44, 45]; silica gel by varying the conditions of forming or calcining the gel[49], and aluminas prepared at different temperatures of dehydration of the hydroxides[50]. Increase in porosity is normally accompanied by an increase in specific surface area and thus by an increase in the magnitude of the selective sorption, e.g. sorption of fatty acids from water on a series of steam-activated carbon blacks[51] and on steam activated charcoals[52].

For carbons heated to varying temperatures after activation sorptive capacity tends to fall off as the final temperature of preparation exceeds 800°C.[53]. This is due to a closure of the pore structure which is general for carbons at temperatures in the range 700 - 1500°C. For aluminas

Fig. 20

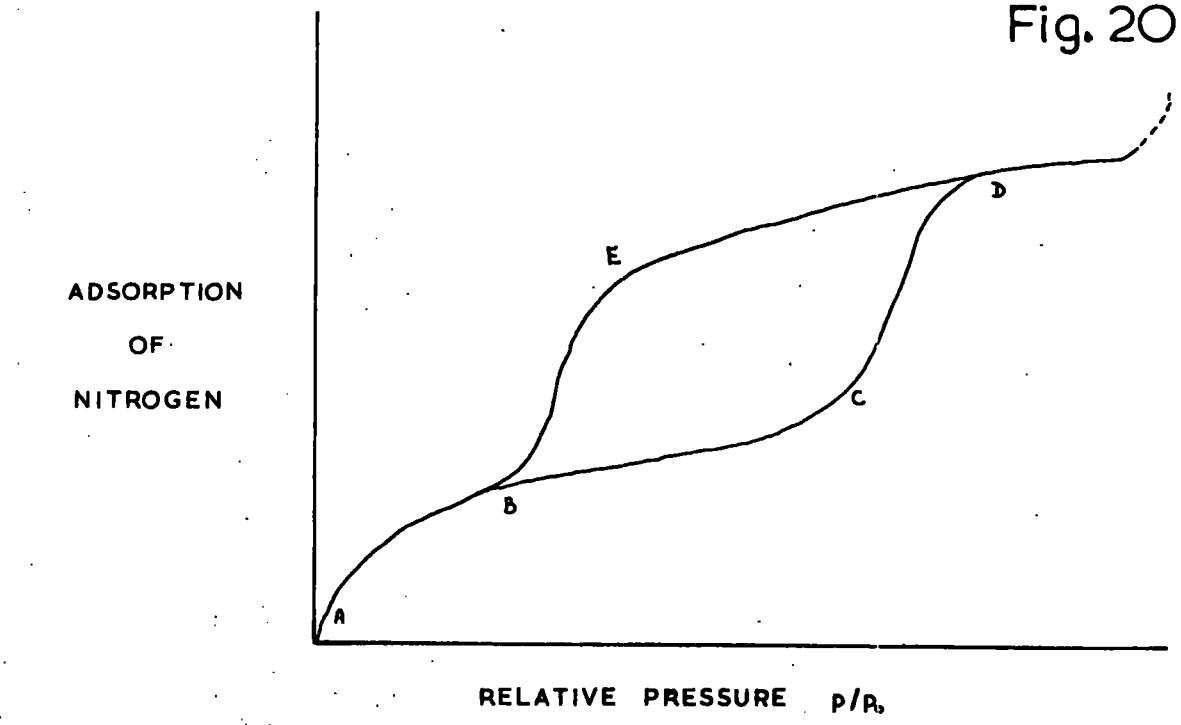
ADSORPTION
OF
NITROGEN
A
B
C
D
E
RELATIVE PRESSURE p/p₀

Fig. 21

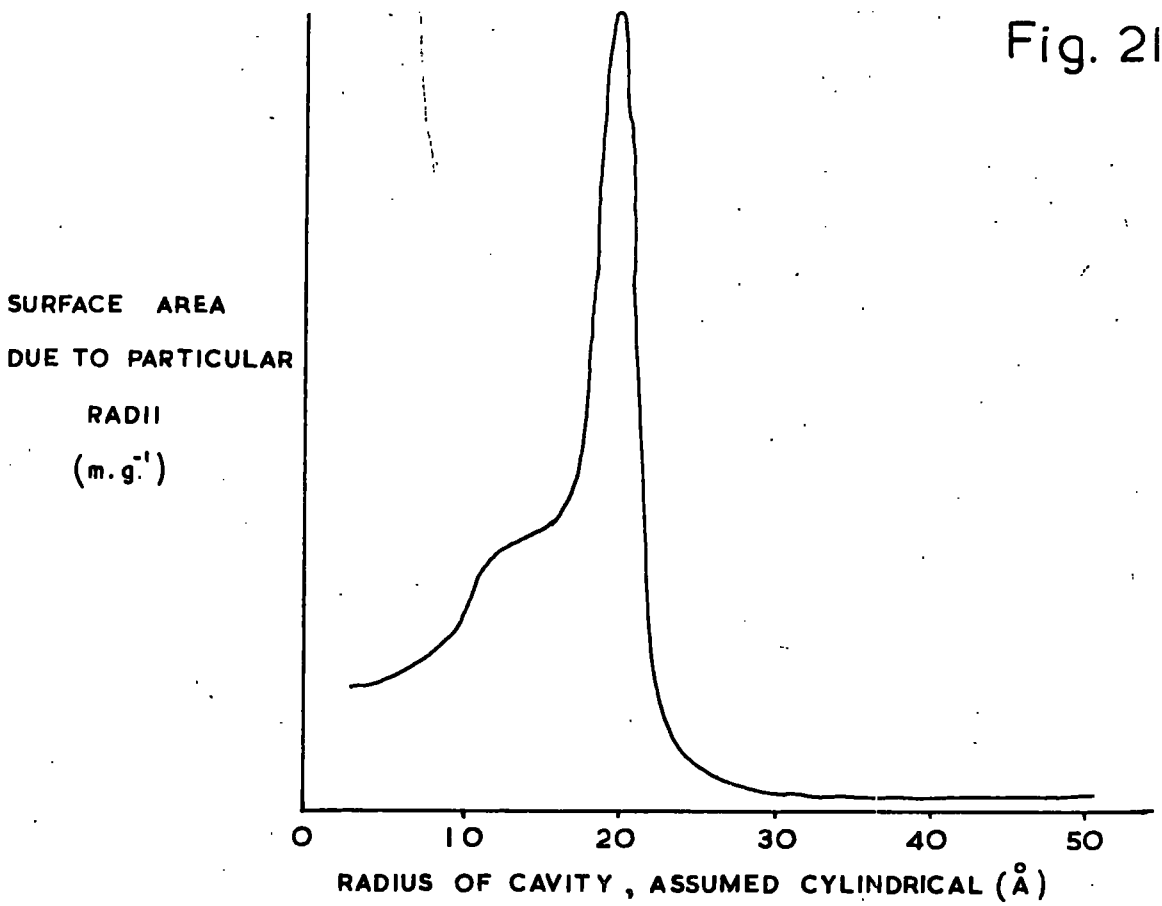
SURFACE AREA
DUE TO PARTICULAR
RADII
(m.g.⁻¹)
0
10
20
30
40
50
RADIUS OF CAVITY, ASSUMED CYLINDRICAL (Å)

prepared from a variety of crystalline hydroxides, de Boer et al.[50] found lauric acid sorption saturation values for pentane to be strongly dependent on the temperature of dehydration and the nature of the hydroxide. The lowest and most diverging values were found for aluminas obtained from crystalline hydroxides heated just above their decomposition temperature and the results were considered to be the outcome of a well developed porous structure giving rise to steric effects. At increasing temperatures of pre-treatment, the specific lauric acid sorption expressed as millimoles of acid per $100m.^2$ of surface area converged to a constant value at heating temperatures above $800^{\circ}C.$ irrespective of the starting material. It was noted that on pre-heating the alumina from approximately $500 - 800^{\circ}C.$ that the surface area determined by low temperature nitrogen sorption decreased to one half the original value, whereas the lauric acid sorption per $100m.^2$ of surface area increased by one half the value at $500^{\circ}C.$ The authors conclude that the steric factors at $500^{\circ}C.$ on the lauric acid sorption explains these results.

(c) Heterogeneity of the Surface

The experimental observation that the heat of chemisorption decreases as surface coverage increases has been ascribed either to the heterogeneous nature of the surface, with some sites more active than others[54] or to the repulsive interaction between adsorbed molecules[55]. Halsey and Taylor[56] have shown that there is a limit to the latter effect and large changes in heats of adsorption must be due to the populating of the most energetic sites, the heat of adsorption decreasing with the filling of less active sites.

Infrared spectroscopy has revealed that adsorption of a compound may give rise to several absorption bands corresponding to independant surface species on particular types of surface site. Variations have been found in the frequencies and intensities of bands of adsorbed substances as the coverage of the surface is increased. The infrared spectra of adsorbed species during desorption experiments have shown that certain molecules are removed more readily from the surface than others. Observations such as these point to the presence of surface heterogeneity.

Ammonia, for example, hydrogen bonds to surface hydroxyl groups on silica and alumina[57, 58, 59]. Peri and Hannan[60] have shown that three independant types of surface hydroxyl group exist on alumina surfaces and that these groups interact to different degrees in hydrogen bonding with adsorbed molecules.

In addition to hydroxyl groups, electron deficient Lewis acid sites exist on the surfaces of certain oxides, and which may co-ordinate molecules such as ammonia possessing lone-pair electrons. Proton-donor or Bronsted acid sites, which may in fact be hydroxyl groups or adsorbed water molecules, have been shown to occur on the surface of silica-alumina catalysts by Parry[61]. Spectra were shown which demonstrated that a proton was transferred from the catalyst surface to the adsorbed molecule. Thus the spectrum of the pyridinium ion appeared when pyridine was adsorbed. Yates and Lucchesi[62] found that independant sites existed on the surface of alumina for the adsorption of acetylene and ethylene, although the exact nature of these sites was not defined.

Heterogeneity in oxide surfaces is not always important. It generally involves the presence of both oxide and hydroxide groups (e.g. boehmite) and as both are highly polar, their different discrimination between pairs of sorptives is not always easy to detect. It is thought to be important, however, in the sorption of fatty acids by silica gel, as the occurrence of hydrogen bonding is postulated, analogous to the formation of a dimeric molecule of fatty acid[63]; the double hydrogen bond could not be formed on a surface consisting of oxide groups only

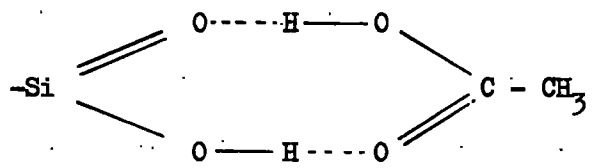

Charcoals and carbon blacks vary enormously and it is useful to consider the surface, not as elementary carbon but as a polynuclear hydrocarbon interspersed with a variety of oxygen complexes, and in some cases with groups containing nitrogen and sulphur. The extent of heterogeneity varies according to the method of manufacture of the carbon and its subsequent thermal history.

The selective sorption of methyl acetate from benzene onto charcoal at low concentrations mentioned earlier can be attributed to the strong interaction of the ester group with some of the polar oxygen complexes. When these are saturated sorption on the remainder of the surface is governed by the electron interaction between the aromatic solid and the aromatic benzene molecules, which is stronger than that between the solid

and the aliphatic ester (see Fig. 19).

A detailed examination of sorption by charcoal from mixtures of the lower aliphatic alcohols with benzene[64] suggests that the small degree of preferential sorption of the alcohols is due to their sorption (possibly by hydrogen-bonding) by oxygen complexes. The individual isotherms (Fig. 22) are S-shaped and characteristic of surface heterogeneity and taken together show that the number of moles sorbed in this way decreases as the homologous series is ascended, possibly reflecting the effect of increasing molecular size. Over the rest of the surface, presumed to be of hydrocarbon character, the benzene is preferentially sorbed in all cases.

The same phenomenon is shown in sorption from the same systems by carbon blacks[65]. On spheron 6, which has an heterogeneous surface, n-butanol is preferentially sorbed at low concentrations, but not at high concentrations. On graphon, which has no appreciable heterogeneity, benzene is preferentially sorbed at all concentrations.

Temperature

With rise in temperature the isotherm usually falls to lower levels (the process of sorption being fundamentally exothermic), particularly at the lowest concentrations, though it may reach almost the same limiting value at high concentrations[66] (Fig. 23). This corresponds to a weakening of the attractive forces between the solute and the solid surface (and between adjacent adsorbed solute molecules) with increasing temperature, and corresponding increase in solubility of the solute in the solvent.

Fig. 22

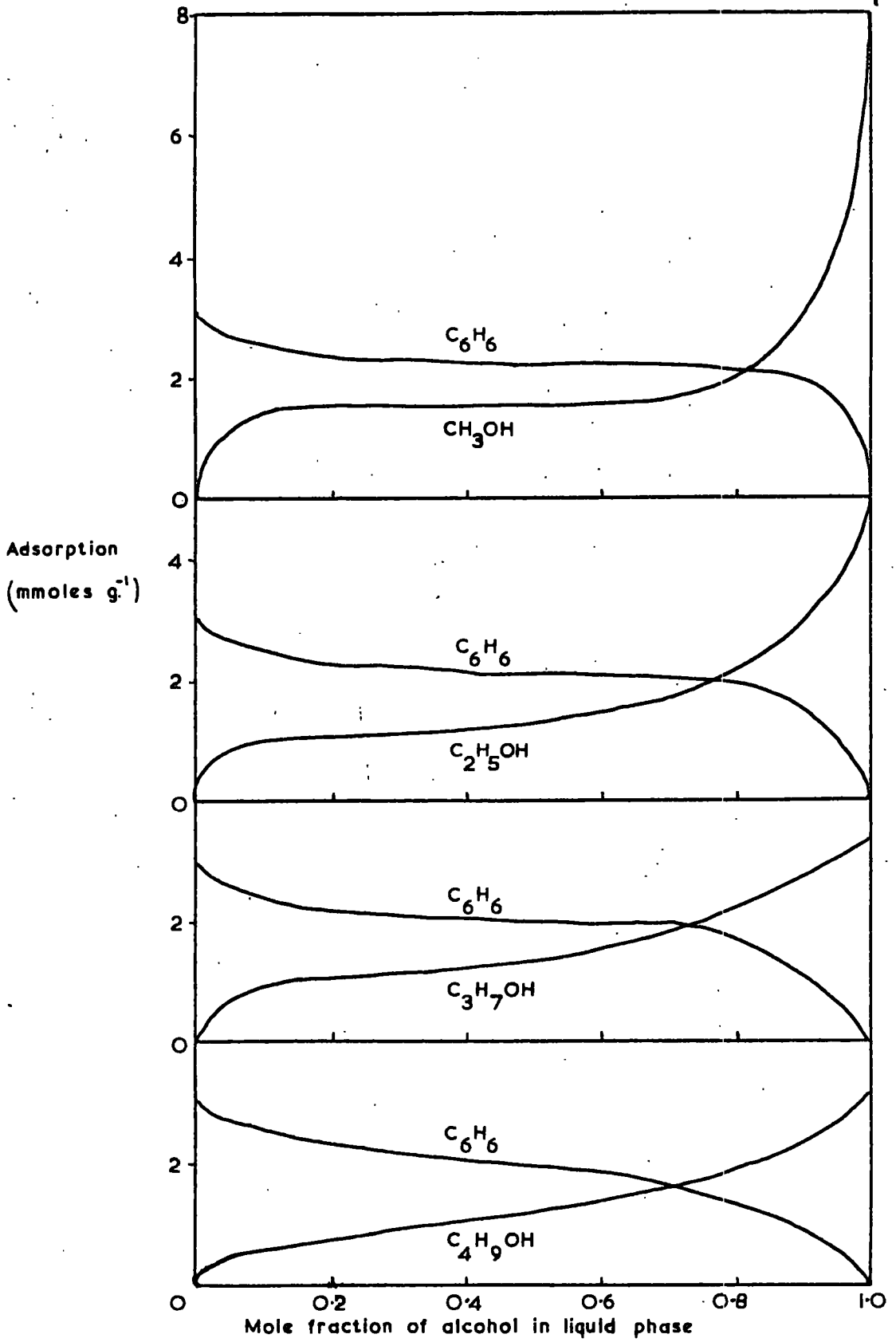

INDIVIDUAL ADSORPTION ISOTHERMS FOR ALCOHOLS FROM BENZENE ON CHARCOAL

Since the temperature range over which sorption experiments can be performed is necessarily limited (by the physical constants of the solvent) temperature coefficients are relatively inexact. Nevertheless the isotherms of Wohler and Wenzels for the sorption of a series of fatty acids from aqueous solution onto Merck animal charcoal illustrate qualitatively the temperature effect[67] (Fig. 24).

It is not proposed to describe the detailed effects of temperature and only an outline summary is presented.

For sorptions from completely miscible liquids, selectivity generally decreases with temperature rise. As the temperature falls multilayer sorption is likely to occur as the critical solution temperature is approached.

For sorptions from liquids of limited miscibility or from solutions of solids, the general effect of temperature rise is to reduce selectivity. The rise in temperature usually increases the limit of solubility, sometimes resulting in greater sorption because higher concentrations become available. In some cases, however, the lowering of solubility with rise in temperature produces opposite effects.

For some systems multilayer sorption of one component (incipient phase separation) occurs if it is sorbed above its melting point, but monolayer sorption occurs if it is sorbed below its melting point.

Although sorption experiments at different temperatures should, in principle, provide interesting thermodynamic data, particularly entropy changes of sorption, deviations from a chosen ideal reference sorption

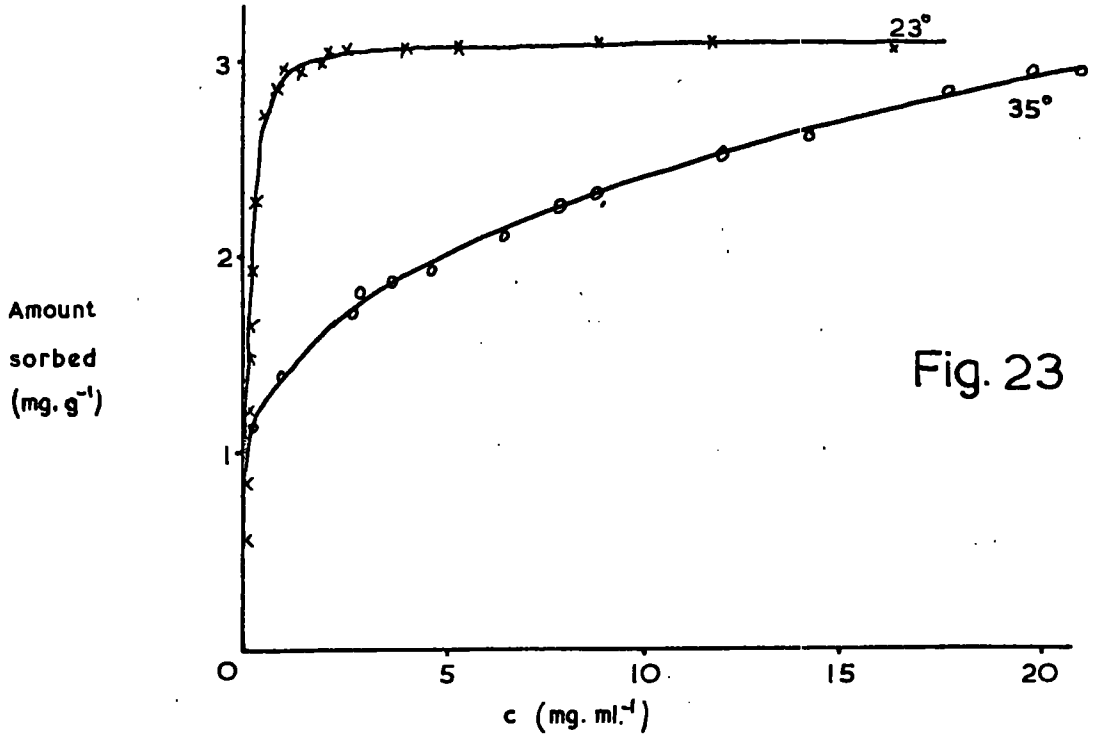

Fig. 23

EFFECT OF TEMPERATURE ON SORPTION OF STEARIC ACID FROM BENZENE BY NICKEL POWDER

Fig. 24

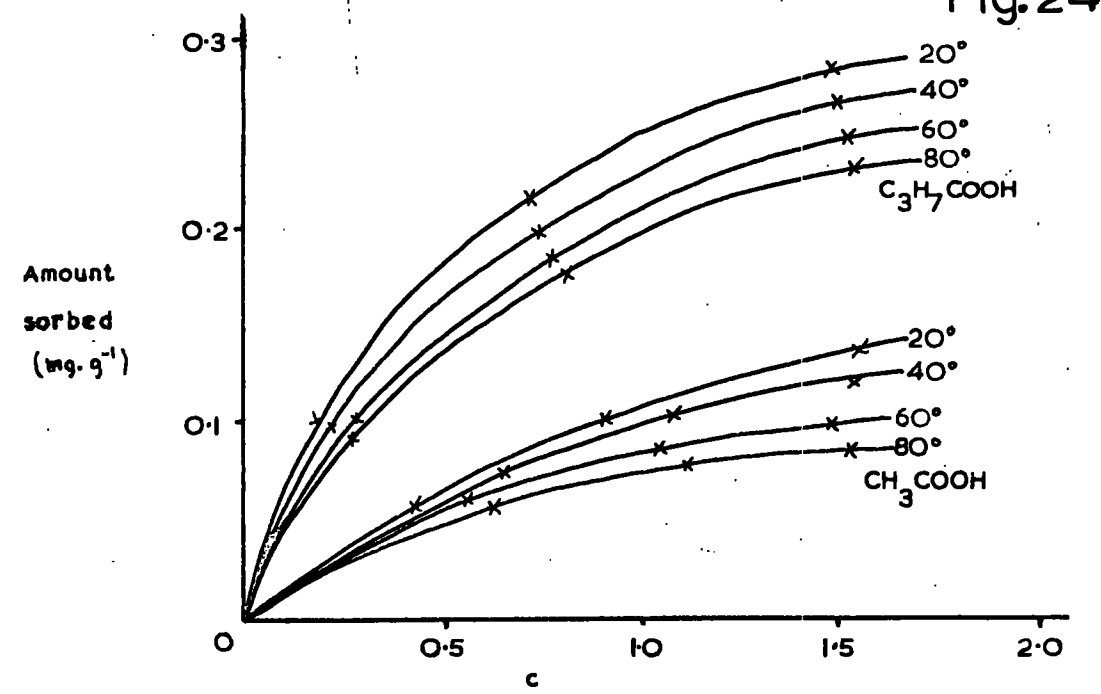

EFFECT OF TEMPERATURE ON SORPTION OF ACIDS FROM WATER BY CHARCOAL

system must often be considered. The assessment of these activity coefficients is not, in general, an easy matter and in consequence most studies of the solid-solution interface have been restricted to assessing the effects of structural changes in the sorptive, the orientation at the interface and the chemical nature of the sorbent, in terms of the forces operating both at the interface and between molecules in the bulk medium.

B - EFFECTS OF HYDROGEN-BONDING IN SOLUTION AND THEIR RELATION TO THE SORPTION PROBLEM

The Hydrogen-bond

$$A \text{——} H \cdots B$$

A hydrogen-bond exists between a functional group A - H and an atom or group of atoms, B, in the same or a different molecule when (a) there is evidence of bond formation and (b) there is evidence that this bond specifically involves the hydrogen atom already bonded to A. In fulfilment of condition (a) above all of the classical methods for detecting chemical bonds have been cited as providing evidence for hydrogen bonds: cryoscopic, vapour pressure and vapour density measurements are typical. Demonstration of condition (b) usually depends upon spectroscopic and diffraction data.

The hydrogen bond A— H···B is usually thought to lie between two closely spaced electronegative atoms, commonly identified as oxygen, nitrogen or fluorine and occasionally chlorine. In these well recognised systems hydrogen-bond formation is accompanied by some or all of the following measurable effects:-

1. Changes occur in the vibrational spectra of A - H and B.

   (a) the frequency of the A - H stretching mode decreases

   $$\begin{matrix} R \\ \diagup \end{matrix} A \leftarrow H \rightarrow \cdots B \qquad \nu_s = 3500 - 2500 \text{ cm.}^{-1},\ 3 - 4\mu$$

   (b) the band width of the A - H stretching mode increases

   (c) the intensity of the A - H stretching mode increases

(d) the frequencies of the A - H deformation modes increase

(e) there are new low frequency modes associated with stretching and bending of the hydrogen-bond itself

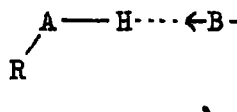

A····B stretch

ν_σ = 250 - 50 cm.$^{-1}$, 40 - 200μ

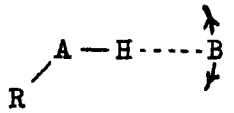

A—H····B bend

ν_β < 50 cm.$^{-1}$, > 200μ

2. The proton magnetic resonance moves towards lower field.

3. The A····B distance is short, compared to the sum of the Van de Waal's radii.

4. Electronic transitions of either the acid or the base may be shifted.

5. The molecular weight is larger than the formula weight, as shown by cryoscopy, vapour pressure and vapour density data.

6. Various properties indicate association: dielectric behaviour, solubility, heat of mixing, molar volume, viscosity etc.

Of these effects, the IR intensity (1c) and the proton magnetic resonance (2) are probably the most sensitive to hydrogen-bond formation whereas the IR frequency (1a) is probably the most easily measured and for the purposes of this thesis only values of $\Delta(\nu_s)$ will be considered.

Infra-red Spectroscopy

Phenol provides a good example of change in IR stretching frequency on hydrogen-bonding: the OH group stretching frequency in cyclohexane is

3622 $cm.^{-1}$ and 3400 $cm.^{-1}$ in a dioxan-cyclohexane solvent mixture of dioxan weight fraction 0-0131. The shift of 222 $cm.^{-1}$ is attributed to hydrogen bonding between the phenol and dioxan molecules[68] and its magnitude is regarded as a measure of the strength of the bond.[69] This interaction between phenol and dioxan is an extreme example of a solvent effect which occurs to lesser degrees in benzene, where the cloud is involved, and carbon tetrachloride in which interaction with the C - Cl dipoles is important. Systematic experimental investigation of these solvent shifts has been made by Bellamy, Hallam and Williams[70] who compared relative frequency shifts of different solutes in the same series of solvents (Fig. 25).

All hydrogenic stretching frequencies were found to yield linear B.H.W. plots having a characteristic slope, S, and no discontinuity was observed on passing from non-polar to polar solvent. In the above plot the relative frequency shift $(\nu_{vapour} - \nu_{solvent})/\nu_{vapour}$ for the pyrrole N - H frequency is plotted against the relative frequency shift for the phenol O - H frequency in ten solvents. This eliminates all those properties of the solvents which operate to a similar extent in the two cases.

Cutmore and Hallam[71] on examination of the slopes of the B.H.W. plots (S values) find that in the case of the S values of N - H bonds, a relationship with the pK_a values of the bases exist, i.e. $S = 0.375\ pK_a + 2.35$, covering primary bases of all structural types with basicities from pK_a -3 to +12. Another relationship, $S = 0.273\ pK_a + 1.35$ is found for

Fig. 25

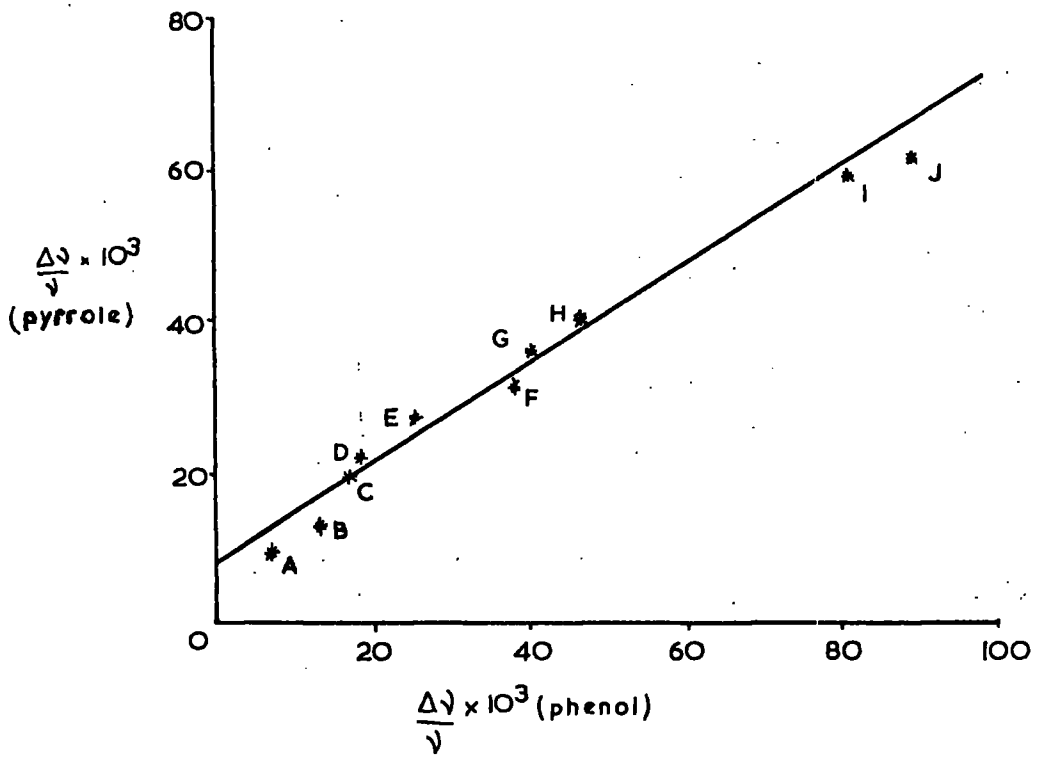

A. n-Hexane
B. Carbon tetrachloride
C. Chloroform
D. sym.Tetrachloroethane
E. Benzene
F. Methyl cyanide
G. Methyl acetate
H. Acetone
I. Diethyl ether
J. Dioxan

all secondary bases. Whereas $\Delta\nu$ values replace the acid character of the solute in a given solvent, S values are independant of solvent and reflect the absolute acidity of the solute. Pimentel and McClellan[72] also illustrate the correlation between $\Delta\nu$ and acid strength with data for ten acids of various strengths in four bases.

Other workers have demonstrated a relationship between $\Delta\nu$ and the increase in half-band width on hydrogen-bonding[73], $\Delta\nu$ and the X·····Y distance[74] in a bond of the type X - H···Y and $\Delta\nu$ and the X - H bond length.[74]

Dipole Moment

Much evidence is available[75 - 80] that in the case of those compounds capable of hydrogen bonding through the hydrogen atom of an hydroxy or amino group and an oxygen atom of the dioxan molecule, the dipole moments determined in dioxan are all greater than those in benzene. This increase is partly due, presumably, to the displacement of electrons along the O - H or N - H bond towards the oxygen or nitrogen atom on hydrogen bonding with dioxan. Smith and Walshaw[80] conclude from a study of the dipole moments of substituted anilines in benzene and dioxan, that in the hydrogen-bonded complexes with dioxan an appreciable increase in molecular polarisation and hence in dipole moment is partly the consequence of an increased mesomeric effect of the amino group. If this is so, then, in the case of substituted phenols the dipole moment increase in dioxan becomes the result of an increase in O - H bond moment occasioned by hydrogen bonding and an associated decrease in C - O bond moment effected

by increased mesomerism.

Ibbitson and Sandall[68] have attempted to relate the O - H bond moment increase when a series of p-substituted phenols are hydrogen bonded to dioxan, with the shifts in O - H stretching frequency, and find a proportionality which is illustrated in Fig. 26.

In the calculation of O - H bond moment increase, x, it was assumed that all the increase in dipole moment of the phenol in dioxan was located in the O - H bond. The values of $\Delta\nu$ are the shifts in O - H stretching frequency relative to the frequency of phenol in cyclohexane. From Fig. 26 it is clear that an increase in frequency shift parallels an increase in O - H bond moment, both variables being influenced by the nature of the P-substituent, an electron attracting substituent having a greater effect than an electron releasing substituent. Since the nature of the electrical effect of the substituent group affects both the acidity of phenols and the basicity of anilines, it proved of interest to compare the acid strengths of the phenols with the O - H bond moment increase (Fig. 27). The anticipated linear decrease of pK_a with increase in O - H bond moment was realised, as shown in Fig. 27.

The trends observed in Figs. 26 and 27 may be expected theoretically. The force constant between the oxygen and hydrogen atoms of the hydroxyl group is related to the stretching frequency of the bond, and a decrease in the latter corresponding to a decrease in force constant is indicative of a stretched bond. Also stretching of the OH bond on interaction with dioxan produces an increase in bond moment and an increasing ionising tendency.

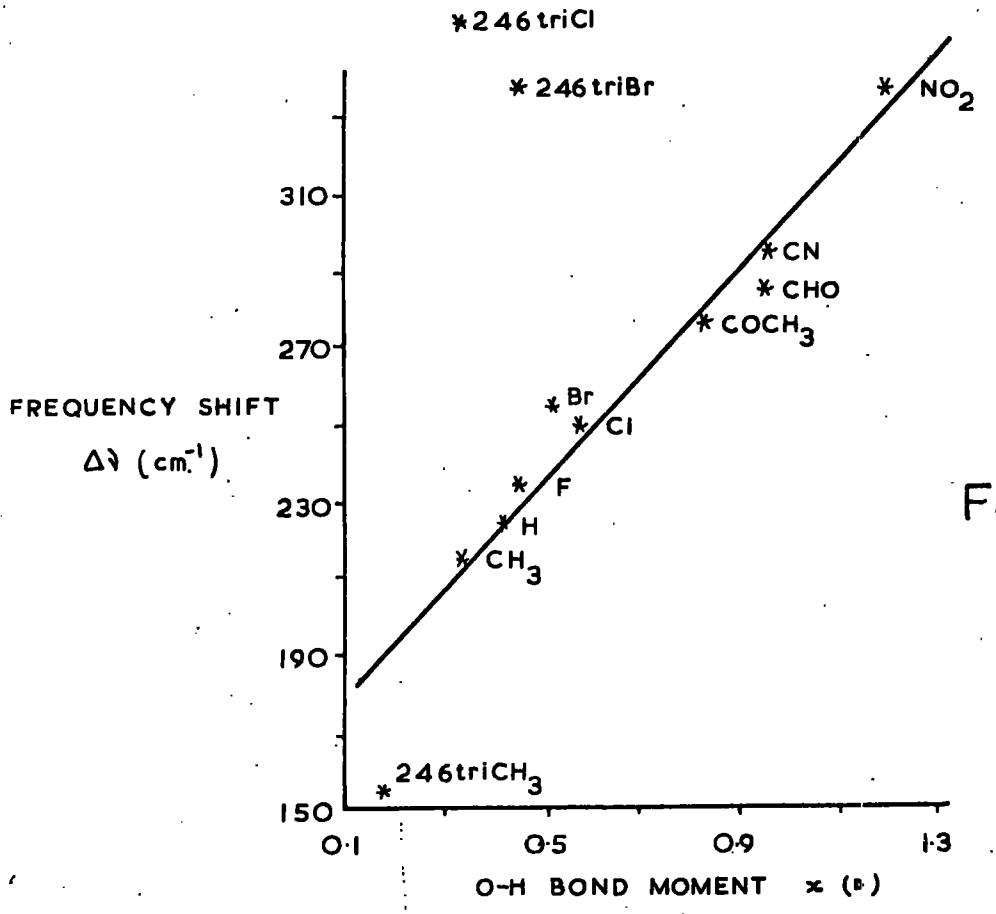
*246triCl
*246triBr
*NO2
310
*CN
*CHO
*COCH3
270
FREQUENCY SHIFT
Δν (cm.-1)
*Br
*Cl
*F
230
*H
*CH3
190
*246triCH3
150
0·1
0·5
0·9
1·3
O-H BOND MOMENT x (D)

Fig. 26

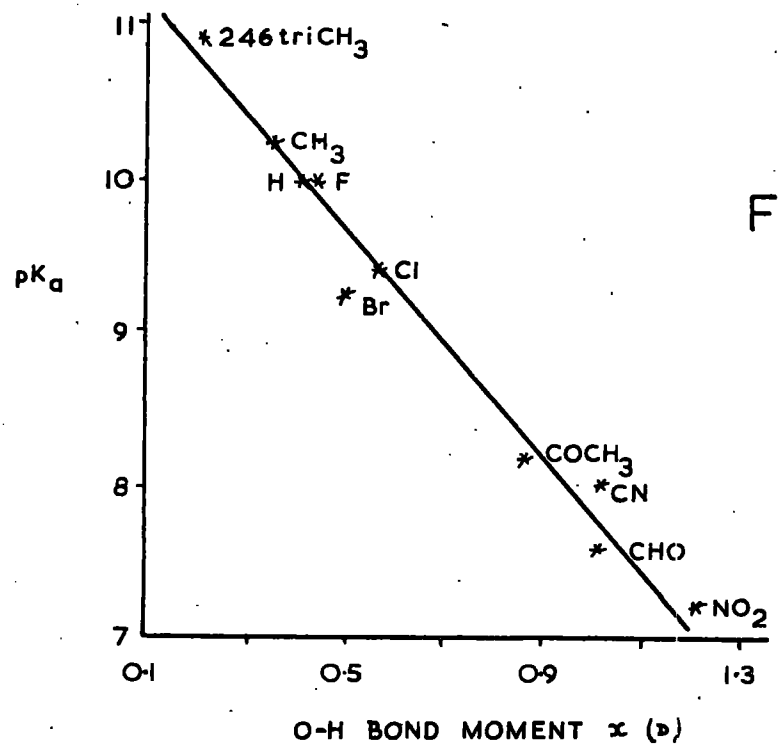
11
*246triCH3
*CH3
10
H *F
pKa
*Cl
*Br
9
*COCH3
*CN
8
*CHO
*NO2
7
0·1
0·5
0·9
1·3
O-H BOND MOMENT x (D)

Fig. 27

A similar relationship between ν_{OH} and dipole moment was observed by Richards and Walker[81] in a study of solvent effects on intermolecular hydrogen-bonding in O - halo phenols. These authors found that on plotting the dipole moments of the phenols against the O - H stretching frequencies in a series of solvents that a linear relationship existed. They concluded that the association effects between phenols and carbon tetrachloride, benzene and dioxan, differ only in magnitude but not in kind.

Sorption at the Solid-Solution Interface

In the section dealing with "Polarity of Sorptive" it was concluded that in order to observe the effect of changing polarity of a sorptive molecule upon its sorption characteristics at the solution-solid interface it was necessary that sorptive-solvent interactions in the mobile phase be a minimum. For this reason Eric, Goode and Ibbitson[12] used cyclohexane as solvent and studied the sorption of a series of p-substituted phenols onto an activated alumina. It was considered that the strong interactions at the ionic surface would more than outweigh the weaker interactions in solution, and in consequence the effect of changing polarity of the sorptive with p-substitution on sorption affinity would be observed. Since this study established the mechanism of sorption as one of hydrogen-bonding between the hydrogen atom of the hydroxy-group and receptive sites on the surface, these workers considered that the O - H bond moment would prove a more fundamental property than resultant dipole moment for comparison with sorption affinity. It was also

envisaged that since bonding to a dioxan molecule produces an increase in O - H bond moment, the same effect would be realised on sorption to alumina. As a consequence of these considerations the values of the O - H bond moments necessary to explain the observed moments of the phenols in dioxan were calculated, the assumption being made that the increase in O - H bond moment due to hydrogen-bonding to dioxan (x) is equal to the decrease in C_{ring}-O bond moment due to increased mesomerism. On comparing the values of x with the thermodynamic free energy changes on sorption evaluated from $-\Delta G^{o} = RT\ln K$ (where K is the equilibrium constant of the sorption process), an increase in $-\Delta G^{o}$ with x was observed. In general electron attracting substituents produced a greater change in both $-\Delta G^{o}$ and x than electron releasing substituents, although some anomalous behaviour was observed with 2, 4, 6-trisymmetrically substituted phenols. Perhaps steric factors and intra-molecular hydrogen-bonding are responsible for this behaviour. In confirmation of this trend, Sandall[38] finds that the equilibrium constants for the sorption process on an activated alumina from cyclohexane solution are p-isopropylphenol 1860, phenol 2800, p-nitrophenol 2770.

A property of association similar to the equilibrium constant for sorption is the association constant K_x for complex formation. Hulett, Pegg and Sutton[82] investigated the formation of complexes due to hydrogen bonding between a series of phenols and trimethylamine in cyclohexane solution. They demonstrated a linear relationship between ln K_x and $(\Delta\mu)^{\frac{1}{2}}$ being the excess dipole moment of the complex over the sum of the moments

for phenol and trimethylamine. If hydrogen-bonding to an alumina surface is considered analagous to such complex formation then discussion of sorption affinity in relation to fundamental bond moment change is condoned.

C - THE PRESENT INVESTIGATION

The present investigation is a study of the sorption characteristics at an alumina-dioxan interface of a series of p-substituted phenols in which the p-substituents consist of -H, $-CH_3$, $-C(CH_3)_3$, - Cl, - NO_2, - CN. Sorption has been carried out by the static method and the results expressed in the form of sorption isotherms. Also an evaluation from ultra-violet spectroscopy of the tendency of the process

$$\text{phenol} + \text{dioxan} \rightleftharpoons \text{complex} \qquad \text{(I)}$$

to occur in solution, has been carried out.

Evidence that hydrogen-bonding is primarily responsible for sorption of non-ionic solutes on alumina is available from a number of sources[11, 36, 83].

From the results of the investigation it was hoped

(1) to elucidate the orientation of phenol molecules sorbed on the surface of the alumina and to confirm the hydrogen-bonding mechanism of sorption,

(2) to define an index of sorption and assess the effect of structural changes in the phenol molecule, and

(3) to compare sorptive affinity as measured by this index of sorption with the association constant of process (I) and also with other previously determined OH bond parameters such as near-infrared stretching frequency and bond moment.

SORPTION STUDIES

In the tables of mean values of results in this section, for the sake of convenience, the symbols listed below have been employed.

c	concentration in moles litre^{-1}
w	weight in grams
v	volume in mls. of stock phenol solution made up to 50 ml. before sorption
c^o	concentration of the phenol before sorption in moles litre^{-1}
p^o	moles of the phenol in 50 ml. of solution before sorption
n^o	total moles in 50 ml. of solution before sorption
x_1^o	mole fraction of the phenol in solution before sorption
$c_{eq.}$	equilibrium concentration in liquid phase after sorption
p^ℓ	moles of the phenol in liquid phase after sorption
n^ℓ	total moles in liquid phase after sorption
x_1^ℓ	mole fraction of the phenol in liquid phase after sorption
$x_{1\ sat.}^\ell$	mole fraction of the phenol in a saturated dioxan solution at 35°C.
$\Delta x_1^\ell = x_1^o - x_1^\ell$	
m	number of grams of sorbent used for the sorption
D.F.	dilution factor
A	limiting sorption value calculated from the Jowett equation in the form

$$\frac{n^o . \Delta x_1^\ell}{m} = A - (A - a)^{-Bx_1^\ell}$$

SORPTION OF A SERIES OF PARA-SUBSTITUTED PHENOLS FROM DIOXAN ONTO ACTIVATED ALUMINA AT 35°C.

Treatment of Materials Prior to Sorption

(a) The Sorbent

All sorption experiments were carried out on the same batch of aluminium oxide, "Camag" M.F.C., neutral and of 100 - 200 mesh. According to the manufacturers the alumina was heated to 800°C. in preparation and is designated γ- type. It has a Brockman activity of 1 and a B.E.T. surface area, determined by low temperature nitrogen sorption, of $155 m.^2 g.^{-1}$. The alumina has also been characterised by Ibbitson and Vallance[84] and is discussed towards the end of this section. For each sorption experiment the sorbent was dried for 48 hours at 120°C.; longer heating at 120°C. produced no further loss in weight.

(b) The Solvent

Dioxan of laboratory reagent grade was allowed to stand in contact with fresh sodium wire for three days, refluxed over molten sodium for four days, then fractionally distilled from molten sodium under anhydrous conditions and used immediately.

(c) The Sorptives

Phenol, p-cresol, p-chlorophenol and p-t-butylphenol of laboratory reagent grade were first fractionally distilled three times, recrystallised from dry 40 - 60 petroleum ether and stored over phosphorus pentoxide until required for the sorption experiments. p-Nitrophenol of laboratory

reagent purity was recrystallised from water twice and dried over phosphorus pentoxide. p-Cyanophenol of similar purity grade was recrystallised twice from a mixture of benzene and 80 - 100 petroleum ether, dried over paraffin wax and stored over phosphorus pentoxide.

Physical constants of the solvent and sorptives are recorded in the table below.

TABLE 1

	Mol. Wt.	m.p.(°C.)	b.p.(°C.)
DIOXAN (dens. at 20°C., 1.0336 g. ml.$^{-1}$)	88.10	11.8	101
PHENOL	94.11	43	182
p-CRESOL	108.14	34	202
p-CHLOROPHENOL	128.56	43	220
p-TERT. BUTYLPHENOL	150.21	99	237
p-NITROPHENOL	139.11	114	-
p-CYANOPHENOL	119.12	113	-

Determination of Solubilities

For reasons outlined in the Discussion later it was necessary to know saturation solubilities of the phenols in dioxan at 35°C. and so preliminary work involved the determination of saturation mole fractions which were, as expected, very high. Crystals of the purified phenols (see P.63) and dioxan were allowed to attain equilibrium over two days in a water bath thermostatted at 35°C. A calibration graph was set up as described under "Sorption Procedure" using a dioxan solution of the

phenol and measuring absorbances at a convenient wavelength in the ultra-violet with the SP.500 Spectrophotometer. A sample of the saturated phenol solution was removed with a warm pipette, suitably diluted (by weight) and its absorbance measured, thus enabling its original concentration and mole fraction to be calculated. The results are reported below:-

TABLE 2

Compound	Saturation mole fraction in dioxan at 35°C.
Phenol	0.938
p-Cresol	0.843
p-Tert. butylphenol	0.604
p-Chlorophenol	0.929
p-Nitrophenol	0.429
p-Cyanophenol	0.440

Sorption Procedure

Sorption was found to be reversible in that it was observed that if an equilibrium between a dye in solution and alumina was established and the alumina then transferred to fresh solvent, within a few hours there was a measurable concentration of dye desorbed from the alumina and present in the solvent.

Initial investigations revealed that sorption was rapid during the first hour at all temperatures but the time for attaining equilibrium varied from about 90 hours at 45°C. to about 10 days at 25°C. For practical convenience a sorption temperature of 35°C. was employed.

The sorption experiment was carried out in 100 ml. glass stoppered flasks which had been cleaned in chromic acid cleaning mixture, rinsed with water and acetone and blown dry. A stock solution of the phenol in dioxan was prepared, chosen volumes were measured into the flasks and made up to 50 ml. by addition of the appropriate volume of dioxan. For each chosen concentration, three identical flasks were prepared.

A 2 gram (wet-weight) quantity of alumina, preheated for 48 hours at 120°C. was poured whilst still hot into each flask which was then sealed with a quick drying solution of cellulose acetate in acetone. The flasks were almost completely immersed in a water thermostat bath maintained at 35°C. and allowed to attain equilibrium over 5 days. The flasks were shaken frequently during this period.

The phenol concentrations in solution after sorption throughout these studies were measured by means of a Unicam SP.500 Photoelectric Quartz Spectrophotometer. This instrument provides a means of investigating the transmission characteristics of compounds in solution over a wavelength range of 200 - 1000 mμ. A hydrogen discharge lamp, supplied with a stabilised current of 300mA provides radiations of wavelengths 200 - 320 mμ. For the wavelength range 320 - 1000 mμ a tungsten lamp, operated from two large capacity 6 volt accumulators, is used. These accumulators also operate the photo-cells and amplifier circuit. The monochromator unit consists of a quartz prism and collimating mirror, with a slit aperature calibrated from 0.01 to 2.00 mm. Two photocells

are employed, a red sensitive cell for use above 625 mμ, and an ultra-violet sensitive cell for use below 625 mμ. The photo-cell current is fed to a two-stage amplifier and passes to an indicating meter which is adjusted to zero by a potentiometer calibrated in both optical density (absorbance) and percentage transmission scales.

After 5 days a series of phenol solutions of graded concentration, chosen to cover the expected range of equilibrium concentrations, was prepared from the original stock phenol solution stored under similar conditions to the sorption solutions. Absorbances were measured in the ultra-violet at an arbitrary wavelength (selected to give accurately readable values) and in a Suprasil cell of suitable thickness so enabling a calibration graph to be constructed. The seal on each sorption flask whilst still in the thermostat was carefully broken, a portion of the clear supernatant liquid transferred to the silica cell and several readings of absorbance recorded. Where necessary dilution of the sorption solutions was carried out in order to obtain a sufficiently accurate absorbance measurement.

The mean absorbance reading for each sorption solution was applied to the calibration graph and thus the equilibrium concentration of phenol in the liquid phase determined and the amount of phenol sorbed calculated.

Isotherms were drawn by plotting the moles of phenol sorbed $\frac{(n^{o}\Delta x_1^{l})}{m}$ against the relative mole fraction $(x_1^{l}/x_{1\ \text{sat.}}^{l})$. The curves appeared to be approaching an asymptotic value of sorption up-take probably corresponding

to monolayer coverage. To avoid unwarranted assumptions about the ideality of the system the Jowett empirical equation[2] was used to estimate the value of the asymptote.

$$\frac{n^{o}\Delta x_1^{\ell}}{m} = A - (A - a)\, e^{-B\, x_1^{\ell}/x_1^{\ell}\ \text{sat.}}$$

where A is the asymptotic value (a constant) and a and B are constants.

The limiting sorption values (A) were calculated for each sorptive from the above equation.

Experimental Results

1. PHENOL

(a) The Calibration Graph

A stock solution was prepared by dissolving 0.2135 g. of phenol in 50 ml. of dioxan solution and taking 1 ml. of the latter up to 100 ml. of molarity 4.537×10^{-4}. The absorbances of a series of solutions of graded concentration prepared from the stock solution were measured at 274 mμ in a 1 cm. Suprasil cell and a graph of concentration against absorbance was drawn. This was found to be a straight line and its equation was calculated by the method of least squares, so enabling equilibrium concentrations to be calculated from absorbance readings.

TABLE 3

ml. of stock soln.	ml. of dioxan	$c \times 10^4$	d
1	9	0.404	0.104
2	8	0.908	0.180
4	6	1.815	0.359
6	4	2.722	0.525
8	2	3.630	0.708
10	0	4.537	0.864

Equation to the line : $d = 1{,}870\ c + 0.020$

(b) The Sorption Experiment

A stock solution was prepared by dissolving 4.0466 g. of phenol in dioxan at 20°C. to give 500 ml. of solution, chosen volumes of which were then diluted to 50 ml. with dioxan to give a series of solutions of graded concentration. Each solution was prepared in triplicate, 2 g. portions of dried alumina were added and the sorption experiment carried out as previously described. After sorption, the equilibrium concentrations were calculated from absorbances, measured in the near ultra-violet, of diluted solutions.

TABLE 4

v	$c^o \times 10^2$	$p^o \times 10^3$	n^o	$x_1^o \times 10^3$
10	1.7199	0.85995	0.58744	1.4639
16	2.7518	1.37590	0.58796	2.3401
22	3.7837	1.89185	0.58847	3.2149
27	4.6437	2.32185	0.58890	3.9427
32	5.5036	2.75180	0.58933	4.6694
38	6.5355	3.26775	0.58985	5.5400

d	$c \times 10^4$	D.F.	$C_{eq.} \times 10^2$	$p^l \times 10^3$
0.580	2.99511	40	1.1981	0.59904
0.423	2.15402	100	2.1540	1.07702
0.460	2.35470	133	3.1388	1.56941
0.392	1.98812	200	3.9762	1.98812
0.471	2.41535	200	4.8307	2.41535
0.568	2.93268	200	5.8654	2.93268

n^{ℓ}	$x_1^{\ell} \times 10^3$	$(x_1^{\ell}/x_{1sat.}^{\ell}) \times 10^3$	$(n^{\circ}\Delta x_1^{\ell}/m) \times 10^4$	$\frac{x_1^{\ell}}{x_{1sat.}^{\ell}} \sqrt{\frac{n^{\circ}\Delta x_1^{\ell}}{m}}$
0.58718	1.0202	1.0875	1.303	8.346
0.58766	1.8327	1.9536	1.492	13.094
0.58815	2.6684	2.8445	1.608	17.690
0.58857	3.3779	3.6008	1.663	21.652
0.58900	4.1007	4.3713	1.676	26.082
0.58951	4.9748	5.3031	1.667	31.529

Limiting sorption value, $A = 1.682 \times 10^{-4}$ moles per gram of alumina.

PHENOL

FIG. 28

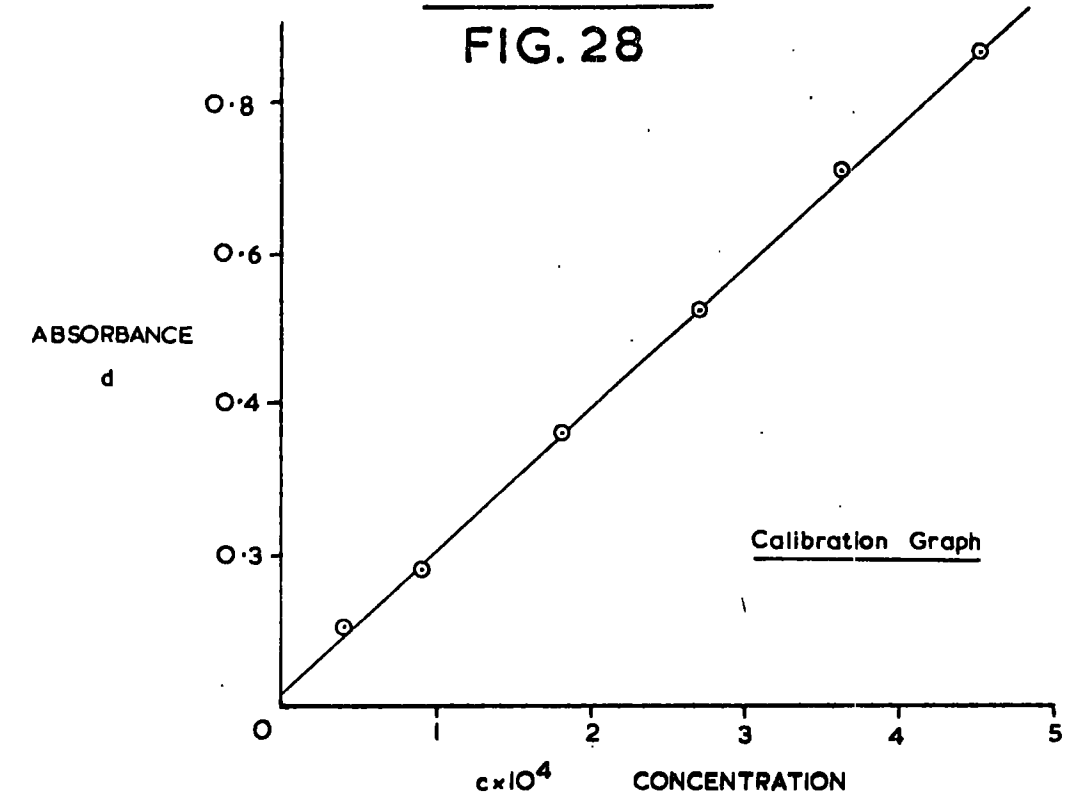

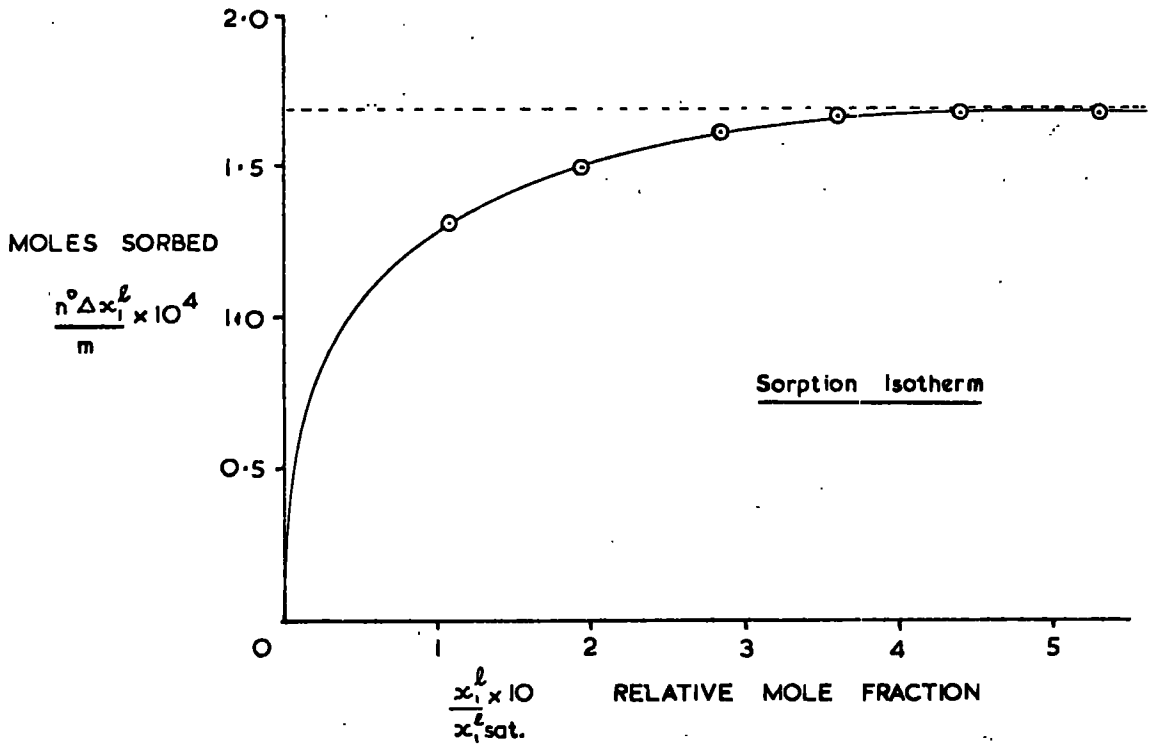

2. p-CRESOL

(a) The Calibration Graph

A stock solution was prepared by dissolving 0.3401 g. of p-cresol in 50.9050 g. of dioxan giving a mole fraction of p-cresol of 5.16152×10^{-3}. The absorbances of a series of solutions of graded concentration prepared from the stock solution were measured at 297.5 mμ in a 2 mm. Suprasil cell and a graph of mole fraction against absorbance was drawn from which equilibrium mole fractions were read.

TABLE 5

wt. of soln.	wt. of dioxan (g.)	$x_1^l \times 10^3$	d
1.2027	9.3556	0.6159	0.078
2.9717	7.6076	1.5191	0.183
5.0736	5.0892	2.7007	0.314
7.3503	2.7674	3.9311	0.442
8.4806	1.8553	4.4404	0.497

(b) The Sorption Experiment

A stock solution was prepared by dissolving 3.4005 g. of p-cresol in 509.05 g. of dioxan so that 1 g. of solution contained 0.61363×10^{-4} moles of the phenol and 1.12749×10^{-2} moles of dioxan. Chosen volumes of the stock solution were then diluted to 50 ml. with dioxan to give a series of solutions of graded concentration. Each solution was prepared in triplicate, 2g. aliquots of dried alumina were added and the sorption experiment carried out as previously described. After sorption, the equilibrium mole fractions were calculated from absorbances measured in the near ultra violet.

TABLE 6

wt. of soln.	$p^o \times 10^3$	moles of dioxan	n^o
8.0342	0.4930	0.484471 + 0.090585	0.575552
17.2946	1.0612	0.381226 + 0.194995	0.577282
25.5397	1.5672	0.288499 + 0.287958	0.578024
33.8974	2.0800	0.194072 + 0.382190	0.578342
42.7469	2.6231	0.093129 + 0.481967	0.577719
50.9144	3.1243	- 0.574055	0.577179

$x_1^o \times 10^3$	d	$x_1^\ell \times 10^3$	$(x_1^\ell / x_{1\ sat.}^\ell) \times 10^3$
0.8566	0.065	0.507	0.601
1.8384	0.167	1.378	1.635
2.7113	0.261	2.215	2.628
3.5966	0.350	3.037	3.603
4.5404	0.452	4.010	4.757
5.4131	0.569	4.884	5.793

$(n^{o}\Delta x_1^{\ell}/m) \times 10^4$	$\frac{x_1^{\ell}}{x_{1\ sat.}^{\ell}} \Big/ \frac{n^{o}\Delta x_1^{\ell}}{m}$
1.007	5.968
1.328	12.312
1.433	18.339
1.493	24.133
1.531	31.071
1.557	37.206

Limiting sorption value, A = 1.567×10^{-4} moles per gram of alumina.

p-CRESOL

FIG. 29

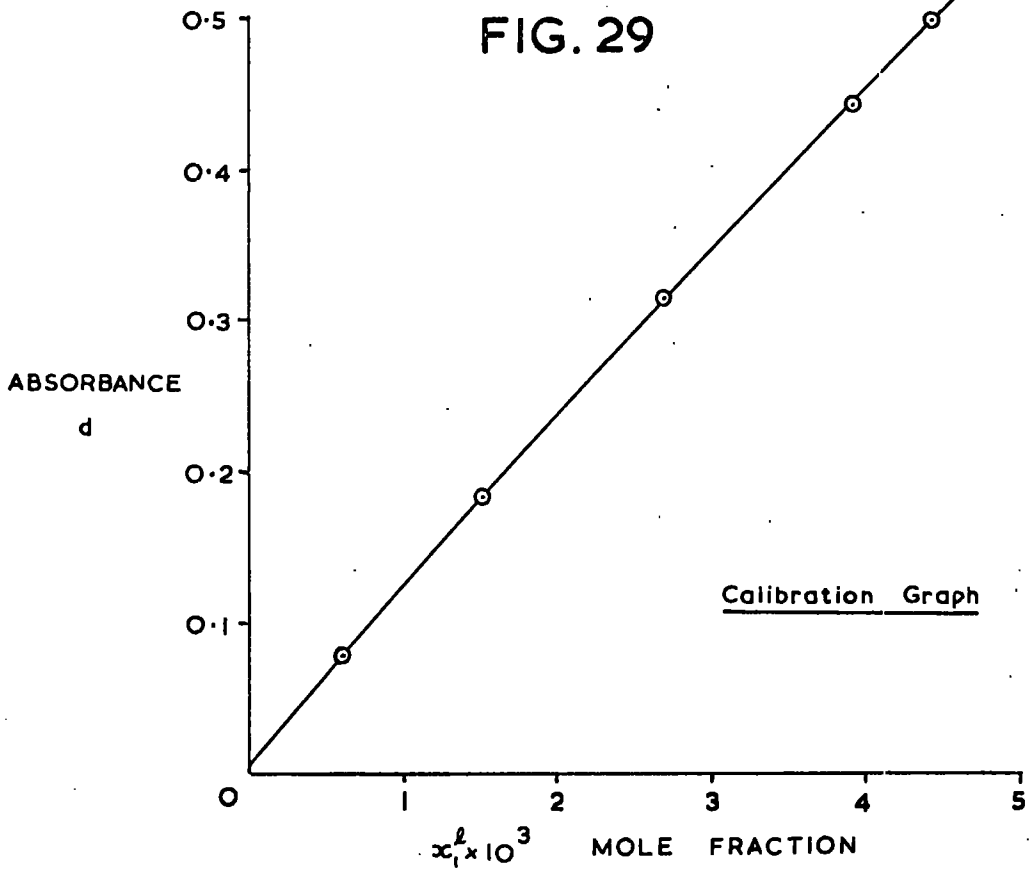

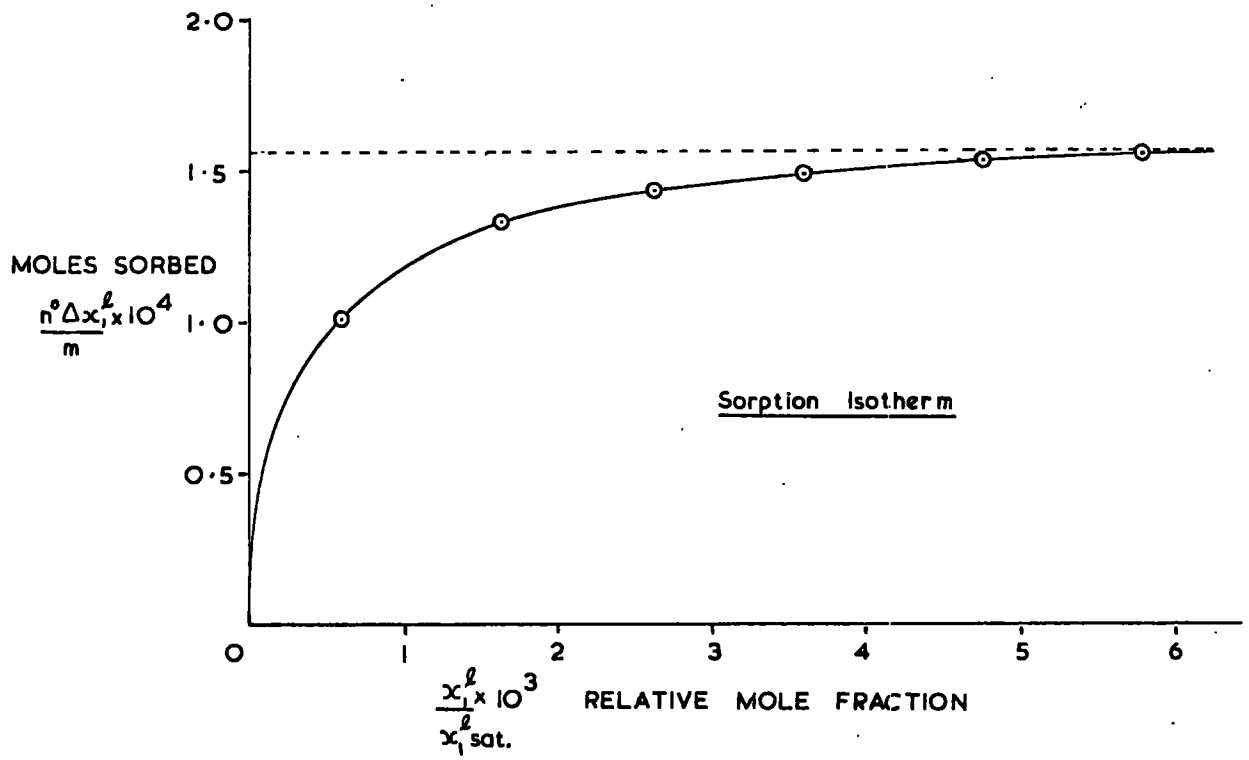

3. p-TERT. BUTYLPHENOL

(a) The Calibration Graph

A stock solution was prepared by dissolving 0.5090 g. of p-t-butylphenol in 50 ml. of dioxan solution of molarity 6.7767×10^{-2}. The absorbances of a series of solutions of graded concentration prepared from the stock solution were measured at 292 mμ in a 1 mm. Suprasil cell and a graph of concentration against absorbance was drawn. This was found to be a straight line and its equation was calculated by the method of least squares, so enabling equilibrium concentrations to be calculated from absorbance readings.

TABLE 7

ml. of stock soln.	ml. of dioxan	c x 10^2	d
0.5	4.5	0.678	0.118
1.0	4.0	1.355	0.196
1.5	3.5	2.033	0.280
2.0	3.0	2.711	0.355
2.5	2.5	3.389	0.433
3.0	2.0	4.066	0.517
3.5	1.5	4.744	0.584
4.0	1.0	5.422	0.657
5.0	0	6.777	0.804

(b) The Sorption Experiment

500 ml. of a stock solution were prepared by dissolving 5.2878 g. of p-t-butylphenol in dioxan at 20°C. Chosen volumes of this solution were then diluted to 50 ml. with dioxan to give a series of solutions of graded concentration. Each solution was prepared in triplicate, 2g. aliquots of dried alumina were added and the sorption experiment carried out as previously described. After sorption, the equilibrium concentrations were calculated from absorbances measured in the near ultra-violet.

TABLE 8

v	$c^o \times 10^2$	$p^o \times 10^3$	n^o	$x_1^o \times 10^3$
4	0.5632	0.2816	0.58686	0.4798
12	1.6896	0.8448	0.58742	1.4382
20	2.8160	1.4080	0.58799	2.3946
29	4.0833	2.0417	0.58862	3.4686
38	5.3505	2.6753	0.58926	4.5401

d	$c_{eq.} \times 10^2$	$p^1 \times 10^3$	n^1
0.072	0.208	0.1040	0.58668
0.183	1.195	0.5975	0.58718
0.305	2.279	1.1395	0.58772
0.444	3.521	1.7605	0.58834
0.585	4.777	2.3885	0.58897

$x_1^{\ell} \times 10^3$	$(x_1^{\ell}/x_{1sat.}^{\ell}) \times 10^3$	$(n^{\circ}\Delta x_1^{\ell}/m) \times 10^4$	$\frac{x_1^{\ell}}{x_{1sat.}^{\ell}} \Big/ \frac{n^{\circ}\Delta x_1^{\ell}}{m}$
0.1773	0.2934	0.8876	3.306
1.0176	1.6842	1.2353	13.634
1.9388	3.2089	1.3400	23.947
2.9923	4.9525	1.4018	35.330
4.0554	6.7120	1.4281	47.000

Limiting sorption value, A = 1.452 moles per gram of alumina.

p-TERT. BUTYLPHENOL

FIG. 30

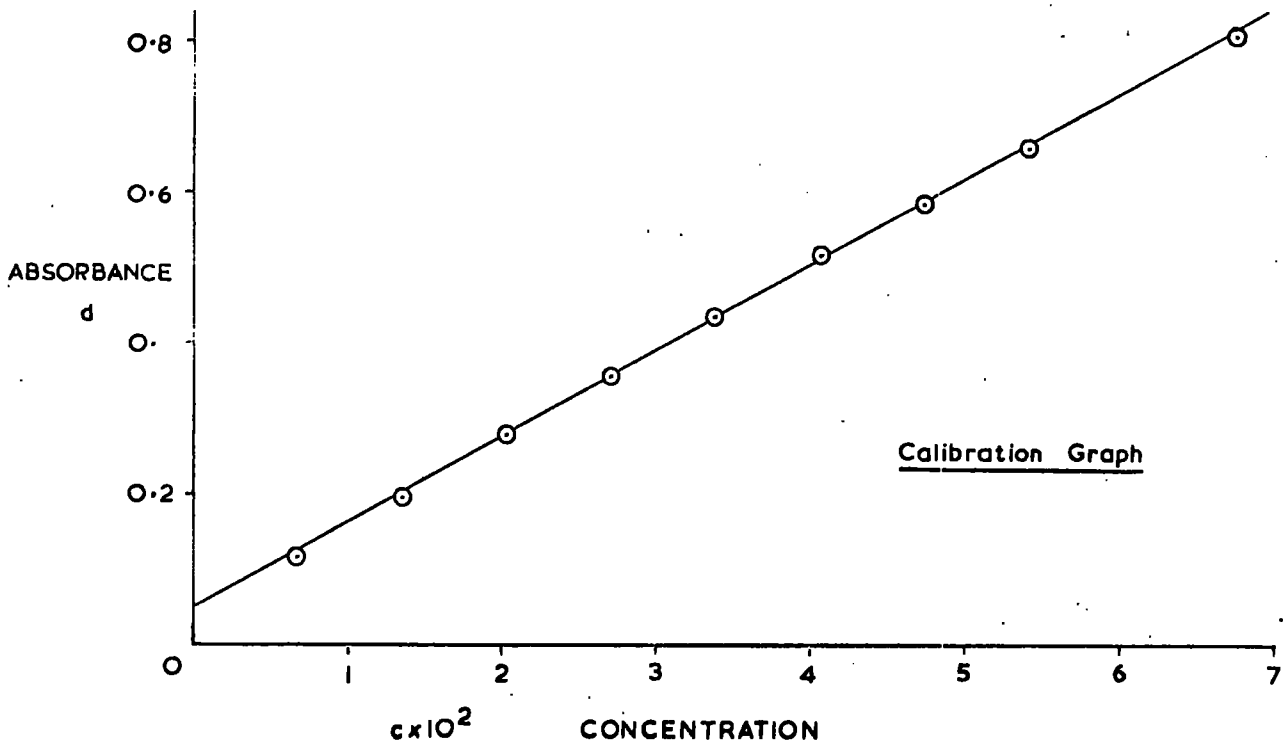

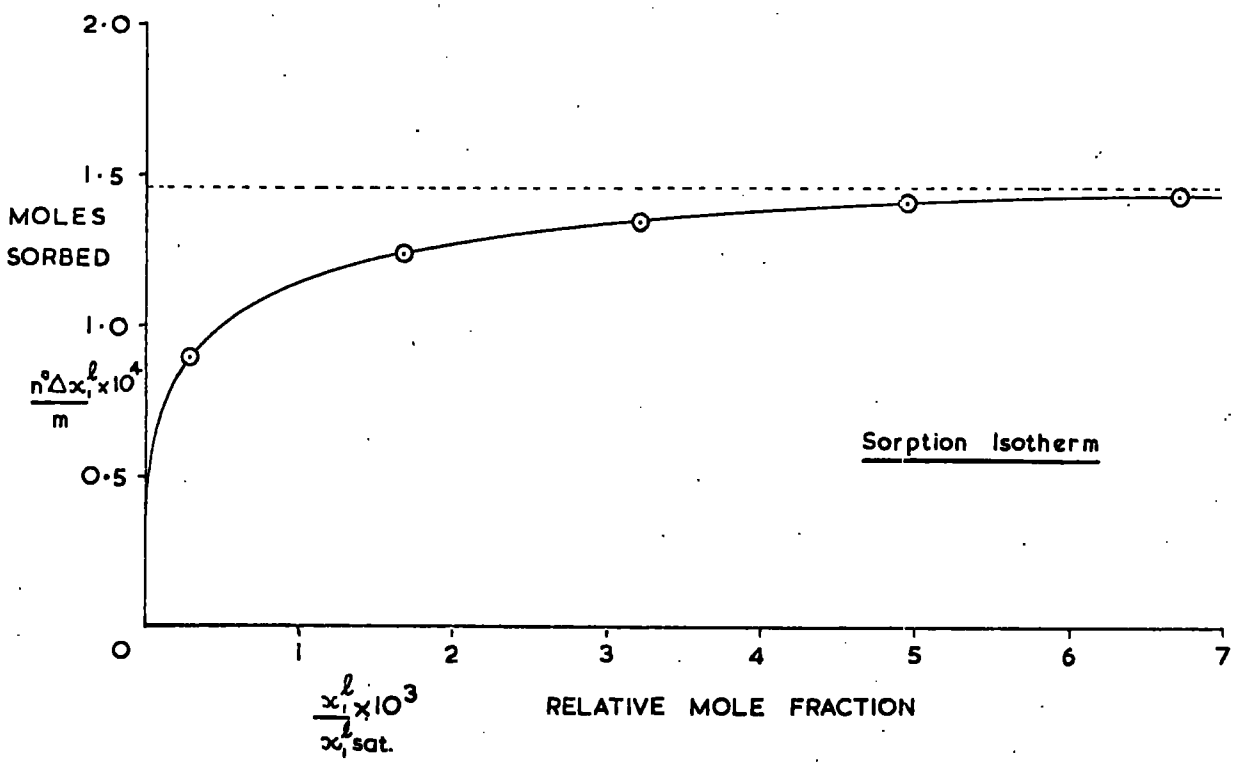

4. p-CHLOROPHENOL

(a) The Calibration Graph

A stock solution was prepared by dissolving 0.3173 g. of p-chlorophenol in 50 ml. of dioxan solution and diluting 1 ml. of the latter to 100 ml. with dioxan giving a molarity of 4.9356×10^{-4}. The absorbances of a series of solutions of graded concentration prepared from the stock solution were measured at 283 mμ in a 1 cm. Suprasil cell and a graph of concentration against absorbance was drawn. This was found to be a straight line and its equation was calculated by the method of least squares, so enabling equilibrium concentrations to be calculated from absorbance readings.

TABLE 9

ml. of stock soln.	ml. of dioxan	$c \times 10^4$	d
2	8	0.9871	0.190
3	7	1.4807	0.283
4	6	1.9742	0.375
5	5	2.4678	0.467
7	3	3.4549	0.655
10	0	4.9356	0.935

Equation to the line : $d = 1{,}887\ c + 0.003$

(b) The Sorption Experiment

500 ml. of a stock solution were prepared by dissolving 3.1726 g. of p-chlorophenol in dioxan at 20°C. Chosen volumes of this solution were then diluted to 50 ml. with dioxan to give a series of solutions of graded concentration. Each solution was prepared in triplicate, 2 g. portions of dried alumina were added and the sorption experiment carried out as previously described. After sorption, the equilibrium concentrations were calculated from absorbances measured in the near ultra violet.

TABLE 10

v	$c^o \times 10^2$	$p^o \times 10^3$	n^o	$x_1^o \times 10^3$
5.0	0.4936	0.2468	0.58683	0.4206
10.0	0.9871	0.4936	0.58707	0.8408
12.4	1.2253	0.6127	0.58719	1.0434
30.0	2.9614	1.4807	0.58806	2.5179
50.0	4.9356	2.4678	0.58905	4.1895

d	$c \times 10^4$	D.F.	$C_{eq.} \times 10^2$	$p^1 \times 10^3$
0.315	1.6552	10	0.1655	0.0083
0.395	2.0721	25	0.5180	0.2590
0.269	1.4136	50	0.7068	0.3534
0.331	1.7378	133.3	2.3170	1.1585
0.407	2.1392	200	4.2785	2.1393

n^{ℓ}	$x_1^{\ell} \times 10^3$	$(x_1^{\ell}/x_{1sat.}^{\ell}) \times 10^3$	$(n^{o}\Delta x_1^{\ell}/m) \times 10^4$	$\frac{x_1^{\ell}}{x_{1sat.}^{\ell}} \Big/ \frac{n^{o}\Delta x_1^{\ell}}{m}$
0.58659	0.1415	0.1522	0.8189	1.859
0.58684	0.4413	0.4748	1.1727	4.049
0.58693	0.6021	0.6478	1.2957	5.000
0.58774	1.9711	2.1208	1.6079	13.190
0.58872	3.6338	3.9098	1.6368	23.887

Limiting sorption value, $A = 1.637 \times 10^{-4}$ moles per gram of alumina.

p-CHLOROPHENOL

FIG.31

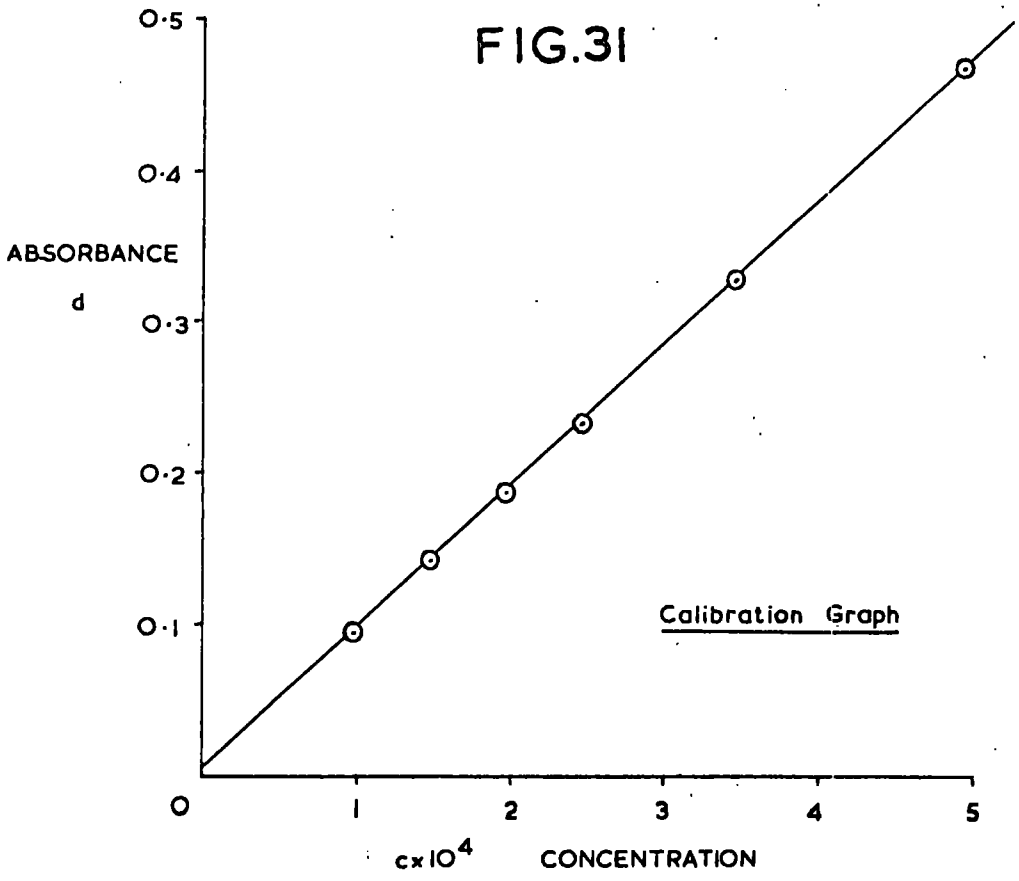

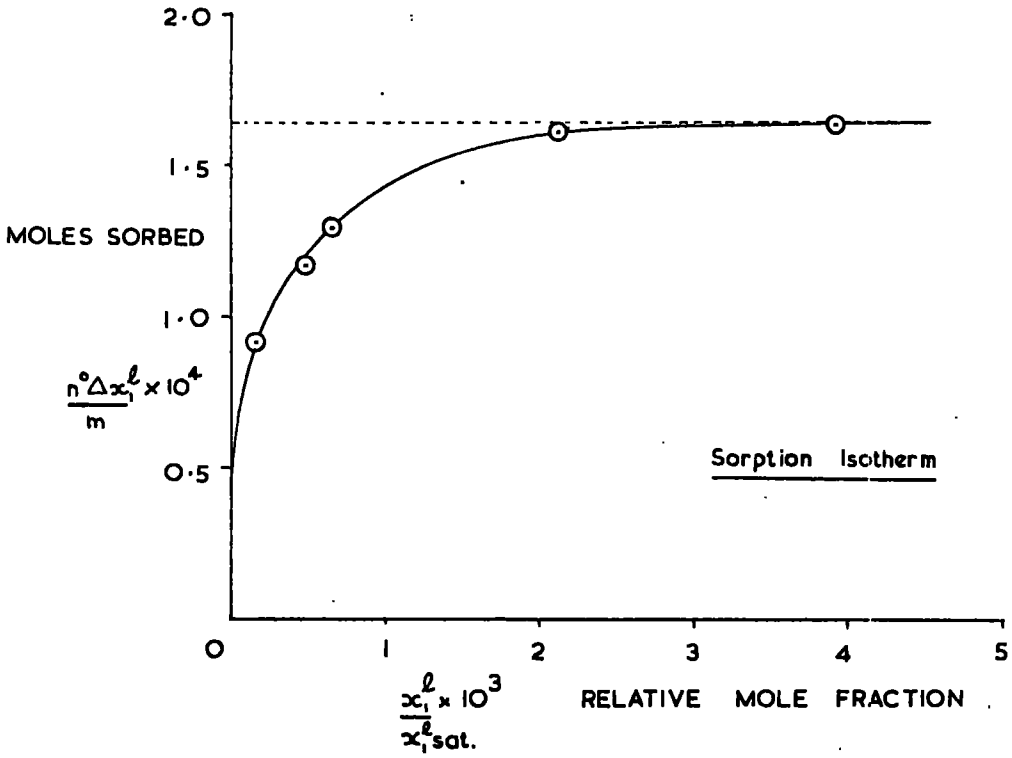

5. p-NITROPHENOL

(a) The Calibration Graph

A stock solution was prepared by dissolving 0.2019 g. of p-nitrophenol in 100 ml. of dioxan solution of molarity 1.4514×10^{-2}. The absorbances of a series of solutions of graded concentration prepared from the stock solution were measured at 360 mμ in a 1 mm. Suprasil cell and a graph of concentration against absorbance was drawn. This was found to be a straight line and its equation was calculated by the method of least squares, so enabling equilibrium concentrations to be calculated from absorbance readings.

TABLE 11

ml. of stock soln.	ml. of dioxan	$c \times 10^2$	d
2	8	0.2903	0.158
4	6	0.5806	0.319
6	4	0.8708	0.473
8	2	1.1611	0.630
10	0	1.4514	0.796

Equation to the line : $d = 54.677\ c - 0.001$

(b) The Sorption Experiment

500 ml. of stock solution were prepared by dissolving 4.8596 g. of p-nitrophenol in dioxan at 20°C. Chosen volumes of this solution were then diluted to 50 ml. with dioxan to give a series of solutions of graded concentration. Each solution was prepared in triplicate, 2 g. portions of dried alumina were added and the sorption experiment carried out as previously described. After sorption, the equilibrium concentrations were calculated from absorbances (measured in the near ultra violet) of diluted solution.

TABLE 12

v	$c^o \times 10^2$	$p^o \times 10^3$	n^o	$x_1^o \times 10^3$
6	0.8384	0.41920	0.58700	0.7141
13	1.8165	0.90825	0.58749	1.5460
21	2.9344	1.46720	0.58805	2.4950
29	4.0523	2.02615	0.58861	3.4423
38	5.3099	2.65495	0.58923	4.5058
46	6.4278	3.21390	0.58979	5.4492

d	$c \times 10^2$	D.F.	$C_{eq.} \times 10^2$	$p^1 \times 10^3$
0.181	0.3328	1	0.3328	0.16640
0.632	1.1577	1	1.1577	0.57885
1.195	2.1873	1	2.1873	1.09365
0.591	1.0827	3	3.2481	1.62405
0.488	0.8949	5	4.4745	2.23725
0.610	1.1170	5	5.5848	2.79240

n^{ℓ}	$x_1^{\ell} \times 10^3$	$(x_1^{\ell}/x_{1sat.}^{\ell}) \times 10^3$	$(n^{o}\Delta x_1^{\ell}/m) \times 10^4$	$\frac{x_1^{\ell}}{x_{1sat.}^{\ell}} \Big/ \frac{n^{o}\Delta x_1^{\ell}}{m}$
0.58675	0.2836	0.6614	1.2635	5.235
0.58716	0.9858	2.2990	1.6466	13.962
0.58767	1.8610	4.3400	1.8641	23.282
0.58820	2.7611	6.4391	2.0048	32.118
0.58882	3.7995	8.8608	2.0809	42.582
0.58937	4.7379	11.0492	2.0976	52.675

Limiting sorption value, $A = 2.118 \times 10^{-4}$ moles per gram of alumina.

p-NITROPHENOL

FIG.32

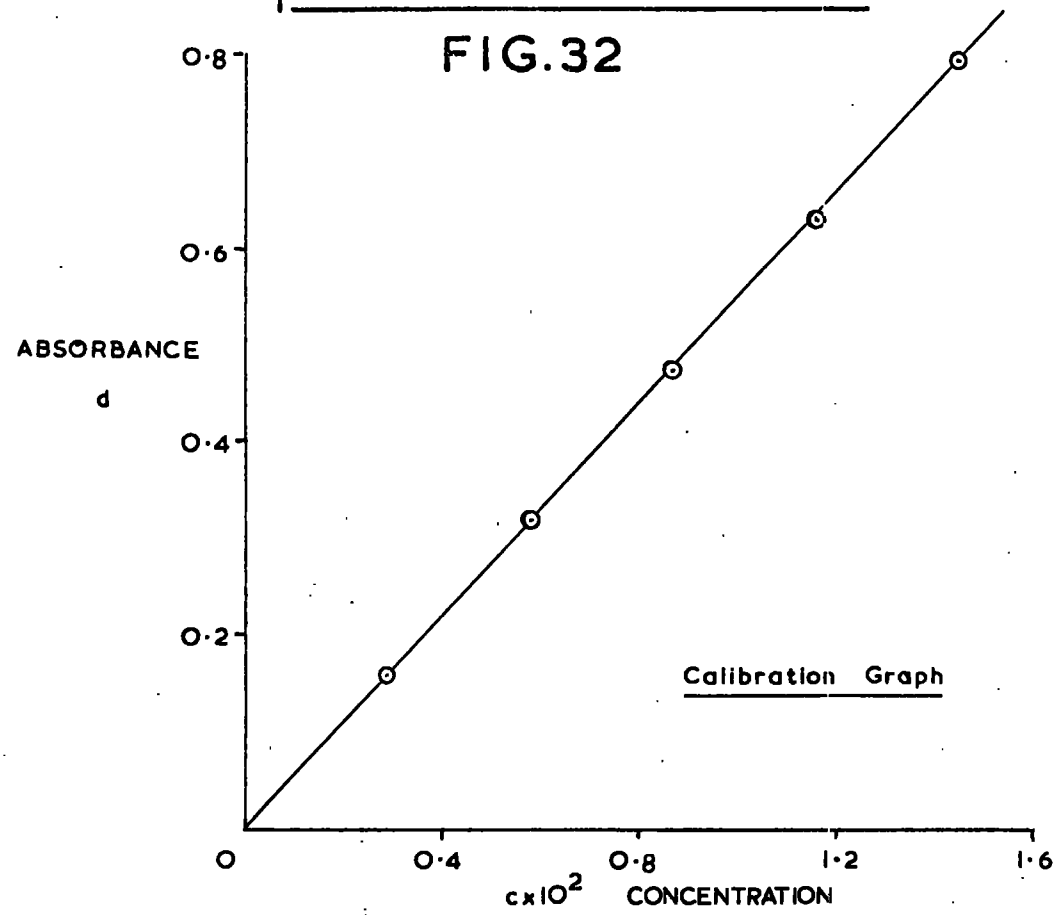

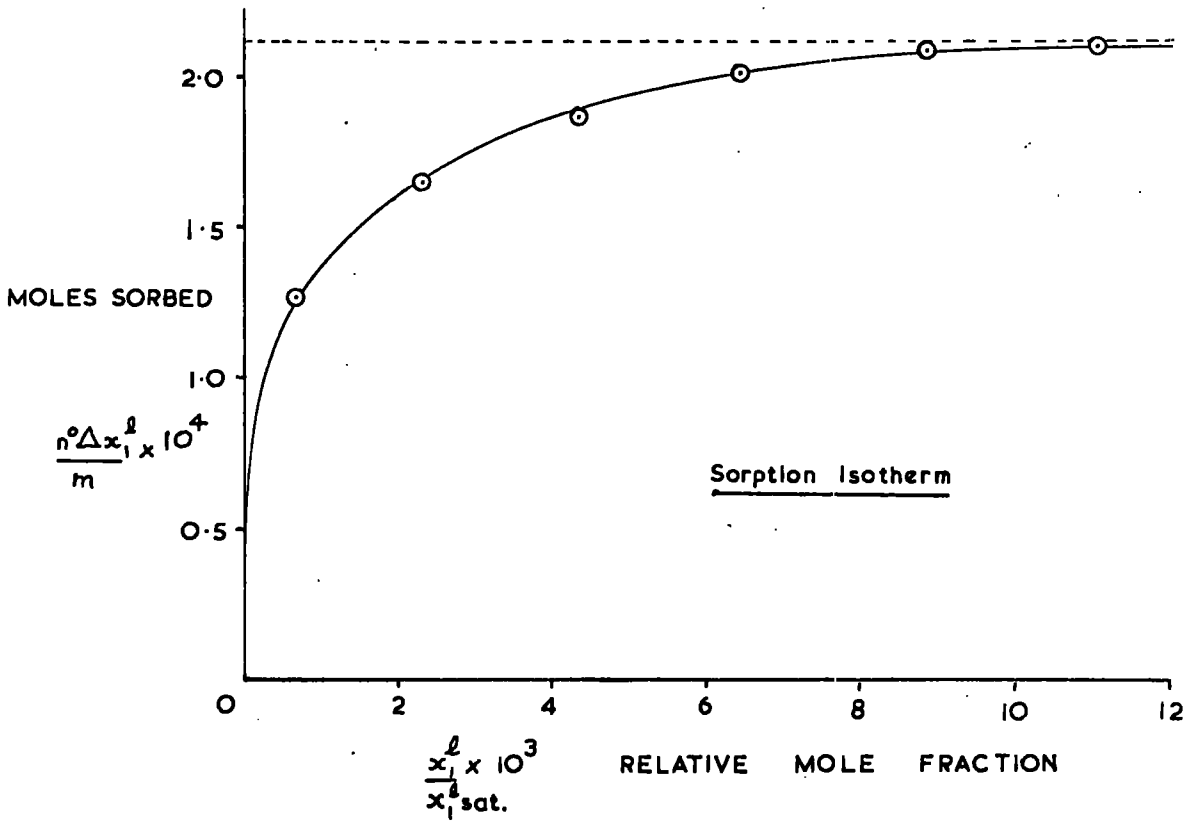

6. p-CYANOPHENOL

(a) The Calibration Graph

A stock solution was prepared by dissolving 0.4060 g. of p-cyanophenol in 51.1059 g. of dioxan giving a mole fraction of p-cyanophenol of 5.84142×10^{-3}. The absorbances of a series of solutions of graded concentration prepared from the stock solution were measured at 292 mμ in a 2 mm. Suprasil cell and a graph of mole fraction against absorbance was drawn. This was found to be a straight line and its equation was calculated by the method of least squares, so enabling equilibrium mole fractions to be calculated from absorbance readings.

TABLE 13

ml. of stock soln.	ml. of dioxan	$x_1 \times 10^3$	d
0.5	4.5	0.5841	0.077
1.0	4.0	1.1683	0.125
2.0	3.0	2.3366	0.243
3.0	2.0	3.5048	0.347
4.0	1.0	4.6731	0.458
5.0	0	5.8414	0.574

Equation to the line : $d = 94.582\ c + 0.019$

(b) The Sorption Experiment

A stock solution was prepared by dissolving 4.1245 g. of p-cyanophenol in 255.3 g. of dioxan so that 1 gram of solution contained 0.01590 g. of the phenol (1.3348×10^{-4} moles) and 0.98410 g. of dioxan (0.01117 moles). Chosen volumes of the stock solution were then diluted to 50 ml. with dioxan to give a series of solutions of graded concentration. Each solution was prepared in triplicate, 2 g. portions of dried alumina were added and the sorption experiment carried out as previously described. After sorption, the equilibrium mole fractions were calculated from absorbances measured in the near ultra violet.

TABLE 14

$W_{soln.}$	$p^o \times 10^3$	$n_{diox.}$	n^o
2.3450	0.3130	0.549566 + 0.026193	0.576072
2.7922	0.3727	0.547238 + 0.031188	0.578799
5.0733	0.6772	0.520948 + 0.056668	0.578293
10.2500	1.3682	0.460388 + 0.114490	0.576246
15.1423	2.0212	0.402521 + 0.169136	0.573678
20.5961	2.7492	0.341318 + 0.230054	0.574121
25.6823	3.4281	0.283114 + 0.286866	0.573408

$x_1^o \times 10^3$	d	$x_1^l \times 10^3$
0.5433	0.033	0.1480
0.6439	0.038	0.2009
1.1710	0.073	0.5709
2.3743	0.174	1.6388
3.5232	0.281	2.7701
4.7885	0.399	4.0177
5.9785	0.511	5.2018

$(x_1^l/x_1^l{}_{sat.}) \times 10^3$	$(n^o \Delta x_1^l/m) \times 10^4$	$\frac{x_1^l}{x_1^l{}_{sat.}} \Big/ \frac{n^o \Delta x_1^l}{m}$
0.3363	1.1386	2.954
0.4565	1.2820	3.561
1.2972	1.7352	7.476
3.7237	2.1191	17.572
6.2943	2.1602	29.138
9.1291	2.2127	41.258
11.8196	2.2268	53.079

Limiting sorption value, $A = 2.247 \times 10^{-4}$ moles per gram of alumina.

p-CYANOPHENOL

FIG. 33

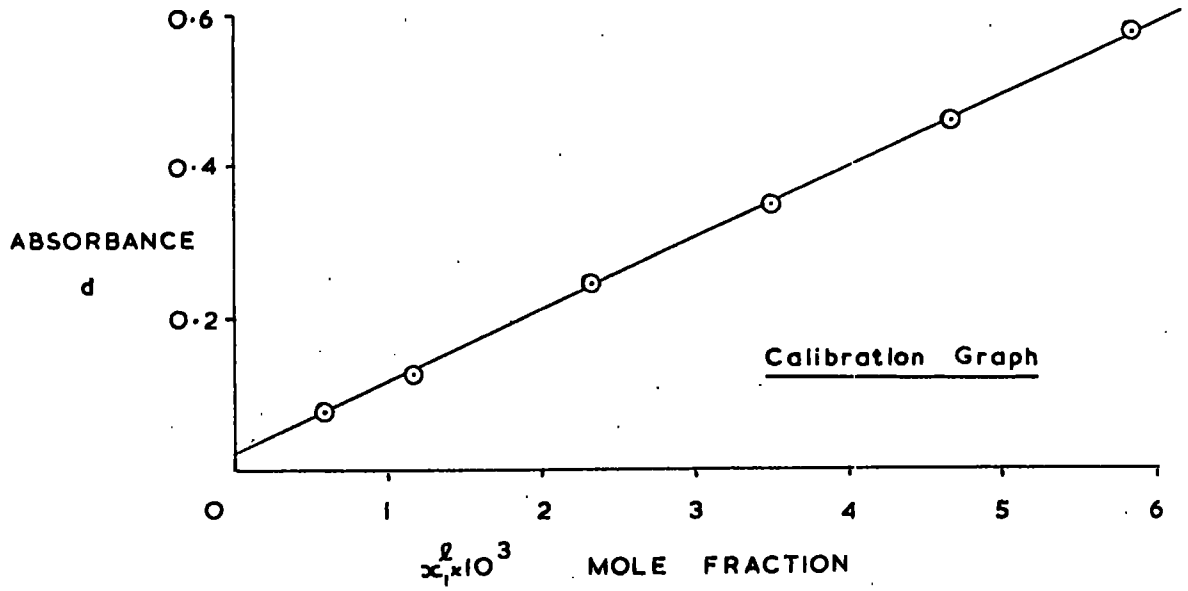

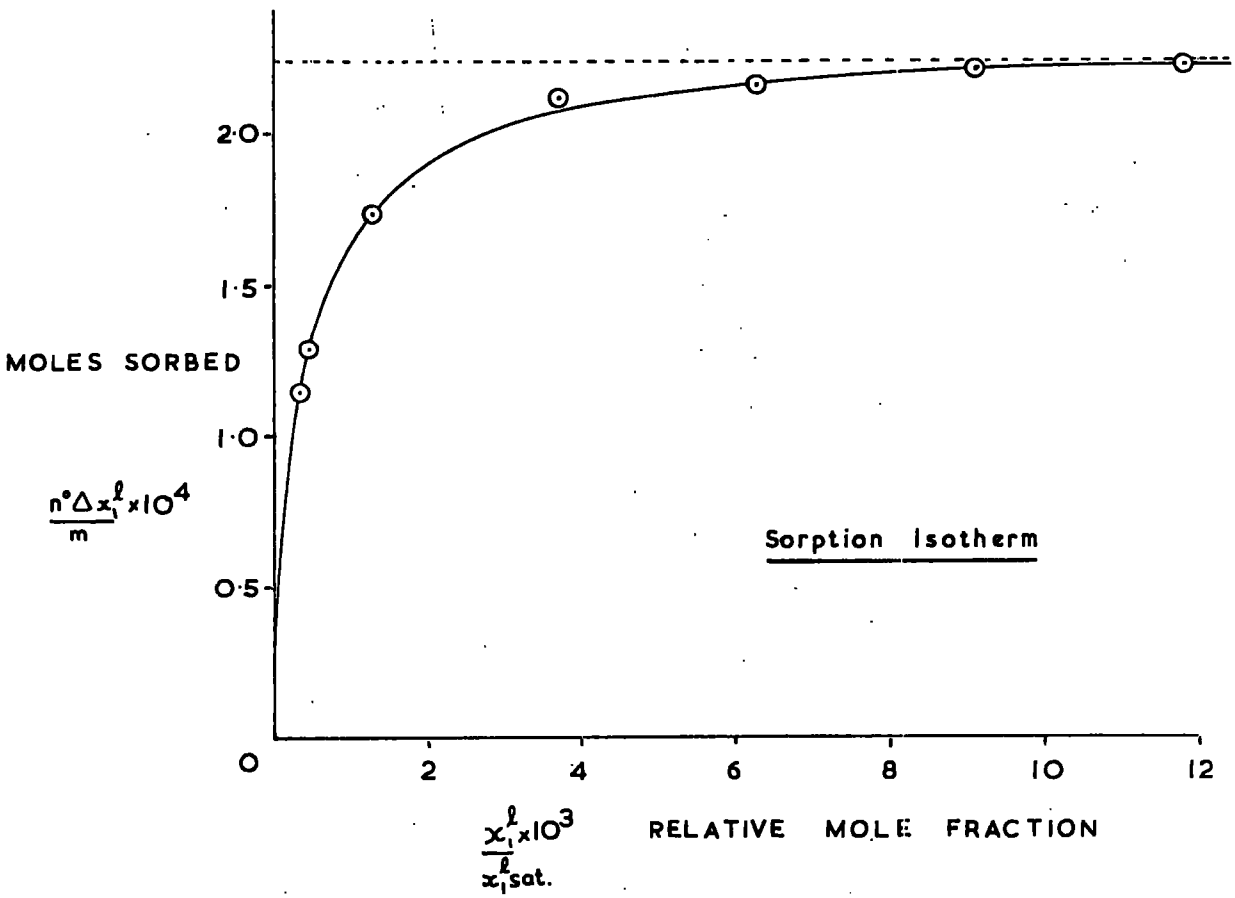

CHARACTERISATION OF THE ALUMINA

The sorption isotherms obtained for p-substituted phenols on the alumina from dioxan can be accounted for in terms of the crystal structure of the alumina, the nature of the exposed surfaces and the surface area accessible to molecules of cross section between 20 and 50 $Å^2$. The area occupied by one molecule of a phenol can then be calculated, compared with a theoretical requirement, and a probable orientation and mechanism of sorption proposed. It is therefore necessary to discuss the structure of the alumina and the nature and extent of its surface.

X-Ray Analysis

The manufacturers state that the high activity alumina used in this work has been heated up to 800°C. and classify it as 'γ-alumina'. Various workers[85-88] have demonstrated the existence of at least six crystalline modifications of nearly anhydrous aluminas formed from pure alumina hydrates: α, γ, δ, θ, κ and χ from a study of X-ray diffraction patterns. Transformations of heated alumina hydrates are complex and there is still some confusion manifest in the literature.

Brown et al.[86] report that gibbsite (hydrargillite, $Al(OH)_3$) begins to decompose between 200 and 300°C. when boehmite (γ-AlO.OH) is slowly formed until the two hydrates are present in roughly equal amounts. At 330°C. the residual gibbsite suddenly decomposes to χ-Al_2O_3 to give a mixture of $\chi.Al_2O_3$ and boehmite. No further change occurs until 530°C. when the boehmite decomposes sharply to γ-Al_2O_3 leaving a mixture of χ- and γ-aluminas in roughly equal amounts, no further changes occurring below 800°C.

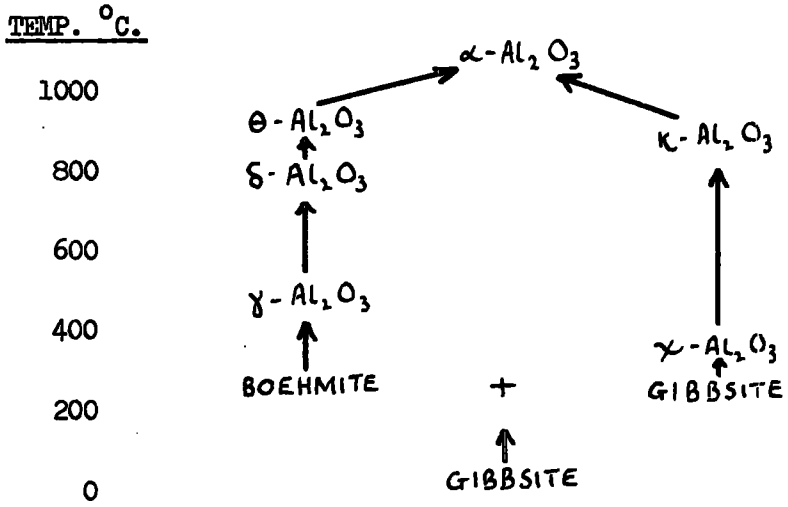

An X-ray powder diffraction pattern was obtained on the sorption alumina using copper K_α filtered radiation and compared with values quoted by Brown[86] (see Fig. 34).

TABLE 15

γ-ALUMINA d, Å		χ-ALUMINA d, Å		SAMPLE USED d, Å	
4.50	wb	4.50	wb	4.75	vw
2.77	vwb				
2.41	mb			2.44	w
2.28	m				
2.20	vvw	2.13	mvb	2.15	w
2.09	?			2.00	w
1.98	msb	1.87	vvw		
1.95	m	1.71	vvw		
1.53	mwb				
1.40	m	1.40	sb		
1.39	s			1.39	ms

w: weak, s: strong, b: broad, v: very

The pattern is not sharply defined and the Stokes broadening indicates

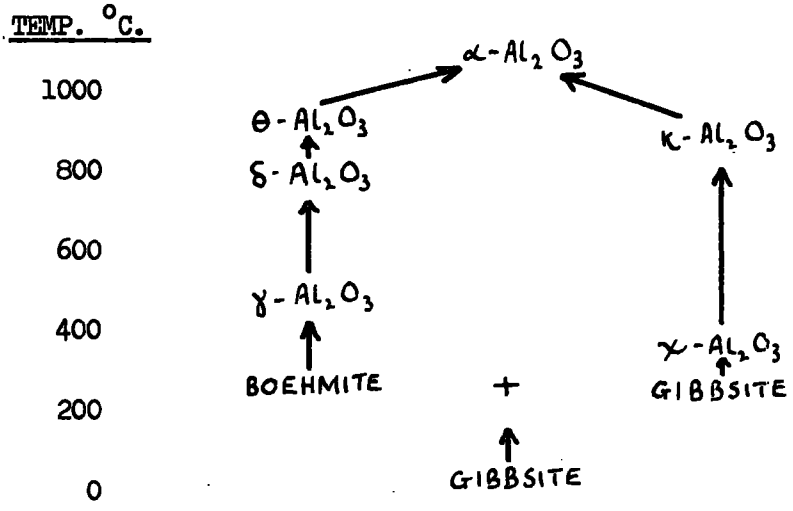

An X-ray powder diffraction pattern was obtained on the sorption alumina using copper K_α filtered radiation and compared with values quoted by Brown[86] (see Fig. 34).

TABLE 15

γ-ALUMINA d, Å		χ-ALUMINA d, Å		SAMPLE USED d, Å	
4.50	wb	4.50	wb	4.75	vw
2.77	vwb				
2.41	mb			2.44	w
2.28	m				
2.20	vvw	2.13	mvb	2.15	w
2.09	?			2.00	w
1.98	msb	1.87	vvw		
1.95	m	1.71	vvw		
1.53	mwb				
1.40	m	1.40	sb		
1.39	s			1.39	ms

w: weak, s: strong, b: broad, v: very

The pattern is not sharply defined and the Stokes broadening indicates

Fig. 34

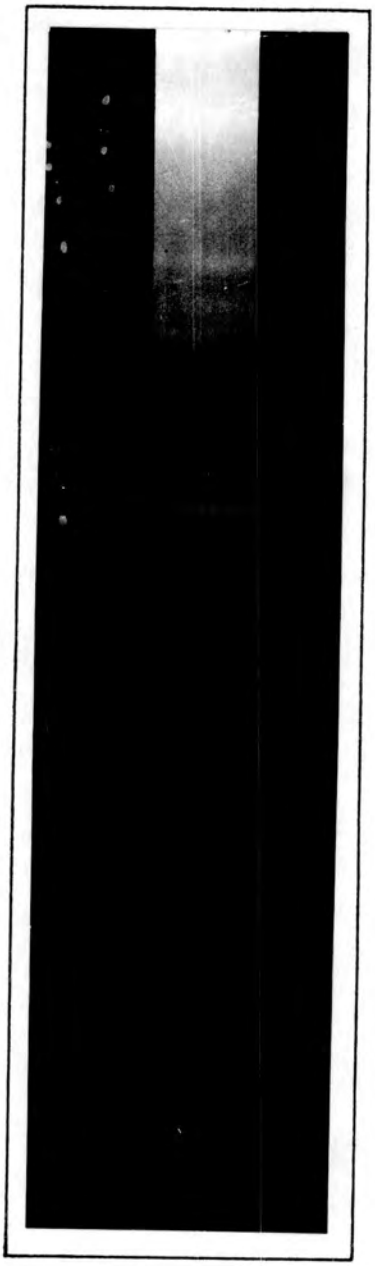

X-RAY POWDER DIFFRACTION PATTERN OF THE SORPTION ALUMINA

the presence of very fine particles (hence the diffuseness), but the appearance of the highly characteristic line at about 2.13Å (shown in patterns of none of the other forms) points to χ-alumina, furthermore the X-ray negative is almost identical to the one shown in Brown's report. It would appear then that the alumina used in this study is calcined gibbsite and is a mixture of χ and γ-anhydrous aluminas with perhaps a trace of δ-alumina.

De Boer et al.[50] report that all aluminas formed between the decomposition temperature of the hydrates and 1000°C. approximate closely in arrangement to a close packed cubic oxygen sub-lattice similar to that of the spinels. Accordingly, the structure can be taken as a pseudo-spinel type but with a cation deficiency, i.e. the thirty two oxygen ions are arranged as in cubic close packing with the appropriate number of aluminium ions (namely $21\frac{1}{3}$) in both tetrahedrally and octahedrally co-ordinated interstices but distributed at random over the twenty four sites normally occupied by the cations. On average, therefore, there are $2\frac{2}{3}$ vacant cation sites per unit cell which is the γ-alumina structure[89] with Lattice parameter 7.95Å.[85]

Constitution of the Surface

It is reasonable to suppose that the alumina crystals cleave to produce a surface formed by planes with simple indices of the oxygen sub-lattice, i.e. 111 or 100, 010, 001 (see Fig. 35). The evidence outlined below supports the view that the 100, 010, 001 faces are exposed in preference to the 111 face and that after the treatment the alumina

Fig. 35

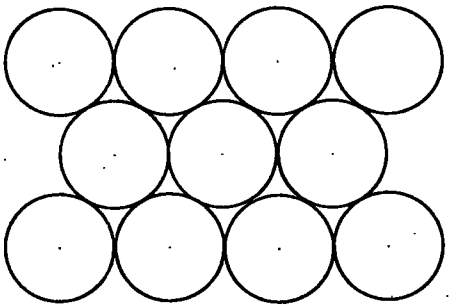

HEXAGONAL CLOSEST PACKING

(111 FACE)

Each oxygen atom occupies 6·84 $\mathring{A}^2$ on the surface.

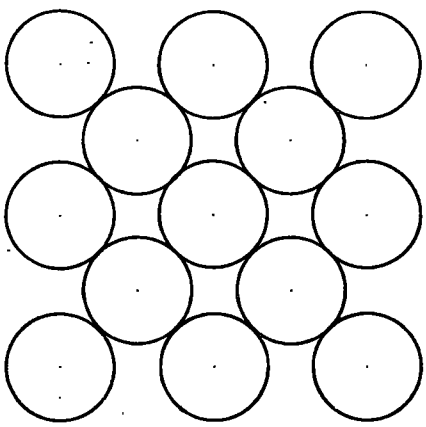

CUBIC CLOSEST PACKING

(100 FACE)

Each oxygen atom occupies 7·90 $\mathring{A}^2$ on the surface.

receives prior to sorption the surface of the alumina is covered by hydroxyl ions rather than oxygen ions for the OH groups play a fundamental role in the adsorption of molecules with which they interact by a process of hydrogen bonding. Again, the hydroxyls readily exchange with D_2O to give deuteroxyl groups at rates inconsistent with the diffusion of any species such as H, OH or H_2O through the bulk of the oxide.

In his investigations on alumina Peri[90] has proposed a theoretical model for the surface which agrees very well with practical results from infra-red and gravimetric studies of surface hydration of γ-alumina. After drying at 100°C. a monolayer of hydroxyl ions was thought to occupy the surface which was then progressively denuded by elimination of water molecules as the temperature was raised. The very high frequencies observed for the oxygen-hydrogen stretching vibrations of hydroxyl groups on alumina prompted Peri to regard these as ions rather than groups covalently bound to surface aluminium atoms although some degree of covalent character is probably present.

Fig. 36 shows a cross-section of a completely hydroxylated ideal surface from which water would be eliminated according to

$$OH^- + OH^- = O^{--} + H_2O$$

giving the ideal state shown in Fig. 37. In practice hydroxyl groups would be removed in a random fashion giving rise to defects such as those in Fig. 38.

Peri considered an array of 10,000 sites and programmed a computer

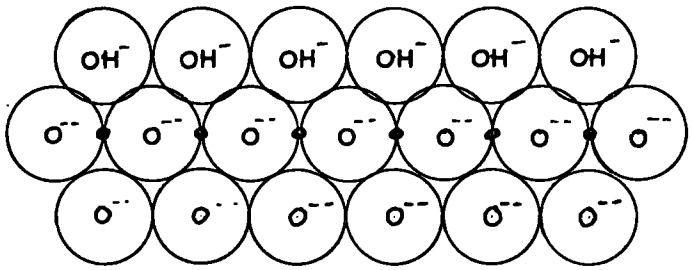

Fig. 36

COMPLETELY HYDROXYLATED SURFACE

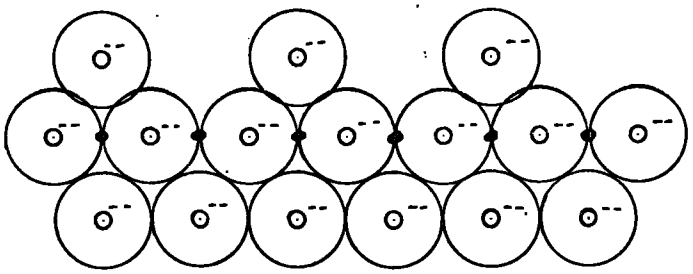

Fig. 37

IDEAL DEHYDROXYLATION.

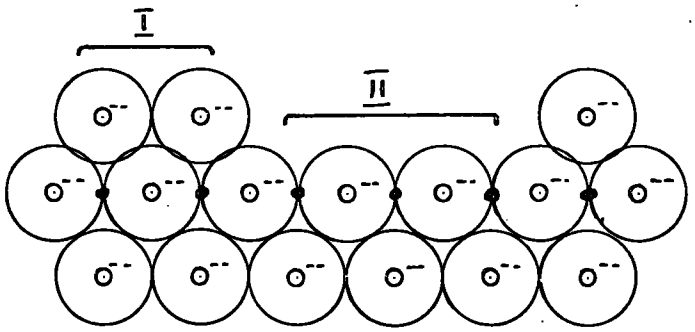

Fig. 38

RANDOM DEHYDROXYLATION SHOWING DEFECTS

to remove at random the maximum number of adjacent hydroxyl pairs without producing defects such as I or II in Fig. 38. He found that only 67% of the original hydroxide layer could be removed giving an ordered lattice with no adjacent aluminium ions and no adjacent oxygen ions (Fig. 39).

Further removal of hydroxyl pairs results in defects and when 90.4% have been removed the remainder (9.6%) are in isolated positions necessitating surface migration of ions for further elimination of water molecules. The remaining 9.6% of the surface hydroxyls find themselves in five possible environments having 0, 1, 2, 3 or 4 nearest oxide neighbours respectively, as shown in Fig. 40.

Peri found in practice that evacuation of alumina at 650°C. left approximately 10% of the surface covered by hydroxyl groups and that a sample in this state gave rise to five hydroxyl bands in the I.R. spectrum. Returning to the model, he assumed that surface migration tended to minimise the number of defects; that mobility of ions increased in the order: oxide ion, hydroxyl ion, proton; and that the band intensity for any of the given types of isolated groups should be proportional to the number of hydroxyl groups appearing on the model. Further dehydration under these conditions demonstrated that the various types of isolated groups were removed at different rates so enabling Peri to assign an absorption band to a particular type:

to remove at random the maximum number of adjacent hydroxyl pairs without producing defects such as I or II in Fig. 38. He found that only 67% of the original hydroxide layer could be removed giving an ordered lattice with no adjacent aluminium ions and no adjacent oxygen ions (Fig. 39).

Further removal of hydroxyl pairs results in defects and when 90.4% have been removed the remainder (9.6%) are in isolated positions necessitating surface migration of ions for further elimination of water molecules. The remaining 9.6% of the surface hydroxyls find themselves in five possible environments having 0, 1, 2, 3 or 4 nearest oxide neighbours respectively, as shown in Fig. 40.

Peri found in practice that evacuation of alumina at 650°C. left approximately 10% of the surface covered by hydroxyl groups and that a sample in this state gave rise to five hydroxyl bands in the I.R. spectrum. Returning to the model, he assumed that surface migration tended to minimise the number of defects; that mobility of ions increased in the order: oxide ion, hydroxyl ion, proton; and that the band intensity for any of the given types of isolated groups should be proportional to the number of hydroxyl groups appearing on the model. Further dehydration under these conditions demonstrated that the various types of isolated groups were removed at different rates so enabling Peri to assign an absorption band to a particular type:

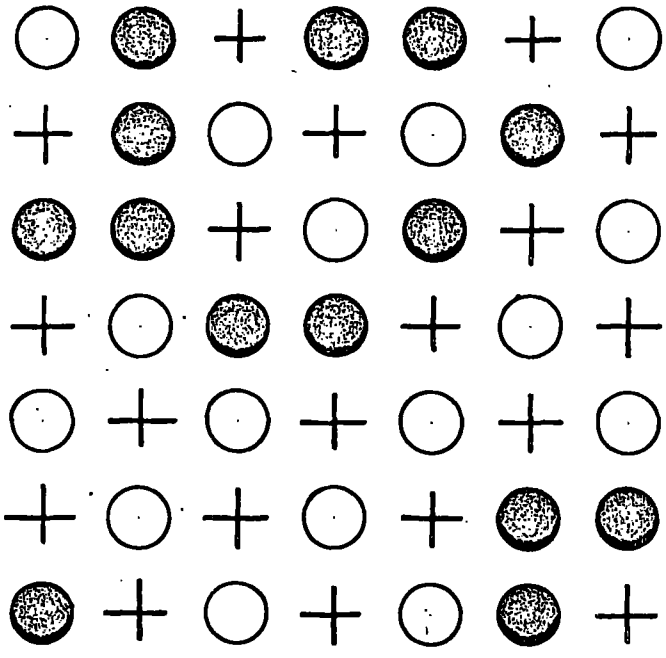

Fig. 39

+ Al^{+++} IONS IN SECOND LAYER

○ O^{--} IONS IN SURFACE LAYER

● OH^{-} IONS IN SURFACE LAYER

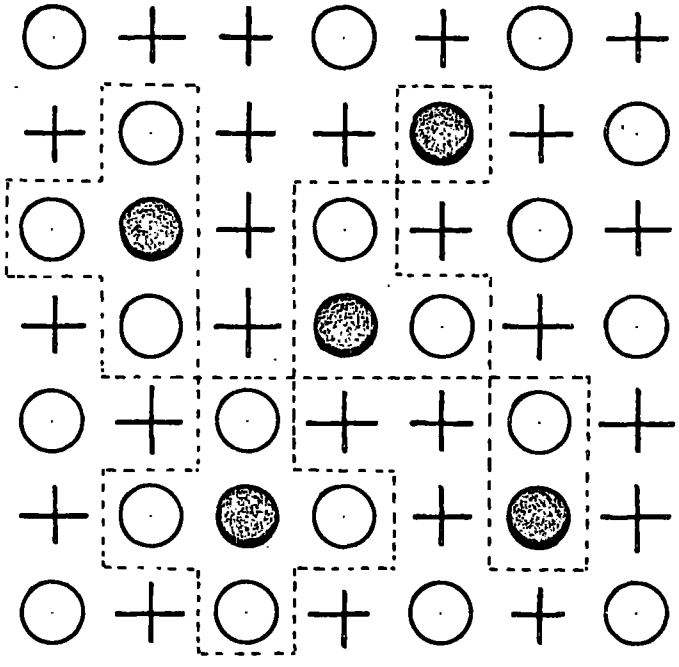

Fig. 40

Absorption band frequency (cm^{-1})	No. of nearest oxide neighbours (Fig.40)
3800	4
3744	2
3700	0
3780	3
3733	1

Peri's speculative model for the surface of γ-alumina gives a plausible explanation of dehydroxylation experiments in terms of defects persisting in boundaries between odd and even surface oxide domains, rather than strained oxide linkages.[91] That his model accounts so well for experimental findings points to the veracity of his assumption that the 100 face is almost exclusively exposed.

Infra-red spectroscopy is of the greatest value in observing perturbation of the surface groups which occurs during adsorption. Hydrogen bonding displaces the frequency of the OH stretching vibration to lower values and considerably broadens and intensifies the absorption band. This is a general finding and occurs for OH groups in solution[92, 72] and also for structural OH groups on surfaces.[58]

It is possible to distinguish between OH groups and water molecules adsorbed on the oxide surface by examination of the I.R. spectrum in the regions 3800 - 3300 $cm.^{-1}$ and 1650 - 1600 $cm.^{-1}$. Molecular water excites an infra-red active deformation vibration with movement of the hydrogen atoms in the plane of the molecule:

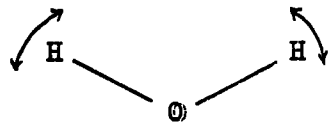

This produces an absorption band in the region of 1630 $cm.^{-1}$ for liquid water. The OH stretching vibrations of liquid water occur at about 3450 $cm.^{-1}$ and show marked evidence for hydrogen bonding.

γ - Alumina upon drying exhibits some interesting spectral changes[60] suggesting that calcination at 600°C. and subsequent exposure to moist air results in molecular water and OH groups on the surface. Reheating causes desorption of some water molecules and forms OH groups from the rest, although at higher temperatures this is reversed and OH groups combine to form water which is removed. Ultimately three types of OH group remain which represent isolated groups on different types of surface site.

Broad absorption bands corresponding to stretching and bending frequencies found in the spectrum of liquid water are shown near 3300 and 1650 $cm.^{-1}$ by undried alumina but after evacuation at 650 - 700°C. well defined absorption maxima at 3698, 3737 and 3795 $cm.^{-1}$ were displayed. These were due to OH stretching vibrations confirmed by deuterium exchange which produced new bands at 2733, 2759 and 2803 $cm.^{-1}$ Quantitative measurements of surface coverage by hydroxyl groups were made by deuterium exchange and showed a 40% coverage after drying at 400°C., a 2% coverage at 800°C. and less than 1% above 900°C., nonetheless the three OH bands were still evident on such very dry alumina.

Groups of a single type could not readily be converted to other types indicating that hydroxyl groups occupied specific sites precluding random motion and the high band frequencies suggest that attachment to

the surface is largely ionic in character, as is γ-alumina itself.[93]

Peri[94] heated γ-aluminas at 800°C. and then resorbed water onto the surface (which even after this treatment would still hold 1-2% of water as hydroxyl groups[60, 95]). He found at the B-point (monolayer coverage) that 6.25 molecules of water per 100Å^2 were rapidly and irreversibly adsorbed, i.e. each molecule required 16Å^2 of surface, and that when exposed to water vapour at saturation pressure (about 200 mm.) at room temperature for 16 hours followed by 2 hours at 100°C. at the same pressure the total adsorption was 12.5 molecules per 100Å^2 or 8Å^2 of surface per molecule. Kipling and Peakall[96] quote 13 molecules per 100Å^2 after evacuation at 25°C. for 100 hours. After dehydration at 800°C. the major part of the surface is probably similar to Fig. 41, though much less ideally. As water molecules reach the surface they are vigorously held: the heat of adsorption of water increases with the temperature at which the alumina is predried and may exceed 100 Kcal. mole^{-1} for very low surface coverages on alumina predried at 538°C.[91] After resorption of 6.25 molecules of water per 100Å^2 the surface is covered by a monolayer of hydroxyl ions: the water has been chemisorbed (Fig. 42). Adsorption of the remaining 6.25 molecules per 100Å^2 to a point of surface saturation implies that one water molecule is physically adsorbed onto a site having the same area as two surface ions.

Evacuation for two hours at 100°C. resulted in 8.3 molecules of water per 100Å^2 (de Boer et al. quoted 8.25 molecules per 100Å^2 after drying at 120°C.) which would correspond to an hydroxyl monolayer (6.25

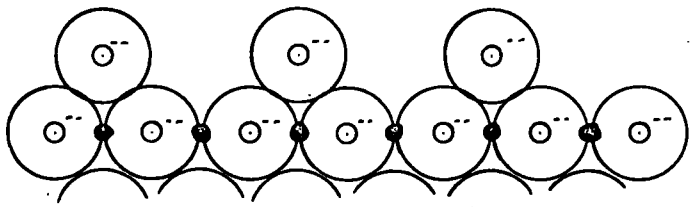

Fig. 41

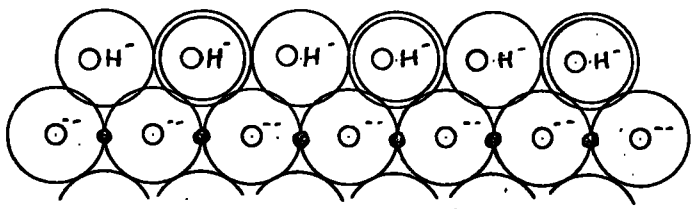

Fig. 42

water molecules chemisorbed) with additional water molecules physically adsorbed on this layer (about one molecule per six ion sites). This is probably the state of the sorbent surface used in these sorption studies; our alumina showed a 3% loss in weight on drying for 48 hours at 120°C. indicating that more than a single monolayer of water molecules probably exists on the "wet" alumina (i.e. before treatment of any kind).

Extent of the Sorbent Surface

Having established the probable nature of the alumina surface it is most important to know its extent and so the area accessible to molecules of the solvent and sorptives used in the sorption study.

Firstly, then, a low temperature (-196°C.) nitrogen sorption was carried out by Ibbitson and Vallance[84] when B.E.T. type II isotherms were obtained. After predrying the alumina at 120°C. for 48 hours sorption saturation values for nitrogen were obtained which gave a surface area of 131.9 $m^2g.^{-1}$ The above workers also attempted a sorption of benzene vapour at 25°C. which gave a result of 102.1 $m^2g.^{-1}$

In view of this discrepancy the author, following the recommendations of Giles and Nakhwa,[97] carried out a sorption of p-nitrophenol from benzene with a view to establishing the specific surface area of the alumina. The experiment was carried out in exactly the same way as the dioxan/phenol sorptions described earlier and the results are reported below.

(a) Solubility Determination

A saturated solution of p-nitrophenol in benzene at 35°C. was

prepared and 41.4518 g. of solution contained 0.9105 g. of p-nitrophenol (determined from absorbance measurements using the calibration graph described below). Thus the saturation mole fraction of p-nitrophenol in benzene at 35°C. was 12.454×10^{-3}.

(b) Calibration

A stock solution was prepared by dissolving 0.9470 g. of p-nitrophenol in 86.7546 g. of benzene at 25°C. giving a p-nitrophenol mole fraction of 6.092×10^{-3}. A series of solutions of graded strength was prepared and absorbances measured in 1 mm. silica cells at 370 mμ and 25°C. The equation to the straight line graph, obtained by plotting p-nitrophenol mole fraction against absorbance, was calculated by the method of least squares.

TABLE 16

p-Nitrophenol mole fraction x 10^3 (x_1^l)	Absorbance (d)
3.655	0.985
3.046	0.813
2.437	0.628
1.828	0.471
1.218	0.305
0.609	0.148

Equation to calibration line: $d = 275.1 \times x_1^l - 0.028$

(c) The Sorption Experiment

A stock solution was prepared by dissolving 6.3010 g. of

p-nitrophenol in 587.7g. of benzene and the sorption solutions prepared in triplicate by suitable dilution of this solution. The alumina was added, the flasks sealed and placed in a water thermostat bath at 35°C. for five days. The absorbances of the supernatant solutions were measured at 370 mμ and 25°C., the equilibrium mole fractions and uptake calculated and the sorption isotherm drawn as before.

TABLE 17

$w_{soln.}$	$n_{pnp} \times 10^3$	n^o	$x_1^o \times 10^3$	d
43.8253	3.3419	0.56424	5.923	0.904
37.6536	2.8712	0.56377	5.093	0.698
32.3839	2.4694	0.56337	4.383	0.536
27.1368	2.0693	0.56297	3.676	0.391
21.8799	1.6684	0.56257	2.966	0.256
15.7418	1.2004	0.56210	2.136	0.126
10.4917	0.8000	0.56170	1.424	0.046
6.1225	0.4669	0.56137	0.832	0.005

$x_1^{\ell} \times 10^3$	$(n^o \Delta x_1^{\ell}/m) \times 10^4$	$\frac{x_1^{\ell}}{n^o \Delta x_1^{\ell}/m(x_{1sat.}^{\ell} - x_1^{\ell})}$	$(x_1^{\ell}/x_{1sat}^{\ell}) \times 10^2$
3.388	7.152	537.94	27.202
2.639	6.917	399.31	21.190
2.052	6.567	308.24	16.476
1.523	6.095	234.16	12.229
1.032	5.438	170.07	8.289
0.560	4.429	108.66	4.495
0.267	3.250	68.92	2.145
0.120	1.998	49.75	0.964

Giles[97] reports that B.E.T. gas type isotherms are obtained from the sorption which was confirmed in this case (see Fig. 43) and following his precedent a modified form of the B.E.T. equation was used to calculate the monolayer capacity.

The standard B.E.T. equation is

$$\frac{v}{v_m} = \frac{c.\ p/p^o}{(1-p/p^o)\ (1+cp/p^o - p/p^o)} \qquad \ldots\ldots\ldots\ldots (12)$$

where v is the amount sorbed

v_m is the amount sorbed at monolayer coverage

p is the gas pressure

p^o is the saturated vapour pressure

c is a constant

This can be rearranged to give a linear plot:

$$\frac{p/p^o}{v(1-p/p^o)} = \frac{1}{c.v_m} + \frac{(c-1)\ p/p^o}{c.v_m} \qquad \ldots\ldots\ldots\ldots (13)$$

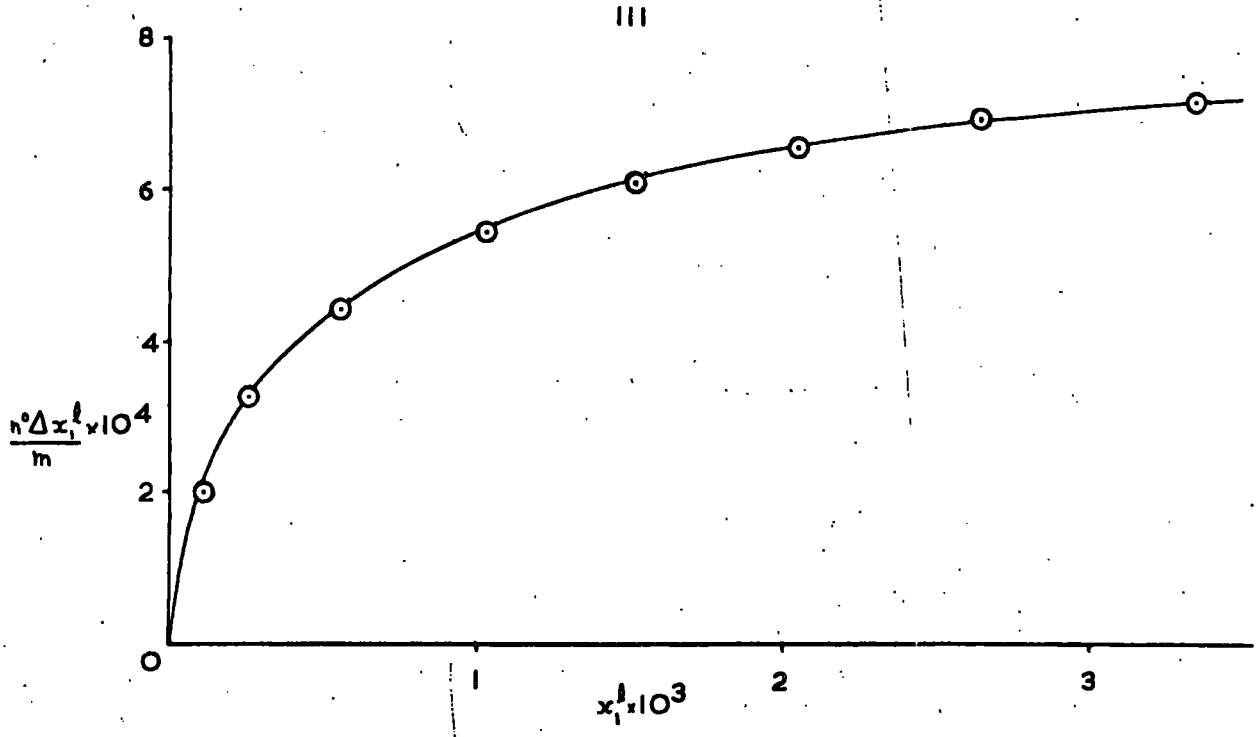
8
6
4
2
0
$\frac{n^o \Delta x_1^l}{m} \times 10^4$
1
2
3
$x_1^l \times 10^3$

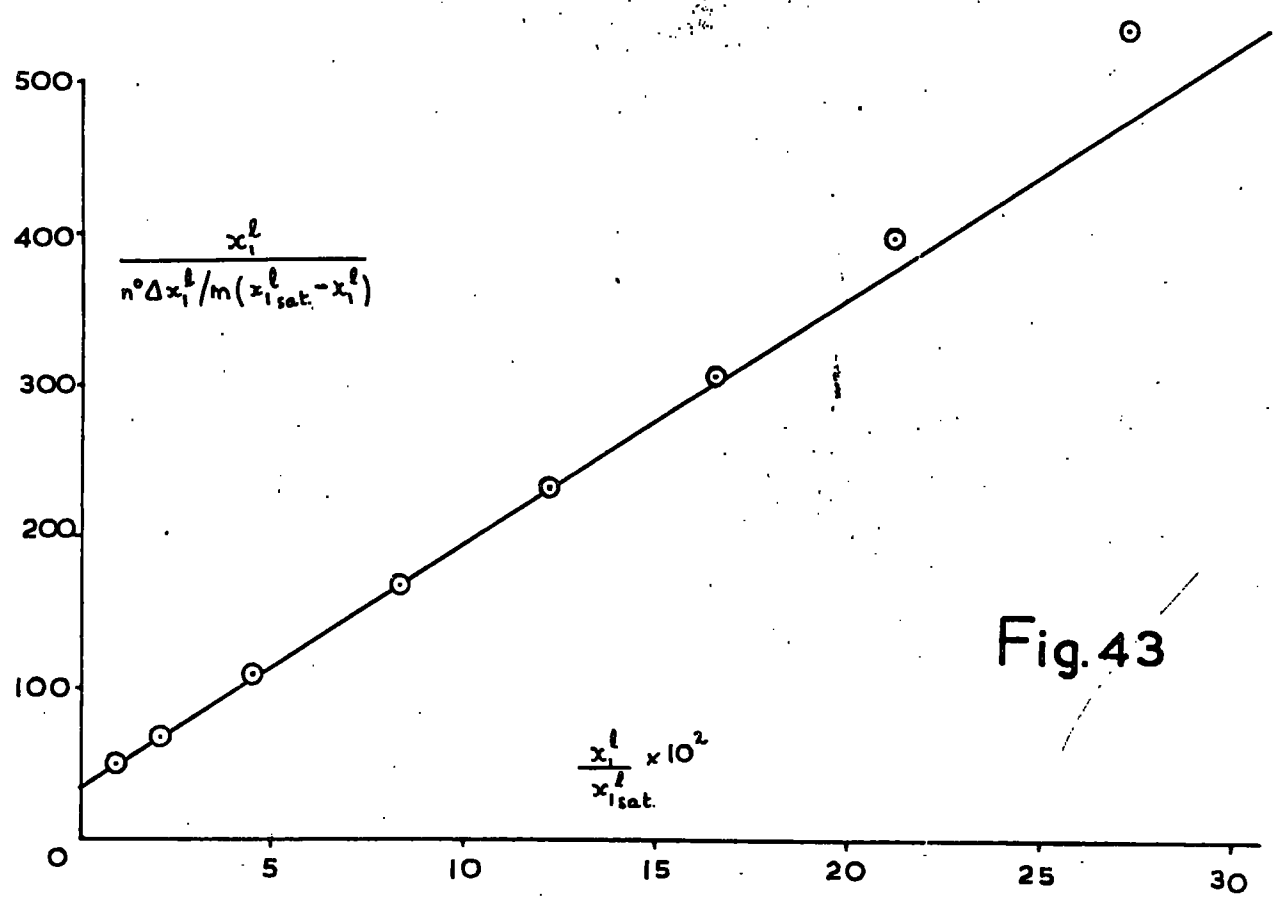
500
400
300
200
100
0
$\frac{x_1^l}{n^o \Delta x_1^l / m (x_{1\,sat.}^l - x_1^l)}$
$\frac{x_1^l}{x_{1\,sat.}^l} \times 10^2$
5
10
15
20
25
30

Fig. 43

For sorption from the liquid phase

v becomes $n^{o}\Delta x_1^{\ell}/m$ - moles of sorptive sorbed per g. of sorbent

v_m becomes $(n^{o}\Delta x_1^{\ell}/m)_{sat.}$ - moles sorbed at monolayer coverage

p/p^{o} becomes x_1^{ℓ}/x_1^{ℓ} sat.

c becomes k - a constant

giving the linear equation

$$\frac{x_1^{\ell}}{n^{o}\Delta x_1^{\ell}/m\ (x_1^{\ell}\ sat. - x_1^{\ell})} = \frac{1}{k(n^{o}\Delta x_1^{\ell}/m)_{sat.}} + \frac{(k-1)}{k(n^{o}\Delta x_1^{\ell}/m)_{sat.}} \frac{x_1^{\ell}}{x_1^{\ell}\ sat.} \quad \ldots\ldots\ldots\ldots\ (14)$$

therefore $(n^{o}\Delta x_1^{\ell}/m)_{sat.} = (\text{slope} + \text{intercept})^{-1}$

From the graph, slope = 1,617.2 and intercept = 35.5

therefore $(n^{o}\Delta x_1^{\ell}/m)_{sat.} = 6.051 \times 10^{-4}$ moles $g.^{-1}$

Taking the cross sectional area of a p-nitrophenol molecule as 25Å^2 [97], a value for the specific surface area of $91.1\ m^2\ g^{-1}$ is obtained.

Finally, other workers have carried out sorptions of fatty acids onto our alumina from non-interacting solvents such as heptane, cyclohexane or pentane and have again been able to calculate a value of the specific surface area of the sorbent used in this study.

The results of all these experiments are summarised in Table 18 and are considered in the "Discussion" section of this thesis in the light of the possibility of localised sorption.

TABLE 18

Sorptive	Solvent	Monolayer Capacity (moles g^{-1} x 10^3)	Molecular Cross-Section ($Å^2$)	Surface Area ($m^2 g^{-1}$)
Nitrogen	-	1.353[84]	16.2	131.9
Benzene	-	0.425[84]	40	102.1
p-Nitrophenol[97]	benzene	0.605	25	91.1
Phenol	cyclohexane	0.651	24	108.0
Phenol	heptane	0.632[98]	24	91.4
Stearic acid[99]	cyclohexane	0.575	20.5	71.0
Lauric acid[50]	pentane	0.587[100]	27.0	95.5

HYDROGEN-BONDING CONSTANTS

Introduction

Ultra violet spectroscopy has been used to determine the equilibrium constant of complex formation in solution by Benesi and Hildebrand,[101] Ketelaar et al.,[102] Nagakura and Baba,[103, 104] Nagakura,[105] and Keefer and Andrews.[106, 107]

Rose and Drago[108] devised a general method for rigorously treating spectrophotometric data for any acid-base system. The general equation for the equilibrium involved is

$$D + P \rightleftharpoons DP,$$

where D is an electron pair donor, e.g. dioxan, and P an electron pair acceptor, e.g. phenol. The expression for the equilibrium constant K is

$$K = {}_{e}c_{C}/(c_{D} - {}_{e}c_{C})(c_{P} - {}_{e}c_{C}) \qquad \ldots\ldots\ldots\ldots\ldots (15)$$

where c_D and c_P are the initial concentrations of D and P respectively

${}_{e}c_{C}$ is the equilibrium concentration of complex.

If the donor molecule does not absorb in the region studied, and assuming additivity of absorbances we have, for a cell of unit path length and a constant wavelength,

$$A = \varepsilon_{C} \cdot {}_{e}c_{C} + \varepsilon_{P} \cdot {}_{e}c_{P} \qquad \ldots\ldots\ldots\ldots\ldots (16)$$

where A is the absorbance of the solution

ε_{C} is the extinction coefficient of the complex

ε_{P} is the extinction coefficient of the electron pair acceptor

${}_{e}c_{P}$ is the equilibrium concentration of P.

Also $$c_{P} = {}_{e}c_{C} + {}_{e}c_{P} \qquad \ldots\ldots\ldots\ldots\ldots (17)$$

Expanding (15) gives

$$K = {}_eC_C/(c_D c_P + {}_eC_C^2 - {}_eC_C \cdot c_D - {}_eC_C \cdot c_P) \quad \ldots\ldots\ldots (18)$$

Eliminating ${}_eC_P$ between (16) and (17) gives

$$A = {}_eC_C (\varepsilon_C - \varepsilon_P) + \varepsilon_P \cdot c_P$$

If A^o corresponds to the absorbance of P alone at its initial concentration, c_P, at the same wavelength and in the absence of D, then:-

$$A^o = \varepsilon_P \cdot c_P$$

and $$A = {}_eC_C (\varepsilon_C - \varepsilon_P) + A^o \quad \ldots\ldots\ldots (19)$$

Rearranging (19) gives ${}_eC_C = (A - A^o) / (\varepsilon_C - \varepsilon_P)$

Substituting this value of ${}_eC_C$ into equation (18) gives

$$K^{-1} = c_D c_P (\varepsilon_C - \varepsilon_P)/(A - A^o) - c_D + (A - A^o)/(\varepsilon_C - \varepsilon_P) - c_P \quad \ldots\ldots\ldots (20)$$

When experimental conditions are such that

$\frac{(A - A^o)}{(\varepsilon_C - \varepsilon_P)} - c_P$ is negligible compared to $\frac{c_D c_P (\varepsilon_C - \varepsilon_P)}{(A - A^o)} - c_D$

then equation (20) becomes

$$K^{-1} = \frac{c_D c_P (\varepsilon_C - \varepsilon_P)}{(A - A^o)} - c_D$$

or $$\frac{1}{(A - A^o)} = \frac{1}{K.c_D.c_P(\varepsilon_C - \varepsilon_P)} + \frac{c_D}{c_D.c_P(\varepsilon_C - \varepsilon_P)} \quad \ldots\ldots\ldots (21)$$

Multiplying equation (21) by c_P gives

$$\frac{c_P}{(A - A^o)} = \frac{1}{K.(\varepsilon_C - \varepsilon_P)} \cdot \frac{1}{c_D} + \frac{1}{(\varepsilon_C - \varepsilon_P)} \quad \ldots\ldots\ldots (22)$$

Equation (22) enables equilibrium constants to be evaluated by the

Nagakura and Baba method since the extra polation of the linear plot of $1/(A - A^{o})$ against $1/c_D$ to $1/(A - A^{o}) = 0$ gives the equilibrium constant K as $K = (-1/c_D)_{extrap.}$

When at a given wavelength the absorption band is due to complex only, equation (16) becomes

$$A = \varepsilon_C \cdot {}_e c_C$$

or $${}_e c_C = A/\varepsilon_C \qquad \ldots\ldots\ldots\ldots\ldots (23)$$

Introducing equation (23) into equation (18) gives

$$K^{-1} = A/\varepsilon_C - c_P - c_D + c_D c_P \varepsilon_C/A \qquad \ldots\ldots\ldots\ldots\ldots (24)$$

Rose and Drago applied equation (24) to the original data of Benesi and Hildebrand on the benzene-iodine system in C Cl_4 as a solvent. Using measured values of c_D, c_P and A, and a series of selected values of ε_C, corresponding K^{-1} values were calculated and plotted against ε_C. Similar calculations for other sets of measured values of c_D, c_P and A gave a series of straight lines, the co-ordinates of whose intersections represent solutions for K and ε_C.

The majority of the intersections occur in a small area indicating good experimental precision and the formation of a 1 : 1 complex is given strong support. Equilibrium constants for the complex were determined for all intersections and the mean deviation calculated. All values outside the mean deviation by a factor of 2.5 were eliminated and a new average determined.

When the terms $A/\varepsilon_C - c_P$ can be neglected, equation (24) reduces to

$$K^{-1} = c_D c_P \varepsilon_C / A - c_D$$

or $$\frac{c_A}{A} = \frac{1}{K\varepsilon_C} \cdot \frac{1}{c_D} + \frac{1}{\varepsilon_C} \qquad \ldots\ldots\ldots\ldots\ldots (25)$$

an equation originally derived by Benesi and Hildebrand. This expression is linear of intercept $1/\varepsilon_C$ and slope $1/K\varepsilon_C$, although small values of K are very much dependant upon the extrapolation and so the line must be constructed by the method of least squares.

A method of evaluation of equilibrium constants of complex formation, similar to that of Rose and Drago, but which numerically designates the "sharpness of fit" of the experimental data was suggested by Grunwald and Coburn.[109]

For the process $D + P \rightleftharpoons DP$,

then if $c_D \gg c_P$ we have for K, the equilibrium constant

$$K = {}_e c_C / c_D (c_P - {}_e c_C) \qquad \ldots\ldots\ldots\ldots\ldots (26)$$

Rearranging equation (26) gives:-

$${}_e c_C = K c_D c_P / (1 + K c_D) \qquad \ldots\ldots\ldots\ldots\ldots (27)$$

An approximate value of K is obtained from the plot of $1/(A - A^o)$ against $1/c_D$ and application of equation (22) (Nagakura and Baba method). This value of K is introduced into equation (27) and a series of values of ${}_e c_C$ calculated corresponding to a series of experimental values of c_D and a constant experimental value of c_P. On the basis of the computed values of ${}_e c_C$ and experimental data for A and A_P (absorbance of free P in the equilibrium mixture), A_C, the absorbance of the complex at equilibrium, is obtained for each experimental point, using equations:

$$ {}_{e}c_{P} = c_{P} - {}_{e}c_{C} \qquad \ldots\ldots\ldots\ldots\ldots (28) $$

$$ A_{P} = {}_{e}c_{P} \cdot \varepsilon_{P} \qquad \ldots\ldots\ldots\ldots\ldots (29) $$

$$ A_{C} = A - A_{P} \qquad \ldots\ldots\ldots\ldots\ldots (30) $$

The validity of the approximate K value used is then tested by fitting the A_C and ${}_{e}c_{C}$ data to equation (31)

$$ A_{C} = \varepsilon_{C} \cdot {}_{e}c_{C} \qquad \ldots\ldots\ldots\ldots\ldots (31) $$

and computing the standard error of fit. In the common case where the error in A_C is approximately constant, independent of ${}_{e}c_{C}$, then $\varepsilon_{C} = \sum {}_{e}c_{C} \cdot A_{C} / \sum {}_{e}c_{C}^{2}$ by the method of least squares.

The calculation is repeated for other values of K, and the standard error of fit of equation (31) is plotted against the assumed value of K. This curve will have a single minimum which indicates the best value of K.

Conrow, Johnson and Bowen[110] have undertaken machine computation of association constants from spectrophotometric data. Activity coefficient effects were assumed to be negligible and Beer's Law assumed to hold for every species involved. The kind of approach used in developing the computer programme was similar to that of Coburn and Grunwald. It was concluded that errors of less than 1% introduced into the concentrations c_P and c_D can cause the calculated value of the equilibrium constant to be in error by more than 50%. The reason for this can be seen by plotting K^{-1} against ε_C as in the Rose-Drago method. The errors can be considered in two groups: errors affecting the slopes

and errors causing displacement in the curves. If a particular set of data gives K^{-1}/ε_C curves differing only slightly in slope then extremely small errors in c_P, c_D and A are sufficient to shift the points of intersection of the curves by large amounts. The curves will differ the most (and hence give the best results) when the concentration of the absorbing species is held constant and that of the non-absorbing species varied over as wide a range as possible e.g. 10 : 1. In order to minimise errors in the displacement of the curves, a region of the spectrum should be chosen in which the contribution of the complex to the observed absorbance is large. Compared to errors in c_P and c_D, the errors in A are less important by a considerable factor. Deduction of the concentration errors greatly enhances the accuracy of K and makes the measured absorbances the limiting factor in the accuracy of the determination. This is a desirable condition since absorbances can be measured at a large number of wavelengths whereas obtaining a large number of concentrations with slopes differing by sufficient amounts is difficult.

To obtain a measure of the reliability of the values of K, the sharpness of fit was calculated for values of K, 10% on either side of the best value. The ratio of the percentage change in fit to 10 (the percentage change in K) was defined as the sharpness, the larger the value the more reliable the value of K. Synthetic data suggested that the sharpness should be 20 or more for a reliably determined value of K.

Experimental

Hydrogen bonding constants for the process

p-substituted phenol + dioxan $\rightleftharpoons$ complex

have been determined from absorbance measurements at a predetermined wavelength in the ultra violet of a series of solutions of the substituted phenol in cyclohexane-dioxan solvent mixtures of varying composition. The apparatus used, the preparation of solutions and the operational procedure are described below.

(1) Apparatus

A Unicam S.P.500 Photoelectric Quartz Spectrophotometer was again used in this section of the study and details of the instrument have already been given in the Sorption Study Section. In addition, an accurately thermostated cell compartment was used enabling absorbances to be measured at 25°C. and 35°C.

(2) Preparation of Solutions

An approximately 10^{-4} molar solution of the phenol in cyclohexane (solution A) was prepared at 25°C.

100 mls. of a dioxan-cyclohexane solution of approximate dioxan weight fraction 0.3 was prepared by weight (solution B).

Solutions for absorbance measurements were prepared by weighing suitable volumes of solution B (e.g. 0, 0.5, 0.7, 1.1, 1.6, 2.5, 5.0 and 10.0 ml.), diluting with 20 ml. of solution A and making up to 50 ml. with cyclohexane at 25°C. As reference solutions, solvent mixtures of composition identical with the solution under examination were used.

(3) Pre-determination of Optimum Wavelength for Measurement

As a preliminary experiment complete ultra violet spectra were recorded in the range 240 - 340 mμ of approximately 10^{-4} molar solutions of the phenol in cyclohexane and in dioxan respectively. Absorbances were measured at 2mμ intervals and plotted against wavelength, the curves being superimposed. By inspection a wavelength was chosen, at which the difference between the absorbances of the two solutions was a maximum. An optimum wavelength was determined in this way for each phenol studied.

(4) Procedure

Each sample solution of the phenol was, in turn, placed in the cell compartment together with the corresponding reference solution. After standing for ten minutes to allow the attainment of thermal equilibrium, at 25°C. and 35°C., the absorbance of the solution was accurately measured. Experimental results are summarised in Tables 19 to 24 and plots of absorbance against wavelength, and $1/(A - A^{\circ})$ against $1/c_D$ shown in Figs. 44 to 49. Approximate values of K, at 25°C. and 35°C., were found by extrapolating to $1/(A - A^{\circ}) = 0$ by the method of least squares (theory P.116, equation 22, the Nagakura and Baba method).

Experimental Results

TABLE 19 : PHENOL

Temperature = 25°C.

Wavelength = 280.5 mμ ; phenol concentration = 2.9857×10^{-4}M; $A^{o} = 0.144$

c_D	$1/c_D$	A	$(A - A^{o})$	$1/(A - A^{o})$
0.01665	60.060	0.217	0.073	13.699
0.02524	39.620	0.240	0.096	10.417
0.03376	29.621	0.261	0.117	8.547
0.06881	14.533	0.322	0.178	5.618
0.13788	7.253	0.382	0.238	4.202
0.57974	1.725	0.457	0.313	3.195

Temperature = 35°C.

Wavelength = 280.5 mμ ; phenol concentration = 2.9496×10^{-4}M; $A^{o} = 0.154$

c_D	$1/c_D$	A	$(A - A^{o})$	$1/(A - A^{o})$
0.01645	60.790	0.205	0.051	19.608
0.02494	40.096	0.223	0.069	14.493
0.03335	29.985	0.240	0.086	11.628
0.06798	14.710	0.290	0.136	7.353
0.13621	7.342	0.351	0.197	5.076
0.57274	1.746	0.436	0.282	3.546

Extrapolated values at $1/(A - A^{o}) = 0$ correspond to

K_{25} = 15.21 litre $mole^{-1}$

K_{35} = 10.79 litre $mole^{-1}$

PHENOL

Fig. 44

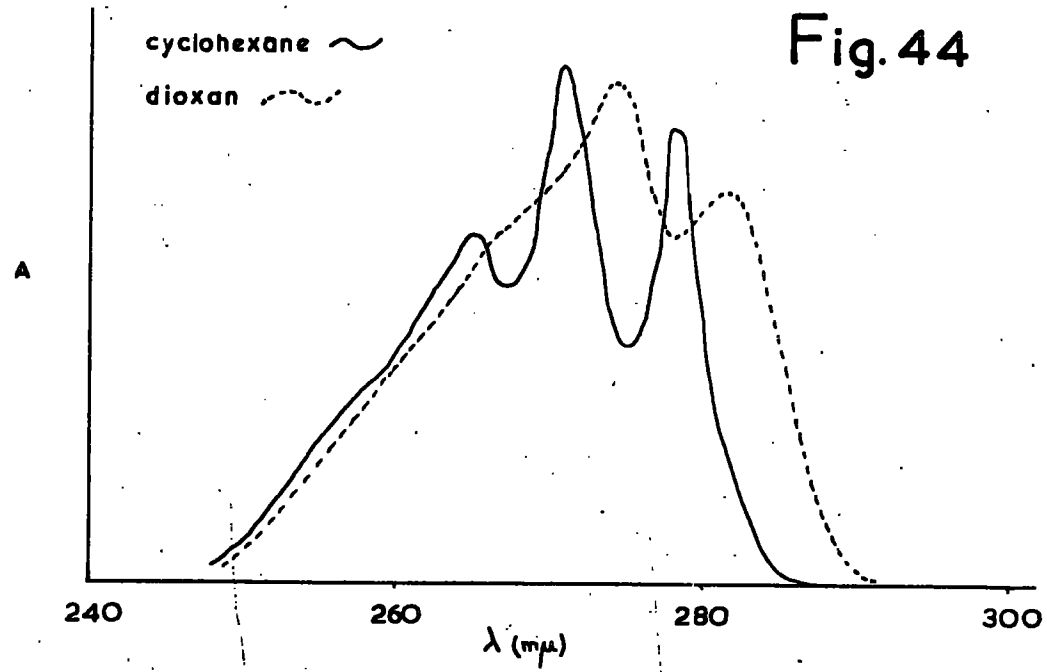

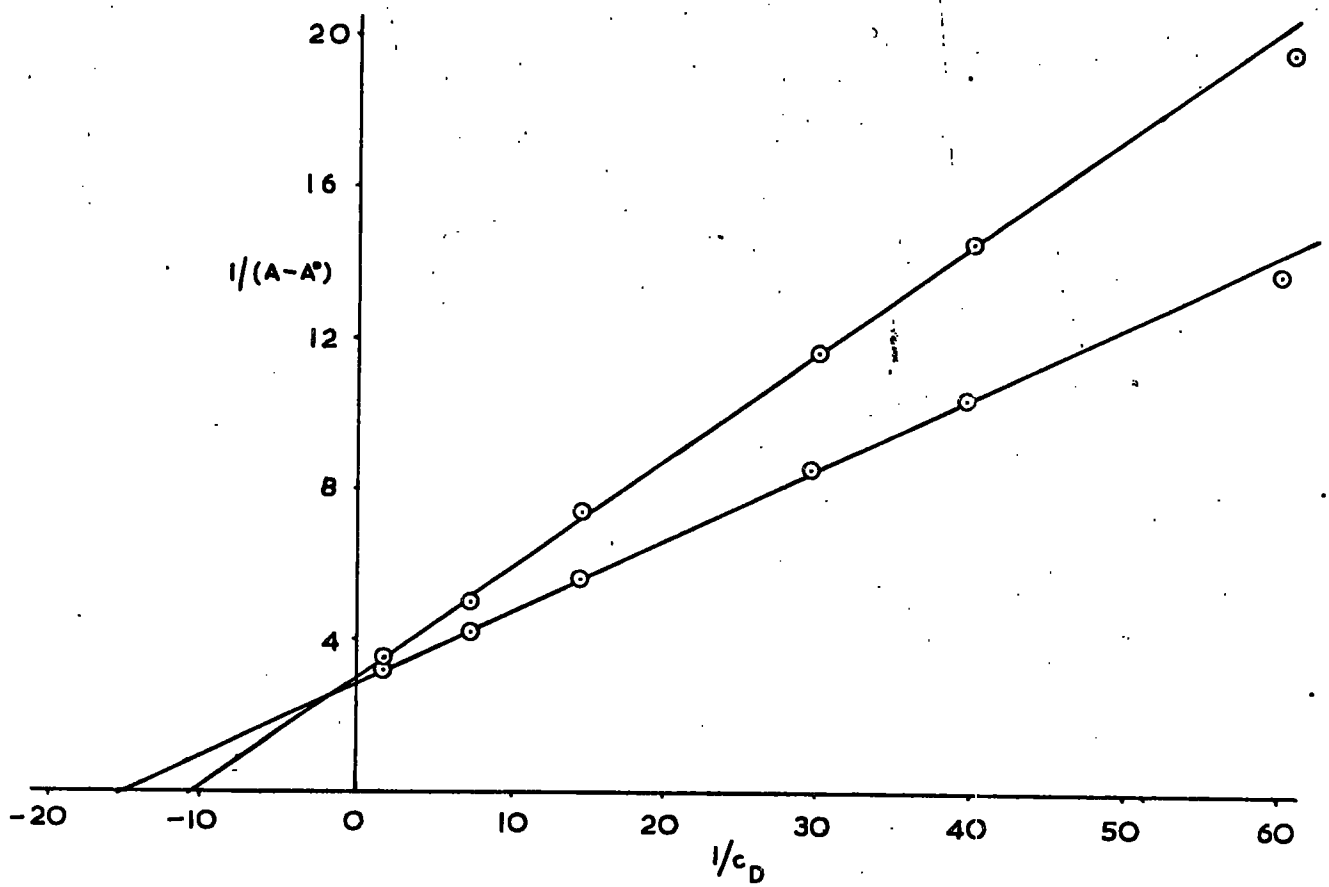

TABLE 20 : p-CRESOL

Temperature = 25°C.

Wavelength = 290 mμ; p-cresol concentration = 3.1470×10^{-4}M; $A^{\circ} = 0.173$

c_D	$1/c_D$	A	$(A - A^{\circ})$	$1/(A - A^{\circ})$
0.02266	44.140	0.246	0.073	13.699
0.03159	31.656	0.267	0.094	10.638
0.05003	19.988	0.303	0.130	7.692
0.07314	13.673	0.338	0.165	6.061
0.11442	8.740	0.380	0.207	4.831
0.22806	4.385	0.433	0.260	3.846
0.45793	2.184	0.474	0.301	3.322

Temperature = 35°C.

Wavelength = 290 mμ; p-cresol concentration = 3.1090×10^{-4}; $A^{\circ} = 0.182$

c_D	$1/c_D$	A	$(A - A^{\circ})$	$1/(A - A^{\circ})$
0.02238	44.680	0.237	0.055	18.182
0.03121	32.043	0.254	0.072	13.889
0.04942	20.233	0.284	0.102	9.804
0.07225	13.840	0.311	0.129	7.752
0.11303	8.847	0.352	0.170	5.882
0.22530	4.438	0.403	0.221	4.525
0.45239	2.211	0.447	0.265	3.774

Extrapolated values at $1/(A - A^{\circ}) = 0$ correspond to

K_{25} = 10.94 litre $mole^{-1}$

K_{35} = 8.81 litre $mole^{-1}$

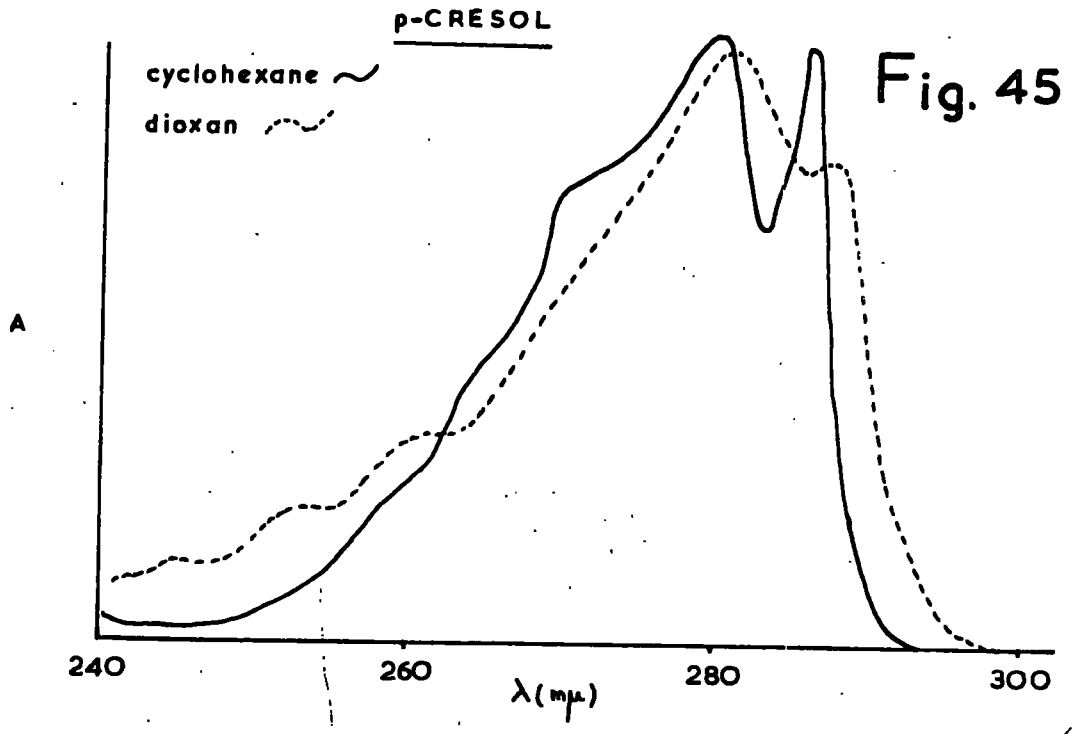
p-CRESOL
cyclohexane
dioxan
A
240
260
280
300
λ(mμ)

Fig. 45

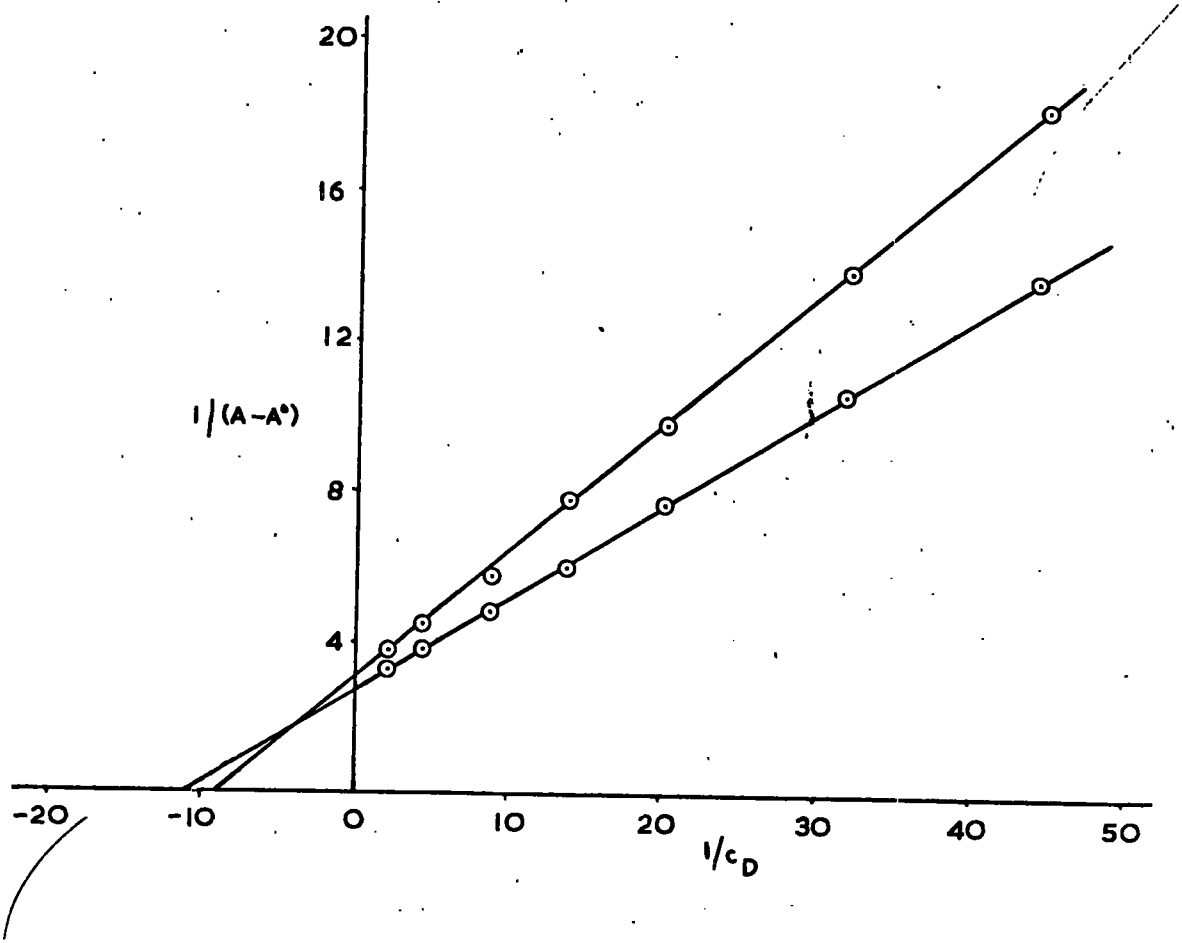
20
16
12
8
4
1/(A-A°)
-20
-10
0
10
20
30
40
50
1/c_D

TABLE 21 : p-t-BUTYL PHENOL

Temperature = 25°C.

Wavelength = 286 mμ ; p-t-butylphenol concentration = 2.9496×10^{-4}; A^{o}=0.317

c_D	$1/c_D$	A	$(A - A^{o})$	$1/(A - A^{o})$
0.01645	60.790	0.358	0.041	24.390
0.02494	40.096	0.372	0.055	18.182
0.03335	29.985	0.388	0.071	14.085
0.06798	14.710	0.432	0.115	8.696
0.13621	7.342	0.480	0.163	6.135
0.57274	1.746	0.549	0.232	4.310

Temperature = 35°C.

Wavelength = 286 mμ; p-t-butylphenol concentration = 4.3026×10^{-4}; A^{o}=o.221

c_D	$1/c_D$	A	$(A - A^{o})$	$1/(A - A^{o})$
0.02246	44.539	0.295	0.074	13.514
0.03105	32.204	0.317	0.096	10.417
0.04962	20.153	0.358	0.137	7.296
0.07192	13.904	0.396	0.175	5.714
0.10328	9.684	0.438	0.217	4.608
0.22528	4.439	0.522	0.301	3.322
0.45030	2.221	0.583	0.362	2.762

Extrapolated values at $1/(A - A^{o}) = 0$ correspond to

K_{25} = 10.42 litre $mole^{-1}$

K_{35} = 8.50 litre $mole^{-1}$

p-t-BUTYL PHENOL

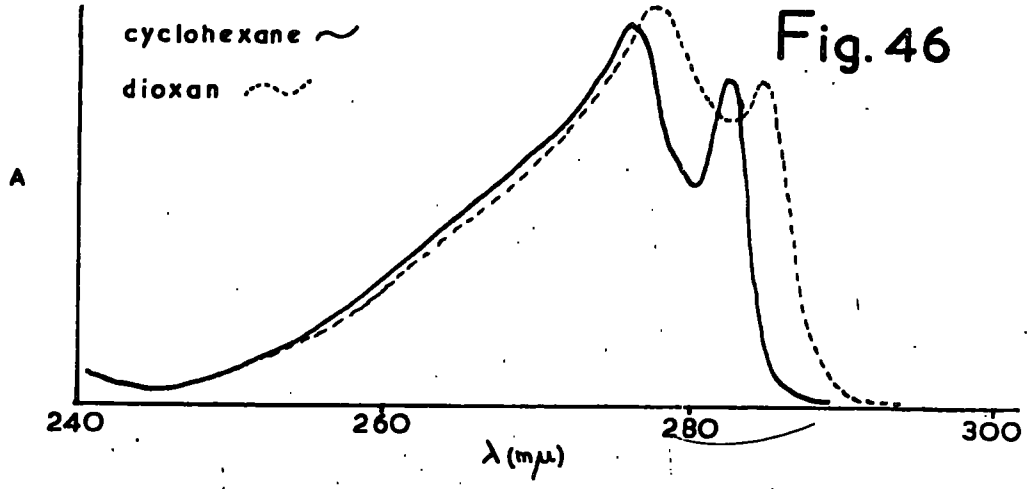

Fig. 46

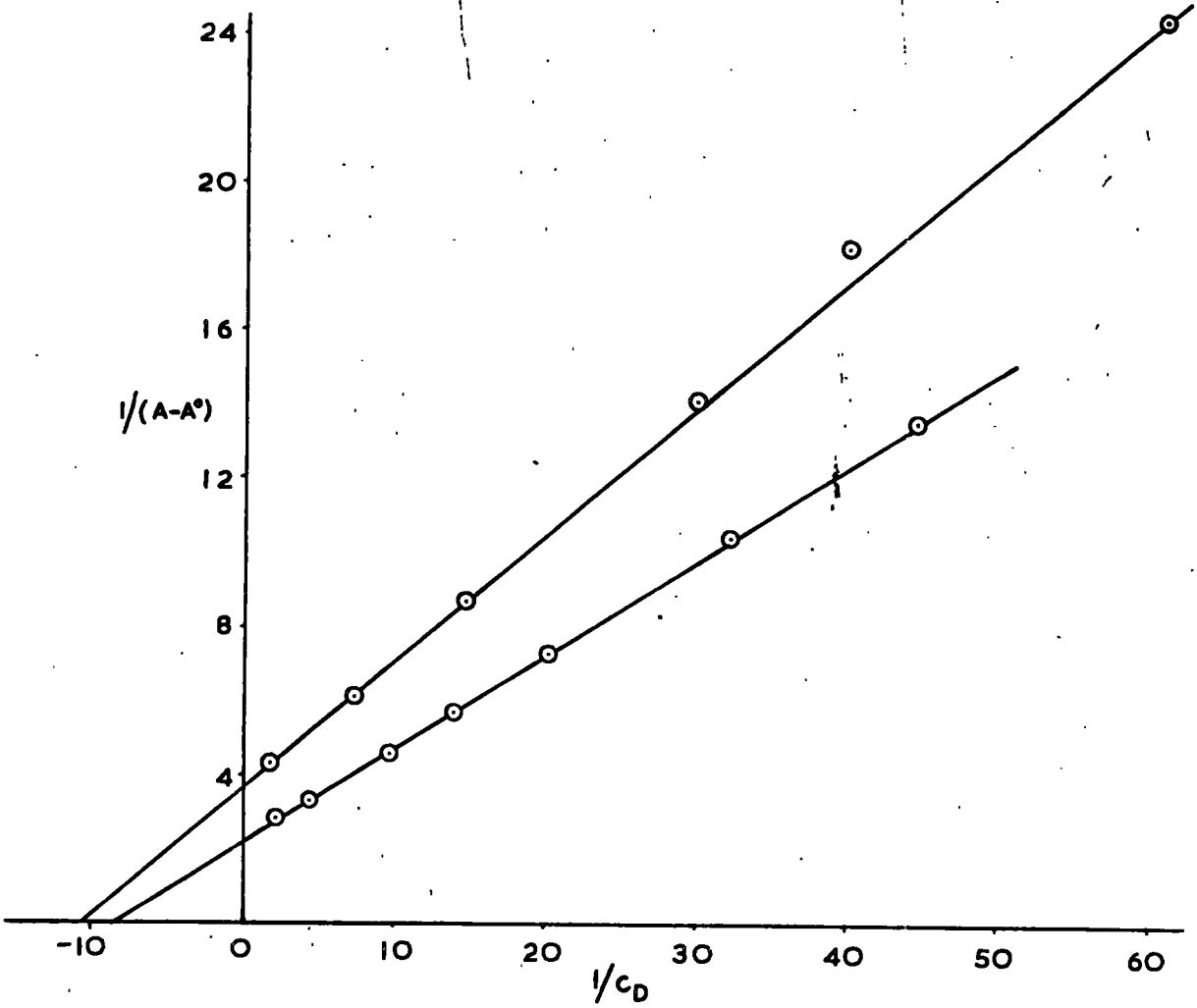

TABLE 22 : p-CHLOROPHENOL

Temperature = 25°C.

Wavelength = 293.5 mμ ; p-chlorophenol concentration = 4.0237×10^{-4}; A°=0.189

c_D	$1/c_D$	A	$(A - A^{\circ})$	$1/(A - A^{\circ})$
0.02322	43.064	0.318	0.129	7.752
0.03251	30.758	0.348	0.159	6.289
0.05118	19.539	0.384	0.195	5.128
0.07451	13.420	0.417	0.228	4.386
0.11637	8.593	0.454	0.265	3.774
0.23443	4.266	0.494	0.305	3.279
0.46830	2.135	0.519	0.330	3.030

Temperature = 35°C.

Wavelength = 293.5 mμ ; p-chlorophenol concentration = 3.9750×10^{-4}; A°=0.192

c_D	$1/c_D$	A	$(A - A^{\circ})$	$1/(A - A^{\circ})$
0.02294	43.591	0.291	0.099	10.101
0.03212	31.134	0.316	0.124	8.065
0.05056	19.778	0.353	0.161	6.211
0.07361	13.584	0.382	0.190	5.263
0.11497	8.698	0.421	0.229	4.367
0.23160	4.318	0.463	0.271	3.690
0.46263	2.161	0.492	0.300	3.333

Extrapolated values at $1/(A - A^{\circ}) = 0$ correspond to

K_{25} = 24.43 litre $mole^{-1}$

K_{35} = 18.28 litre $mole^{-1}$

p-CHLOROPHENOL

Fig. 47

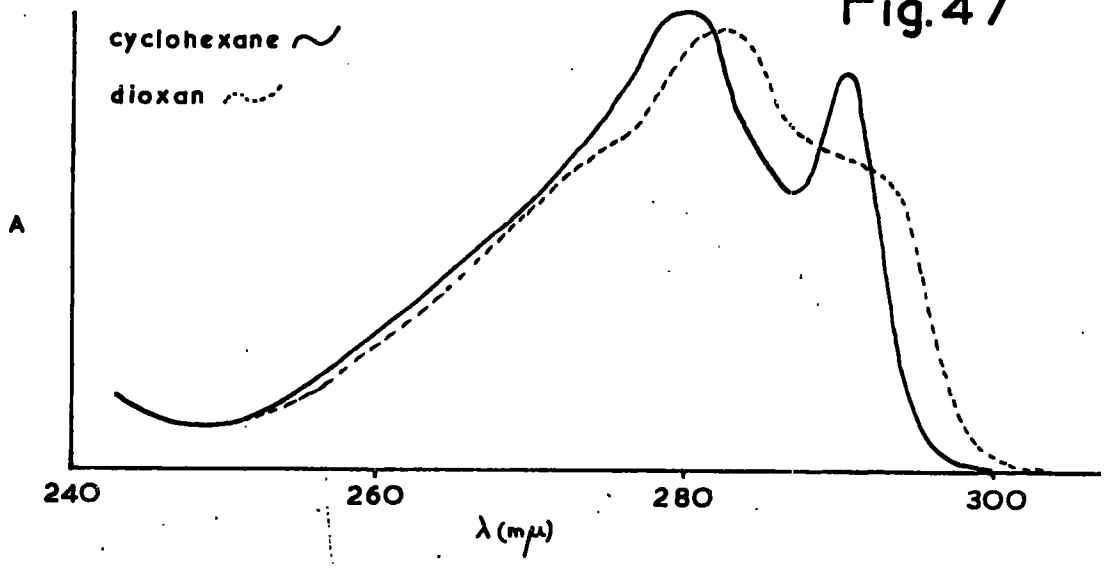

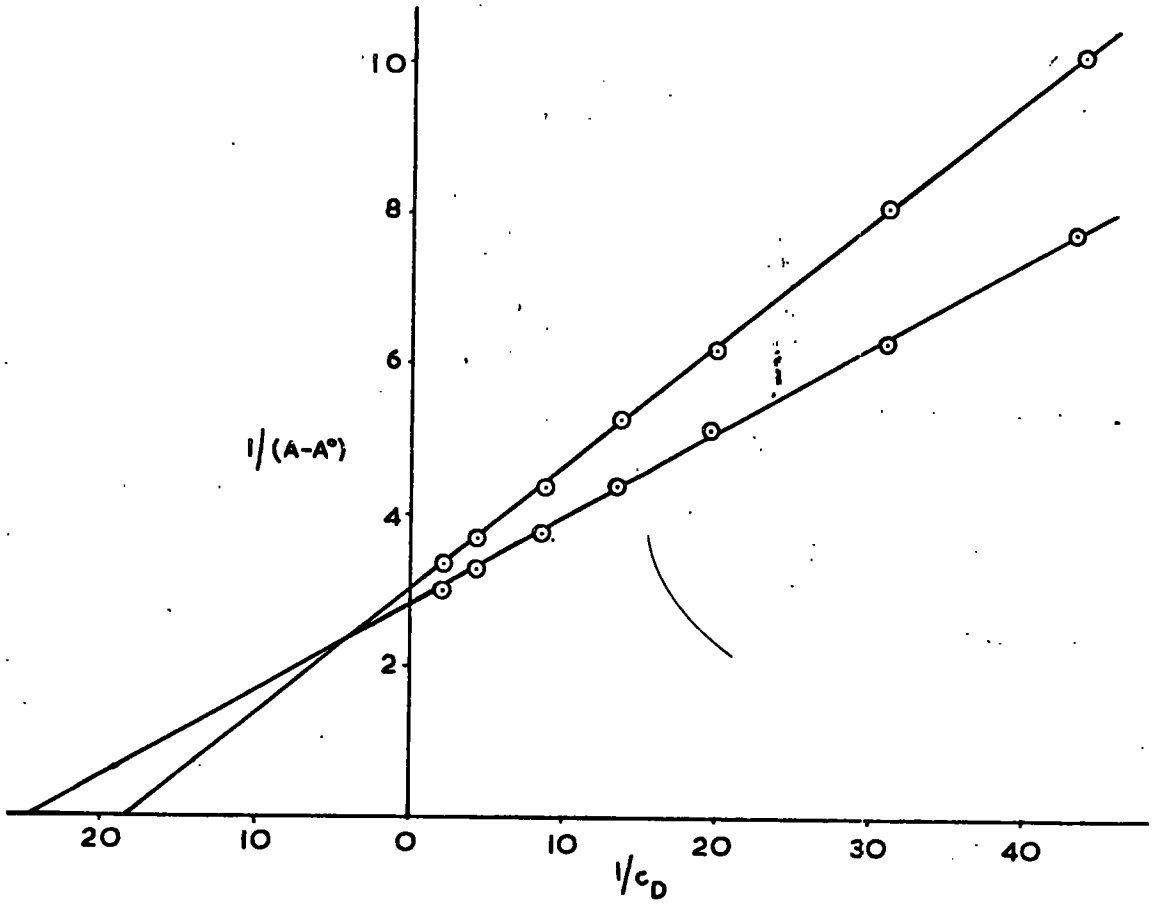

TABLE 23 : p-CYANOPHENOL

Temperature = 25°C.

Wavelength = 252 mμ ; A^0 = 0.147

c_D	$1/c_D$	A	$(A - A^0)$	$1/(A - A^0)$
0.01191	83.956	0.318	0.171	5.848
0.01601	62.465	0.346	0.199	5.025
0.02011	49.719	0.362	0.215	4.651
0.03034	32.964	0.417	0.270	3.704
0.05094	19.631	0.470	0.323	3.096
0.10159	9.844	0.520	0.373	2.681
0.20401	4.902	0.553	0.406	2.463

Temperature = 35°C.

Wavelength = 252 mμ ; A^0 = 0.133

c_D	$1/c_D$	A	$(A - A^0)$	$1/(A - A^0)$
0.01177	84.983	0.255	0.122	8.197
0.01582	63.229	0.291	0.158	6.329
0.01987	50.327	0.315	0.182	5.495
0.02997	33.367	0.357	0.224	4.464
0.05032	19.871	0.400	0.267	3.745
0.10036	9.964	0.469	0.336	2.976
0.20153	4.962	0.511	0.378	2.646

Extrapolated values at $1/(A - A^0) = 0$ correspond to

K_{25} = 50.20 litre $mole^{-1}$

K_{35} = 37.22 litre $mole^{-1}$

p-CYANOPHENOL

Fig. 48

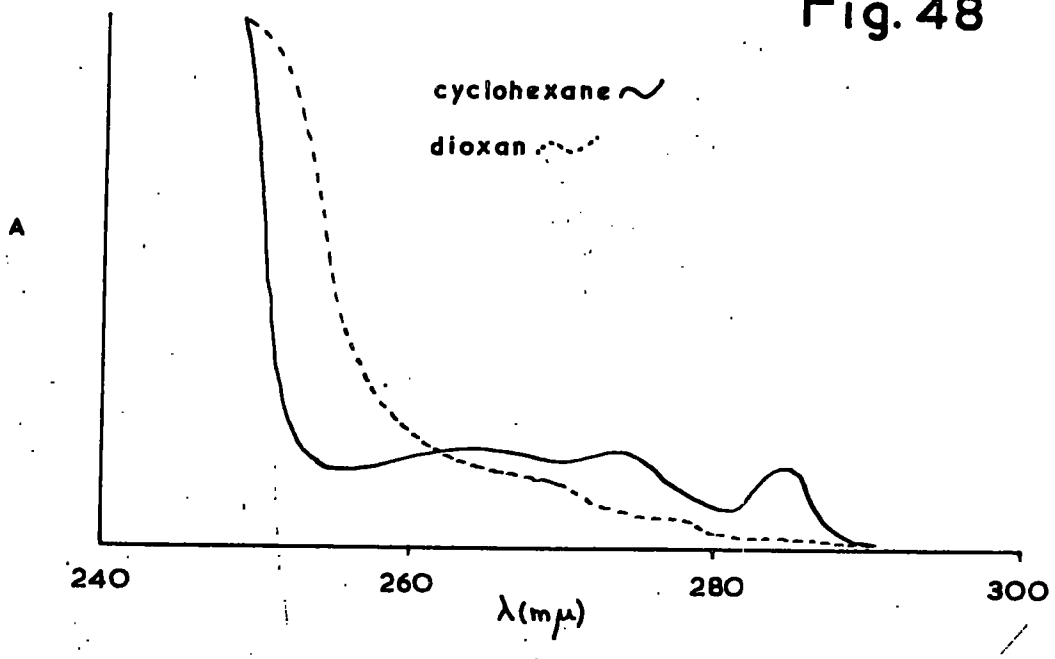

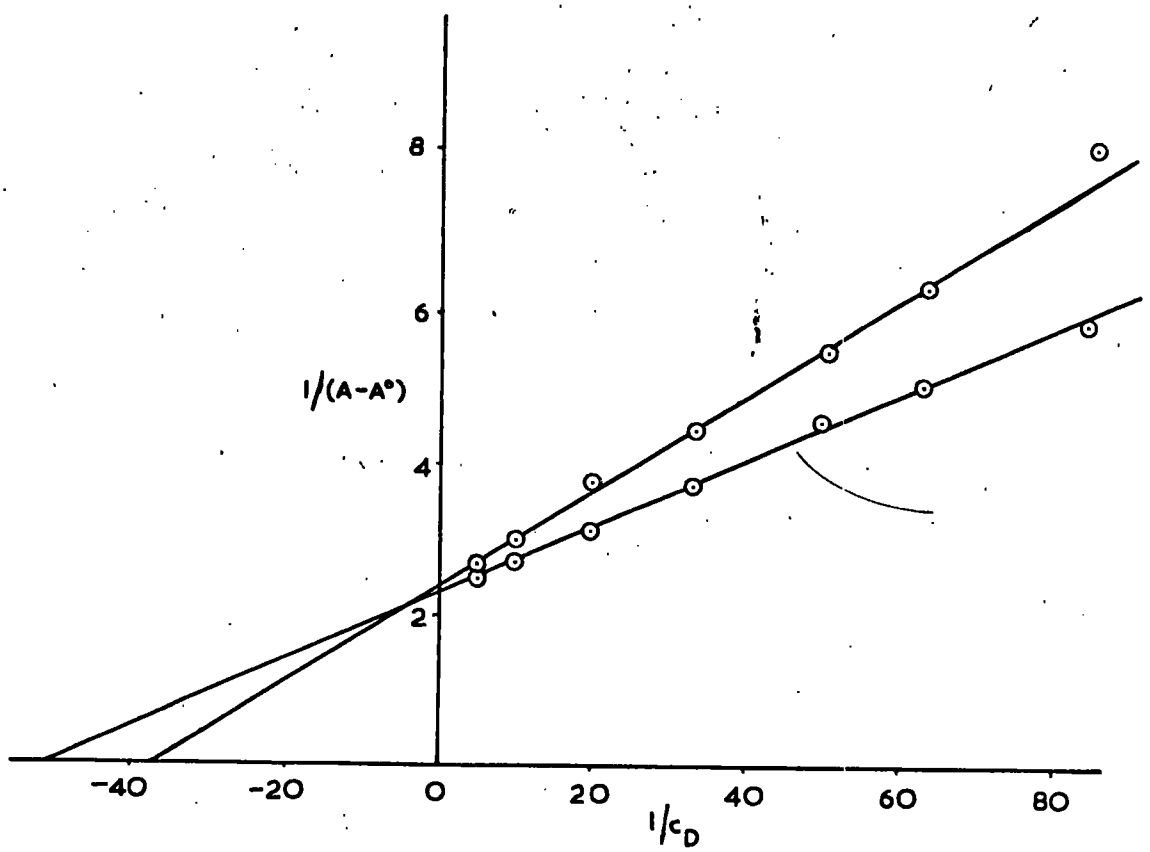

TABLE 24 : p-NITROPHENOL

Temperature = 25°C.

Wavelength = 315 mμ ; A^0 = 0.102

c_D	$1/c_D$	A	$(A - A^0)$	$1/(A - A^0)$
0.01362	73.421	0.258	0.156	6.410
0.01799	55.574	0.281	0.179	5.587
0.02278	43.898	0.300	0.198	5.051
0.03405	29.366	0.325	0.223	4.484
0.05718	17.489	0.360	0.258	3.876
0.11412	8.763	0.393	0.291	3.436
0.22924	4.362	0.418	0.316	3.165

Temperature = 35°C.

Wavelength = 315 mμ ; A^0 = 0.094

c_D	$1/c_D$	A	$(A - A^0)$	$1/(A - A^0)$
0.01346	74.319	0.219	0.125	8.000
0.01778	56.254	0.238	0.144	6.944
0.02250	44.435	0.259	0.165	6.061
0.03364	29.725	0.289	0.195	5.128
0.05649	17.703	0.325	0.231	4.329
0.11274	8.870	0.361	0.267	3.745
0.22645	4.416	0.390	0.296	3.378

Extrapolated values at $1/(A - A^0) = 0$ correspond to

K_{25} = 66.83 litre $mole^{-1}$

K_{35} = 49.00 litre $mole^{-1}$

p-NITROPHENOL

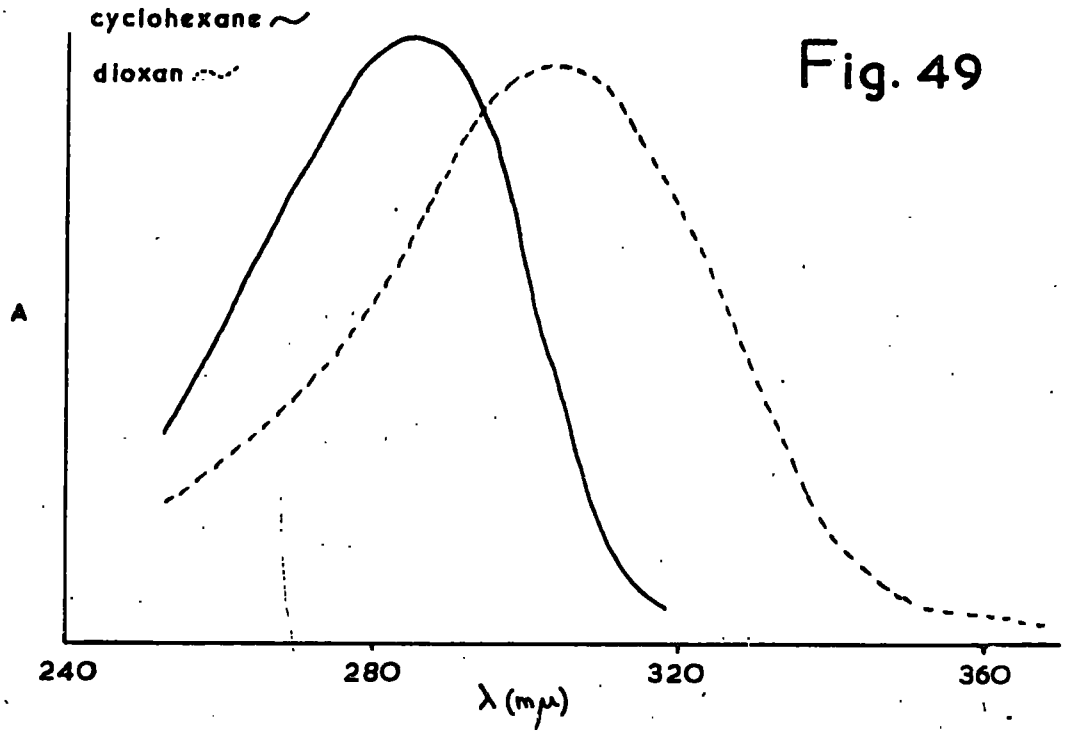

Fig. 49

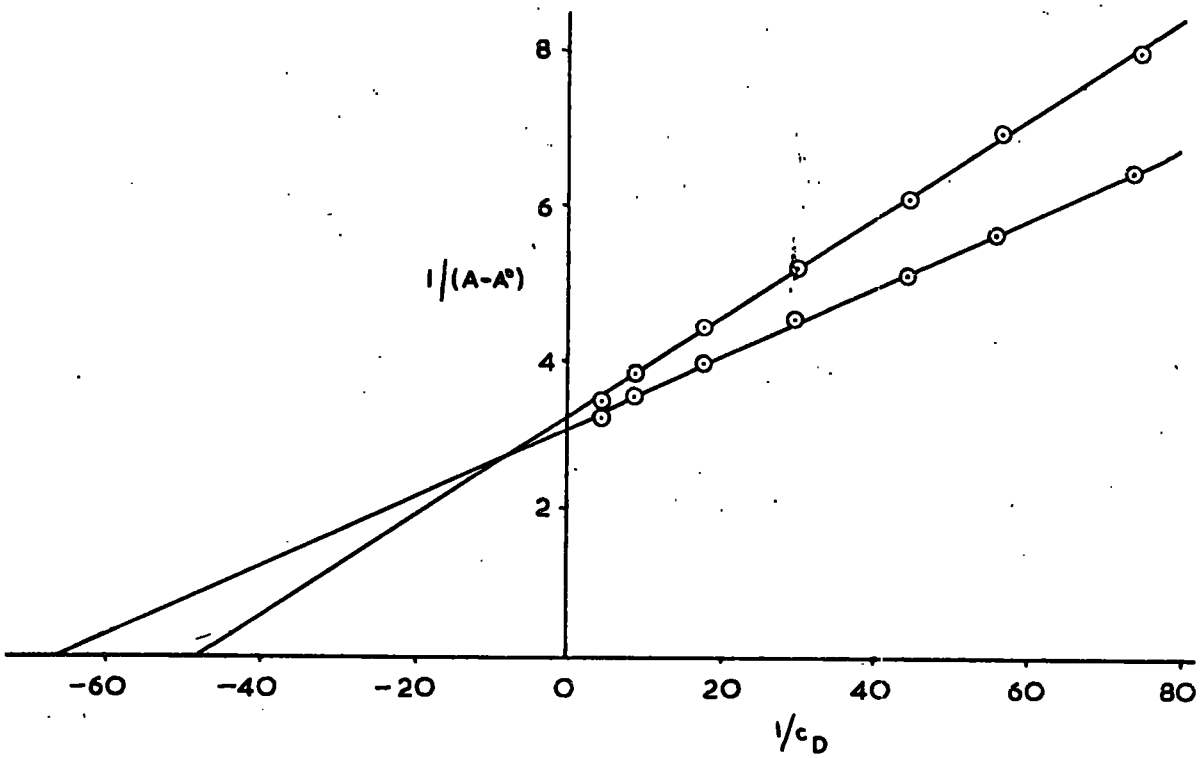

The method of Rose and Drago[108] was next applied to the results and values of the association constant were calculated by means of Equation (20):

$$K^{-1} = \frac{c_D \cdot c_P (\varepsilon_C - \varepsilon_P)}{(A - A^o)} - c_D - c_P + \frac{(A - A^o)}{(\varepsilon_C - \varepsilon_P)}$$

For each value of c_D corresponding values of A, A^o and c_P (Tables 19 to 24) were substituted into Equation 20 so giving a linear relationship between K^{-1} and $(\varepsilon_C - \varepsilon_P)$. As the true value of K^{-1} is constant the straight lines corresponding to different values of c_D should intersect at one point. In practice they do not, and so the mean of the K^{-1} values (the co-ordinates of points of intersection) within the limits stipulated by Rose and Drago ($\pm$ 2.5 mean deviations) is calculated and hence K assessed. A typical Rose-Drago plot is shown in Fig.50 which is for p-cresol at 25°C. (Table 20).

The calculations involved in this analysis are lengthy and tedious and so an I.B.M.1130 computer was programmed to calculate equations to the straight lines, co-ordinates of all intersections, the mean K^{-1} value and the deviation of each K^{-1} value from the mean. Values outside the limits were then rejected and a new mean determined which was taken as the best K value.

The computer was instructed to print out the mean K value, the slope and intercept of each line and values of K and the deviation $(K - K_{mean})$. The results are recorded in Tables 25 to 32 together with the revised mean K value; values of c_D and A have already been

ROSE-DRAGO PLOT FOR p-CRESOL AT 25°C.

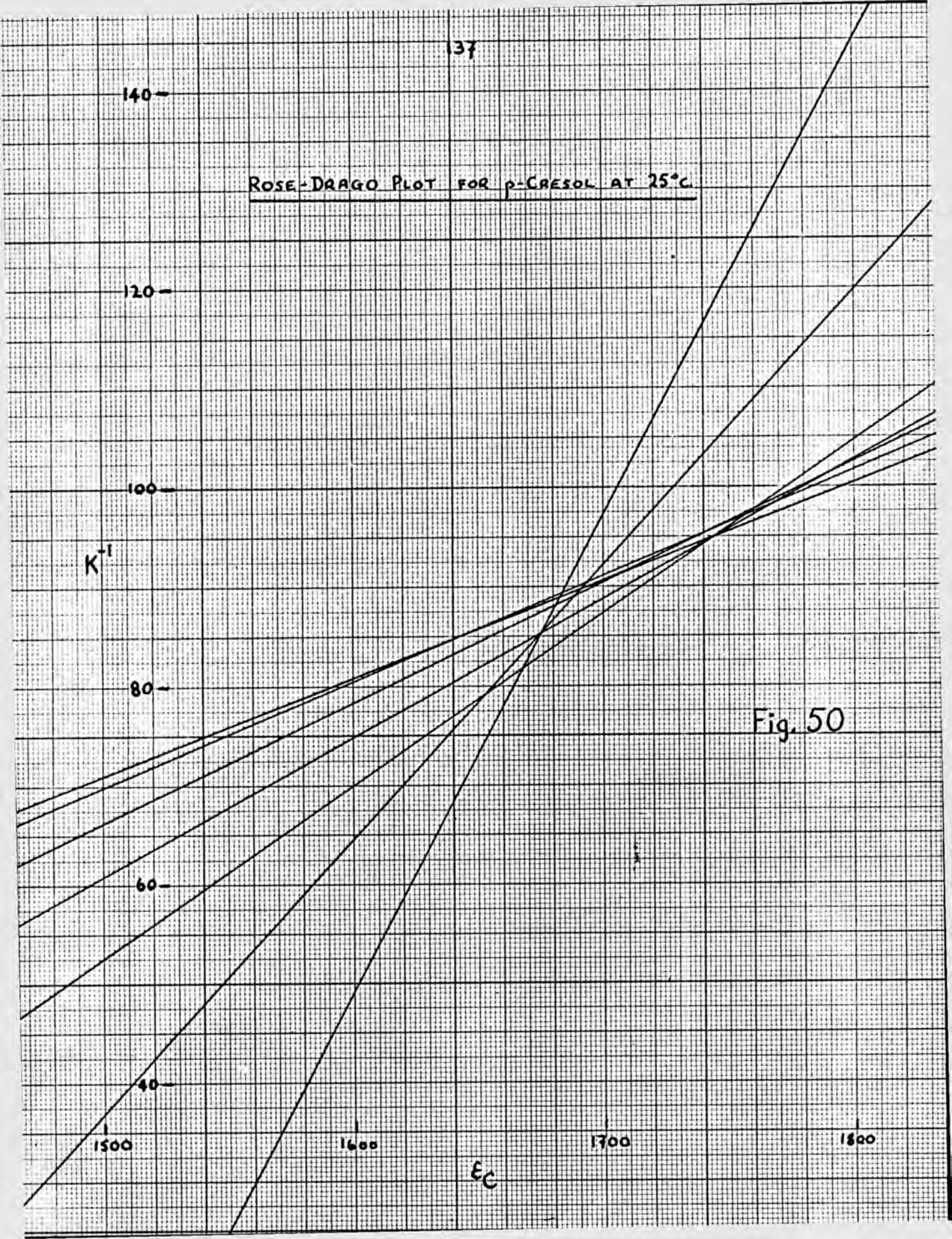

Fig. 50

reported in Tables 19 to 24. A copy of the Fortran computer programme used is shown in Fig.51.

The Rose-Drago analysis could not be applied to p-nitrophenol and p-cyanophenol as the solubilities of these compounds in cyclohexane was extremely small and therefore accurate values of c_p were unobtainable.

```
// JOB T
// FOR
*IOCS (CARD, 1132 PRINTER)
*LIST SOURCE PROGRAM
*EXTENDED PRECISION
      DIMENSION CD(10), AM(10), EM(10), C(10), AK(45), DEV(45)
 8    FORMAT (10X, 47H CALCULATION OF EQUILIBRIUM CONSTANT ROSE-DRAGO)
 9    FORMAT (//, 15X, 3HAVK, /)
      WRITE (3, 8)
      WRITE (3, 9)
      READ (2, 5) M
 5    FORMAT (I 1)
      READ (2, 10) (CD(J), AM(J), J = 1, M)
10    FORMAT (F 10.5, F 10.3)
      READ (2, 20) CA, AM, AMF
20    FORMAT (F 10.0, F 10.3)
      READ (2, 30) EC1, EC2
30    FORMAT (2F 10.0)
      DO 90  J = 1, M
      EA = AMF/CA
      RK1 = (AM(J) - AMF)/(EC1-EA) - CA - CD(J) + (CD(J)*CA*
                          (EC1-EA)/(AM(J) - AMF)
      RK2 = (AM(J) - AMF)/(EC2-EA)-CA-CD(J)+(CD(J)*CA*
                          (EC2-EA))/(AM(J) - AMF)
      EM(J) = (RK2 - RK1)/(EC2 - EC1)
      C(J) = RK1 - EM(J)*EC1
90    CONTINUE
      NSUM = M*(M-1)/2
      K = 0
      DO 2  I = 1, M
      DO 2  J = 1, M
      IF (1 - J) 1, 2, 2
 1    K = K + 1
      AK(K) = (EM(I) - EM(J)/(EM(I)*C(J)-EM(J)*C(I))
 2    CONTINUE
      AVK = 0.0
      DO 3  I = 1, NSUM
 3    AVK = AVK + AK(I)
      AVK = AVK/NSUM
      DO 14 K = 1, NSUM
14    DEV(K) = AK(K) - AVK
 4    FORMAT (F 20.3)
11    FORMAT (//, 15X, 2HCD, 10X, 2HAM, 12X, 2HEM, 16X, 1HC, /)
 6    FORMAT (F 20.6, F 10.3, 2E20.7)
12    FORMAT (//, 15X, 2HAK, 18X, 3HDEV, /)
 7    FORMAT (2F 20.6)
      WRITE (3, 4) AVK
      WRITE (3, 11)
      WRITE (3, 6)(CD(J), AM(J), EM(J), C(J), J = 1, M)
      WRITE (3, 12)
      WRITE (3, 7)(AK(K), DEV(K), K = 1, NSUM)
      CALL EXIT
      END
```

TABLE 25 : PHENOL, 280.5 m ; 25°C.

(for values of c_D, c_p, A and A^o see Table 19.)

Slope x 10^4	Intercept	K	$(K - K_{mean})$
0.660546	-0.044646	27.401640*	10.791359
0.758111	-0.056631	22.444590*	5.834308
0.828756	-0.067362	17.876796	1.266514
1.104352	-0.112227	16.422249	-0.188032
1.663060	-0.204824	15.846901	-0.763380
5.442489	-0.824692	17.088094	0.477812
		15.361261	-1.249020
K_{mean} = 16.610 litre $mole^{-1}$		14.811333	-1.798948
Mean deviation = 2.449		14.777539	-1.832742
Revised K_{mean} = 15.57 litre $mole^{-1}$		14.802691	-1.807589
		14.453623	-2.156658
		14.561113	-2.049168
		14.123941	-2.486340
		14.462642	-2.147638
		14.719808	-1.890473

*reject.

TABLE 26 : PHENOL, 280.5 m , 35°C.

(For values of c_D, c_P, A and A^o see Table 19)

Slope x 10^4	Intercept	K	$(K - K_{mean})$
0.963056	-0.069308	17.765400*	6.185536
1.081912	-0.084809	14.348266*	2.768403
1.163497	-0.098239	12.623776	1.043912
1.505472	-0.152960	11.181900	-0.397963
2.084475	-0.254149	11.345786	-0.234077
6.055116	-0.901790	10.719300	-0.860563
		11.201646	-0.378217
K_{mean} = 11.579 litre $mole^{-1}$		10.210928	-1.368935
Mean deviation = 1.119		10.761446	-0.818416
Revised K_{mean} = 11.11 litre $mole^{-1}$		11.371512	-0.208351
		10.128941	-1.450922
		10.765398	-0.814465
		9.079171*	-2.500692
		10.545521	-1.034342
		11.648959	0.069095

*reject.

TABLE 27 : p-CRESOL, 290 m , 25°C.

(For values of c_D, c_P, A and A^o see Table 20)

Slope x 10^4	Intercept	K	$(K - K_{mean})$
0.984390	-0.078520	11.557106	0.440531
		10.825204	-0.291370
1.067284	-0.092419	10.421437	-0.695137
		10.498123	-0.618452
1.224514	-0.120207	11.142090	-0.025515
		11.300997	0.184421
1.411991	-0.154309	10.393530	-0.723044
		10.079775	-1.036799
1.760858	-0.215591	10.296417	-0.820157
		11.087755	-0.028819
2.787210	-0.386691	11.273973	0.157398
		9.753106	-1.363469
4.818761	-0.729045	10.250096	-0.866479
		11.285825	0.169250
		11.465806	0.349231
		10.670270	-0.446305
K_{mean} = 11.116 litre $mole^{-1}$		11.864384	0.747809
		11.919078	0.802502
Mean Deviation = 0.656		12.827584*	1.711008
		12.488137	1.371561
Revised K_{mean} = 11.03 litre $mole^{-1}$		12.047380	0.930805

* reject.

TABLE 28 : p-CRESOL, 290 m , 35°C.

(For values of c_D, c_P, A and A^0 see Table 20)

Slope x 10^4	Intercept	K	$(K - K_{mean})$
1.268444	-0.097561	8.809408	-0.046061
		8.339136	-0.516333
1.352068	-0.111476	9.052630	0.197160
		8.276108	-0.579361
1.512579	-0.139418	8.899687	0.044217
		8.933981	0.078511
1.749170	-0.176400	8.071447	-0.784022
		9.125798	0.270328
2.077516	-0.236860	8.182586	-0.672883
		8.910152	0.054682
3.183008	-0.414416	8.945159	0.089689
		10.307554*	1.452085
5.323681	-0.767312	8.232071	-0.623398
		9.124633	0.269163
		9.108666	0.253197
		6.864194*	-1.991275
K_{mean} = 8.855 litre $mole^{-1}$		8.774958	-0.080510
		8.868372	0.012903
Mean deviation = 0.504		10.328978*	1.473508
		9.744234	0.888764
Revised K_{mean} = 8.80 litre $mole^{-1}$		9.065102	0.209632

* reject.

TABLE 29 : p-t-BUTYLPHENOL, 286 m , 25°C.

(For values of c_D, c_P, A and A^o see Table 21)

Slope x 10^4	Intercept	K	$(K - K_{mean})$
1.183937	-0.144028	20.622215*	9.825159
		12.158631	1.361575
1.338180	-0.169109	10.856433	0.059376
		10.654862	-0.142193
1.386347	-0.182713	10.963739	0.166683
		4.788873*	-6.008182
1.745002	-0.255934	8.584660	-2.212395
		9.365855	-1.431200
2.466805	-0.401787	10.201214	-0.595841
		9.968376	-0.828679
7.284530	-1.356160	10.164180	-0.632875
		10.740859	-0.056196
		10.343818	-0.453237
		11.031689	0.234633
		11.510431	0.713374

K_{mean} = 10.797 litre $mole^{-1}$ * reject.

Mean deviation = 1.648

Revised K_{mean} = 10.50 litre $mole^{-1}$

TABLE 30 : p-t-BUTYLPHENOL, 286 m , 35°C.

(For values of c_D, c_P, A and A^o see Table 21)

Slope x 10^4	Intercept	K	$(K - K_{mean})$
1.333203	-0.096756	8.582911	0.114364
		7.985110	-0.483435
1.427046	-0.111768	8.108764	-0.359781
		8.014285	-0.454260
1.608911	-0.142664	8.469019	0.000473
		8.634296	0.165749
1.832822	-0.179231	7.653175	-0.815370
		7.968802	-0.499744
2.127874	-0.228803	7.902395	-0.566150
		8.455203	-0.013342
3.331303	-0.418731	8.639216	0.170670
		8.327046	-0.141499
5.485682	-0.758850	8.039191	-0.429354
		8.679401	0.210854
		8.844715	0.376168
		7.769621	-0.698924
		8.794535	0.325989
		8.961144	0.492598
		9.343803	0.875256
		9.337760	0.869214
		9.329072	0.860526

K_{mean} = 8.468 litre $mole^{-1}$

Mean deviation = 0.425

Revised K_{mean} = 8.47 litre $mole^{-1}$

TABLE 31 : p-CHLOROPHENOL, 293.5 m , 25°C.

(For values of c_D, c_P, A and A^o see Table 22)

Slope x 10^4	Intercept	K	$(K - K_{mean})$
0.703285	-0.052334	23.269781	-0.038389
		26.953246	3.645075
0.796847	-0.065013	25.368021	2.059850
		23.951051	0.642880
1.024350	-0.093163	23.578246	0.270075
		23.287425	-0.020745
1.277854	-0.127294	29.776519*	6.468449
		26.203072	2.894901
1.723834	-0.188863	24.125793	0.817623
		23.634712	0.326541
3.043101	-0.367550	23.290160	-0.018010
		22.343908	-0.964262
5.656322	-0.723330	21.283833	-2.024336
		21.707681	-1.600489
		21.646183	-1.661987
		20.359840	-2.948330
K_{mean} = 23.308 litre $mole^{-1}$		21.447144	-1.861026
		21.432219	-1.875951
Mean deviation = 1.536		22.410635	-0.897535
		22.014294	-1.293876
Revised K_{mean} = 22.99 litre $mole^{-1}$		21.387716	-1.920454

* reject.

TABLE 32 : p-CHLOROPHENOL, 293.5 m , 35°C.

(For values of c_D, c_P, A and A^o see Table 20)

Slope x 10^4	Intercept	K	$(K - K_{mean})$
		19.868471*	2.067639
0.892171	-0.060552	19.368244	1.567412
		19.716578	1.915747
0.993450	-0.073139	18.147889	0.347058
		18.009218	0.208387
1.201291	-0.099421	17.654384	-0.146446
		19.053498	1.252666
1.484525	-0.134430	19.664987	1.864156
		17.787309	-0.013522
1.928798	-0.194933	17.740225	-0.060605
		17.391093	-0.409737
3.317962	-0.376168	20.382282*	2.581451
		17.154967	-0.645863
6.042257	-0.737065	17.348089	-0.452742
		17.003693	-0.797138
		14.762331*	-3.038499
		16.311994	-1.488836
K_{mean} = 17.800 litre $mole^{-1}$		16.166097	-1.634733
		17.635251	-0.165579
Mean deviation = 1.124		16.871348	-0.929482
		15.779502	-2.021329
Revised K_{mean} = 17.95 litre $mole^{-1}$			

* reject.

The technique devised by Grunwald and Coburn[109] for calculating equilibrium constants from spectroscopic data enables a 'sharpness of fit' to be calculated for values of K as reported on Page 120. A value of K obtained from the Nagakura and Baba or the Rose and Drago analysis is substituted into Equation 27 enabling a series of values of ${}_{e}c_{C}$ to be deduced.

$$ {}_{e}c_{C} = Kc_{D}c_{P}/(1 + Kc_{D}) \qquad \ldots\ldots\ldots\ldots\ldots (27) $$

Using equations

$$ {}_{e}c_{P} = c_{P} - {}_{e}c_{C} \qquad \ldots\ldots\ldots\ldots\ldots (28) $$

$$ A_{P} = {}_{e}c_{P} \cdot \varepsilon_{P} \qquad \ldots\ldots\ldots\ldots\ldots (29) $$

$$ A_{C} = A - A_{P} \qquad \ldots\ldots\ldots\ldots\ldots (30) $$

corresponding values of A_{C} were calculated.

By the method of least squares the best straight line of the form $A_{C} = m. {}_{e}c_{C} + k$ was fitted to the ${}_{e}c_{C}$, A_{C} data and a corrected value of A_{C} recalculated (designated A_{C}^{*}).

The standard deviation (D), as defined by Grunwald and Coburn was then estimated:

$$ D = \left[\frac{(A_{C} - A_{C}^{*})^{2}}{A_{C}^{*}} + k \right]^{\frac{1}{2}} $$

The above calculation was repeated for a series of values of K and the corresponding standard deviations were plotted against K. The best value of K was taken to be when the standard deviation was a minimum ($D_{min.}$) and the sharpness of fit[108] was estimated by interpolating

D at values of $K \pm 10\%$ of K, calculating the mean value, D^1, and using the definition

$$\text{Sharpness of fit, } S = \frac{(D^1 - D_{min})}{D_{min}} \times 10$$

Here again the calculations are time consuming and tedious and so the computer was programmed to calculate and print out values of D from a prescribed series of K values and the values of A, A^o, c_p and c_D reported in Tables 19 to 22. A copy of the Fortran computer programme used is shown in Fig. 52. The results are reported in Tables 33 to 36 and the plots of K against D in Figs. 53 to 56.

The Grunwald and Coburn analysis, like that of Rose and Drago, could not be applied to p-nitrophenol nor p-cyanophenol owing to the very low solubility of these compounds in cyclohexane and the consequent difficulty in estimating c_p values.

```
// JOB T
// FOR
*IOCS (CARD, 1132 PRINTER)
*LIST SOURCE PROGRAM
*EXTENDED PRECISION
     DIMENSION CD(10), AM(10), AC(10), AAE(10), CC(10), CAE(10), ACC(10), DEV(10)
10   FORMAT (10X, 45H CALCULATION OF EQUILIBRIUM CONSTANT GRUNWALD)
20   FORMAT (//, 11X, 2HGK, 12X, 5HRTSUM, 18X, 1HC, /)
     WRITE (3, 10)
     WRITE (3, 20)
     READ (2, 25) M
25   FORMAT (I 1)
     READ (2, 30) (CD(J), AM(J), J = 1, M)
30   FORMAT (F 10.5, F 10.3)
     READ (2, 31) CA, AMF
31   FORMAT (F 10.0, F 10.3)
     READ (2, 40) N
40   FORMAT (I 2)
     DO 80  I = 1, N
     READ (2, 50) GK
50   FORMAT (F 10.3)
     DO 35  J = 1, M
     CC(J) = GK*CD(J)*CA/(1. + GK*CD(J))
     CAE(J) = CA - CC(J)
     EA = AMF / CA
     AAE(J) = EA*CAE(J)
35   AC(J) = AM(J) - AAE(J)
     SCC = 0.0
     SAC = 0.0
     SCCAC = 0.0
     SCC2 = 0.0
     DO60  J = 1, M
     SCC = SCC + CC(J)
     SAC = SAC + AC(J)
     SCCAC = SCCAC + CC(J) * AC(J)
60   SCC2 = SCC2 + cc(J) * CC(J)
     EN = M
     EM = (SAC*SCC-SCCAC*EN)/(SCC*SCC-SCC2*EN)
     C = (SAC-EM*SCC)/EN
     DO75  J = 1, M
     ACC(J) = EM*CC(J)+C
75   DEV(J) = (AC(J) - ACC(J)) **2/ACC(J)
     SUM = 0.0
     DO79  J = 1, M
79   SUM = SUM + DEV(J)
     RTSUM = SQRT (SUM + C)
     WRITE (3, 90) GK, RTSUM, C
90   FORMAT (F 15.3, 2E20.6)
80   CONTINUE
81   FORMAT (//, 11X, 2HCD, 12X, 2HAM,/)
```

```
82   FORMAT (F 17.5, F 11.3)
83   FORMAT (//, 11X, 2HCA, 12X, 3HAMF, /)
84   FORMAT (E 21.5, F 7.3)
     WRITE (3, 81)
     WRITE (3, 82) (CD(J), AM(J), J = 1, M)
     WRITE (3, 83)
     WRITE (3, 84) CA, AMF
     CALL EXIT
     END
```

```
FEATURES SUPPORTED
EXTENDEN PRECISION
IOCS
CORE REQUIREMENTS FOR
COMMON       0     VARIABLES     302     PROGRAM     482
END OF COMPILATION
```

TABLE 33 : PHENOL

(For values of wavelength, concentrations and absorbances see Table 19)

25°C.		35°C.	
K	D x 10^2	K	D x 10^2
16.40	7.55738	11.80	7.37406
16.10	6.44931	11.50	6.22481
15.90	5.58319	11.30	5.30919
15.80	5.09295	11.20	4.78149
15.70	4.54846	11.10	4.18416
15.60	3.92718	11.00	3.48144
15.50	3.18446	10.90	2.58873
15.40	2.20050	10.80	1.11798
15.30	0.68791	10.70	2.05800
15.20	2.40951	10.60	3.12331
15.10	3.34002	10.50	3.91279
15.00	4.06490	10.40	4.57176
14.90	4.68073	10.30	5.15063
14.70	5.72154	10.10	6.15627
14.40	7.00854	9.80	7.43348
$D_{min.}$ = 0.047		$D_{min.}$ = 0.051	
when K = 15.32 litre $mole^{-1}$		when K = 10.78 litre $mole^{-1}$	
and D^1 = 0.899		and D^1 = 0.770	
S = 181		S = 141	

PHENOL

Fig. 53

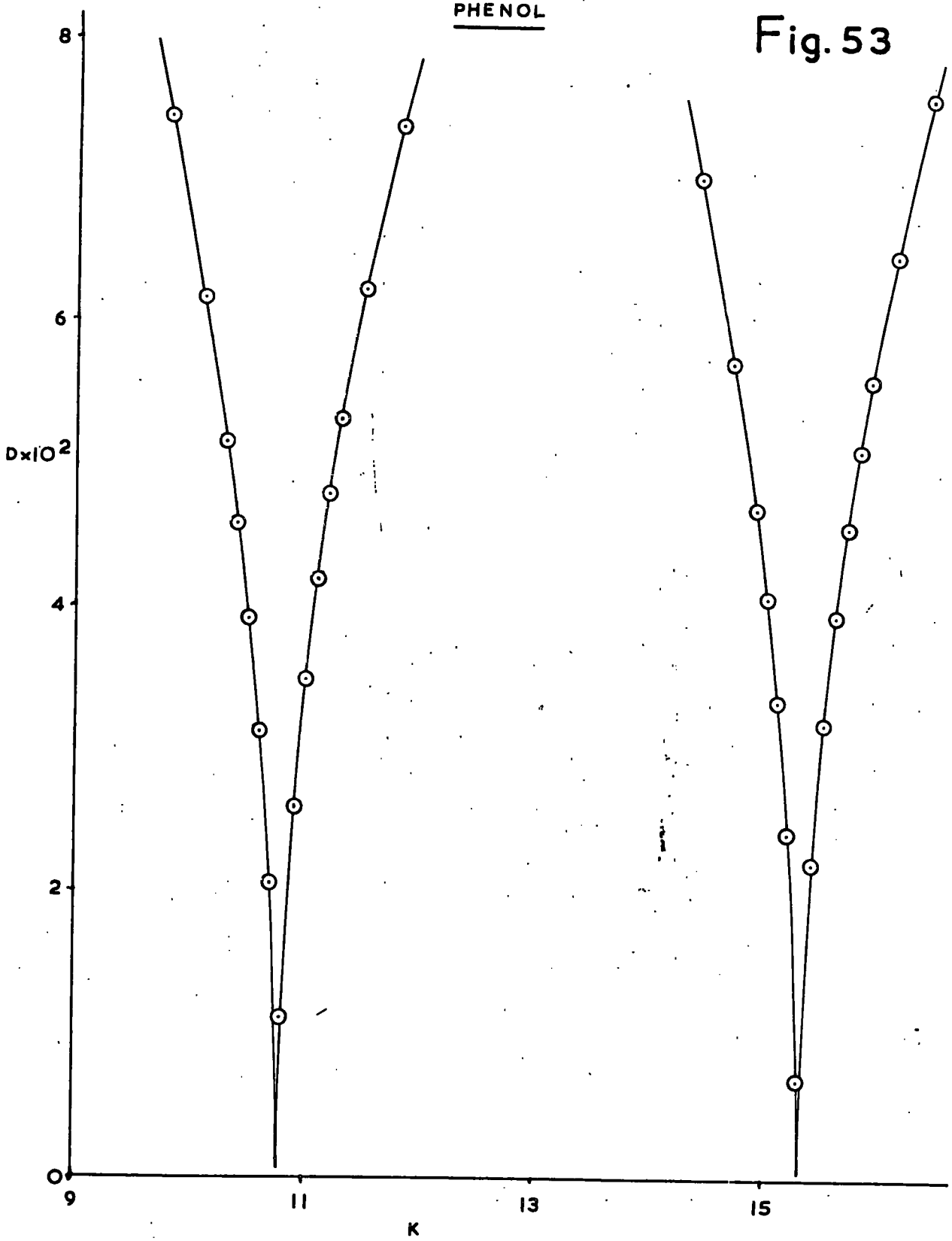

TABLE 34 : p-CRESOL

(For values of wavelength, concentrations and absorbance see Table 20)

25°C.		35°C.	
K	D x 10^2	K	D x 10^2
12.30	8.29558	10.00	8.23872
12.00	6.92489	9.70	6.95628
11.80	5.82414	9.50	5.93579
11.70	5.18312	9.40	5.34823
11.60	4.44772	9.30	4.68376
11.50	3.55983	9.20	3.90320
11.40	2.35259	9.10	2.91456
11.30	1.27726	9.00	1.30987
11.20	2.97095	8.90	2.25893
11.10	4.00641	8.80	3.45861
11.00	4.82766	8.70	4.34315
10.90	5.53103	8.60	5.08003
10.80	6.15709	8.50	5.72665
10.60	7.25548	8.30	6.84884
10.30	8.65995	8.00	8.27257

$D_{min.}$ = 0.066

when K = 11.33 litre $mole^{-1}$

and D^1 = 0.902

S = 127

$D_{min.}$ = 0.092

when K = 8.98 litre $mole^{-1}$

and D^1 = 0.782

S = 75

Fig. 54

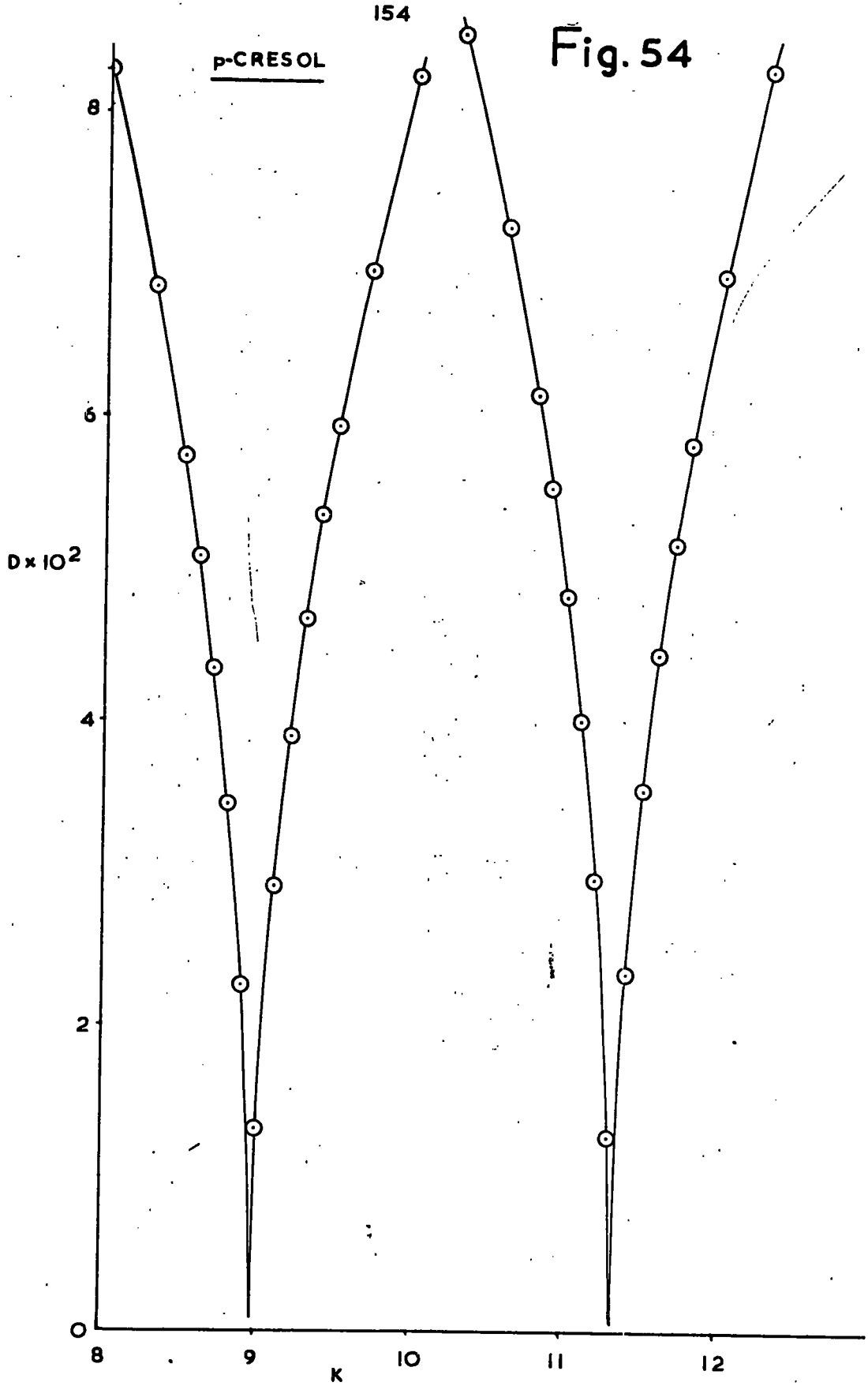

TABLE 35 : p-t-BUTYLPHENOL

(For values of wavelength, concentrations and absorbances see Table 21)

25°C.		35°C.	
K	D x 10^2	K	D x 10^2
11.70	6.96629	9.70	9.69700
11.40	5.91809	9.40	8.18934
11.20	5.09034	9.20	6.98877
11.10	4.61751	9.10	6.29719
11.00	4.08752	9.00	5.51481
10.90	3.47423	8.90	4.59535
10.80	2.72180	8.80	3.43008
10.70	1.64955	8.70	1.53505
10.60	1.41134	8.60	2.66675
10.50	2.59444	8.50	4.07920
10.40	3.39077	8.30	5.99033
10.30	4.03623	8.20	6.75302
10.20	4.59492	8.10	7.44241
10.00	5.55386	7.90	8.67009
9.700	6.75827	7.60	10.26602

$D_{min.}$ = 0.081

when K = 10.65 litre $mole^{-1}$

and D^1 = 0.710

S = 78

$D_{min.}$ = 0.059

when K = 8.68 litre $mole^{-1}$

and D^1 = 0.910

S = 144

p-t-BUTYLPHENOL

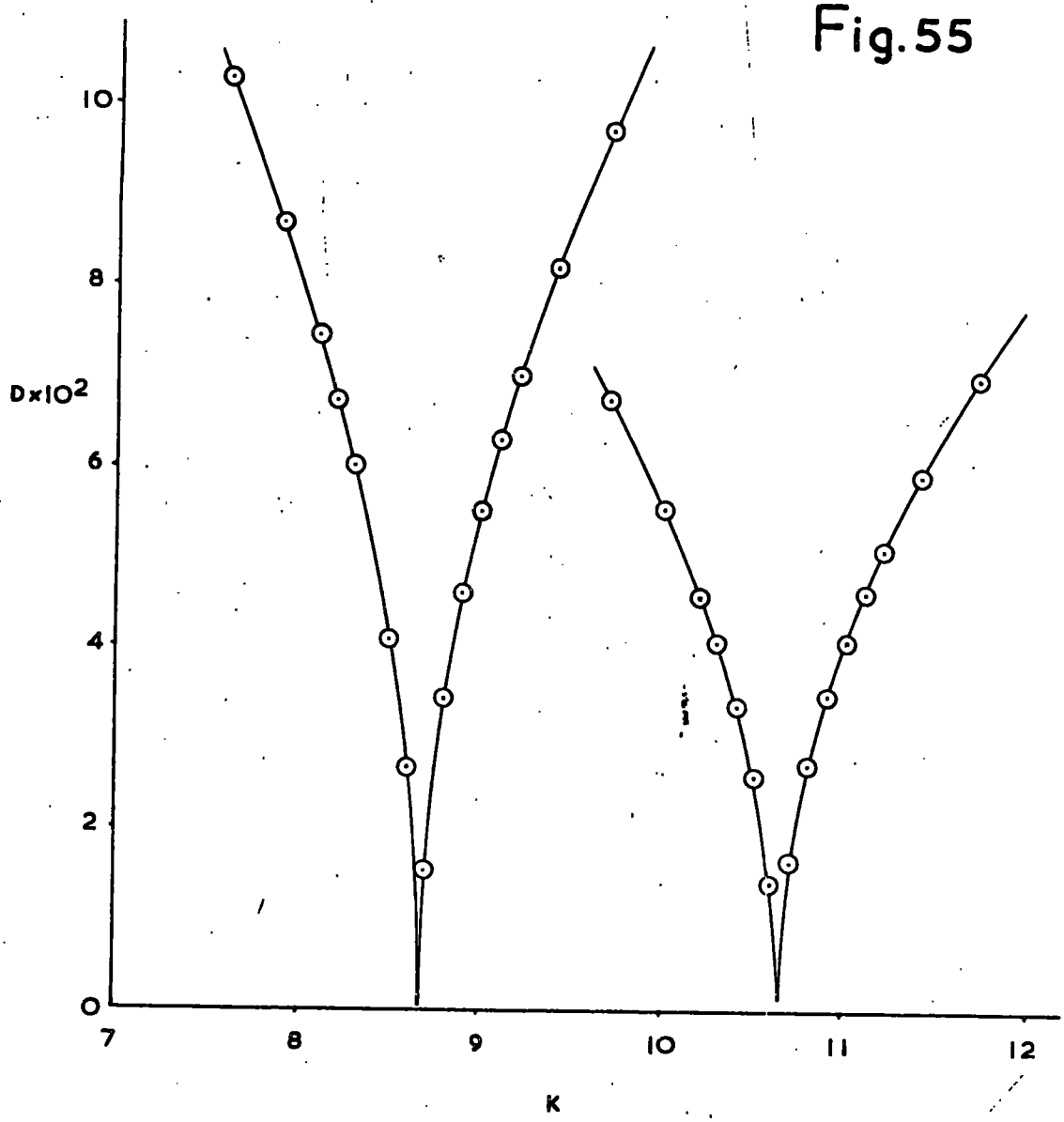

TABLE 36 : p-CHLOROPHENOL

(For values of wavelength, concentrations and absorbances see Table 22)

25°C.		35°C.	
K	D x 10^2	K	D x 10^2
25.00	7.49287	19.400	8.29589
24.70	6.29984	19.100	7.20382
24.50	5.35680	18.90	6.36954
24.40	4.81583	18.80	5.90735
24.30	4.20529	18.70	5.40502
24.20	3.48883	18.60	4.85009
24.10	2.57967	18.50	4.22185
24.00	1.06429	18.40	3.48080
23.90	2.09622	18.30	2.52969
23.80	3.15054	18.20	0.82084
23.70	3.93225	18.10	2.24960
23.60	4.58304	18.00	3.28698
23.50	5.15276	17.90	4.06902
23.30	6.13675	17.70	5.30004
23.00	7.37304	17.40	6.74261

$D_{min.}$ = 0.081

when K = 24.00 litre $mole^{-1}$

and D^1 = 1.163

S = 134

$D_{min.}$ = 0.060

when K = 18.21 litre $mole^{-1}$

and D^1 = 1.058

S = 166

p-CHLOROPHENOL

Fig.56

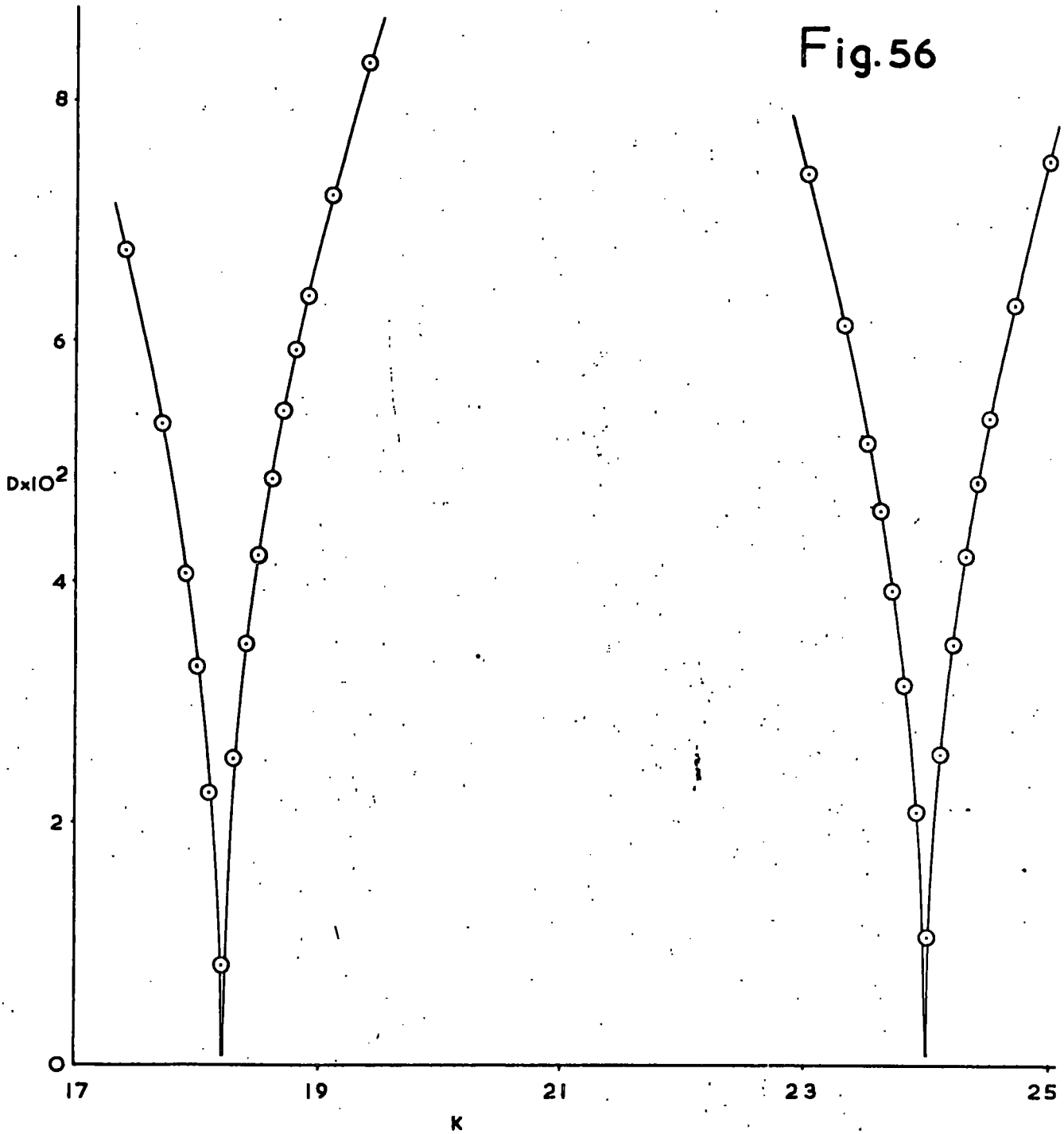

Finally, Table 37 summarises the results of all three methods used for calculating hydrogen bonding equilibrium constants from spectroscopic data.

TABLE 37 : Hydrogen Bonding Constants

Compound	Nagakura & Baba (litre mole^{-1})	Rose & Drago (litre mole^{-1})	Grunwald & Coburn (litre mole^{-1})
25°C.			
Phenol	15.21	15.57	15.32
p-Cresol	10.94	11.03	11.33
p-t-Butylphenol	10.42	10.50	10.65
p-Chlorophenol	24.43	22.99	24.00
p-Cyanophenol	50.20	-	-
p-Nitrophenol	66.83	-	-
35°C.			
Phenol	10.79	11.11	10.78
p-Cresol	8.81	8.80	8.98
p-t-Butylphenol	8.50	8.47	8.68
p-Chlorophenol	18.28	17.95	18.21
p-Cyanophenol	37.22	-	-
p-Nitrophenol	49.00	-	-

DISCUSSION OF RESULTS

Introduction

In correlating properties of the OH bond such as association constant, near infra-red stretching frequency, bond moment and sorption affinity, Hammetts sigma constant has been used in this investigation as a basic measure of the effects of structural change. From the results obtained proposals have been made regarding the nature of the orientations of the sorptive molecules at the alumina-solution interface and a probable sorption mechanism has been suggested. An index of sorption has been defined and used as a measure of sorption affinity in correlating with the Hammett structural parameter.

Qualitative correlations between chemical properties and structure have long been in existence but it is only recently that successful quantitative relationships have been devised. One such relation, which will form the basis for this discussion, is the empirical equation suggested by Hammett in 1937[111, 112] which arose from his observations on the parallelism of the effects of substituents (R) on rate or equilibrium constants in side chain (Y) reactions of benzene derivatives:

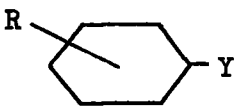

The Hammett equation relates the nature of the substituent R, and the reactivity of the side chain Y:-

$$\log (K/K_o) = \sigma\rho,$$

where K and K_o are rate or equilibrium constants for reactions of the

substituted and unsubstituted compounds respectively; σ' is the substituent constant varying only with the nature and position of R; and ρ is the reaction constant varying with the reaction, the physical conditions under which it takes place and the nature of the side chain Y. The above equation was first restricted to substituents in the meta- and para- positions of the benzene ring and has proved widely applicable in spite of its essentially empirical nature. The expression on the left-hand side of the equation is proportional to the difference in the free energies of reactions of substituted and unsubstituted compounds (if the K are equilibrium constants) or to the difference in energies of activation (if the K are rate constants). For this reason the equation is often referred to as a "linear free-energy relationship", although it is not at all obvious that such a linear free-energy relation should hold.

Jaffe[113] gives a useful summary of sigma constants calculated from carefully vetted experimental results. It has been found that the constants for certain groups (e.g. p-nitro) whilst applicable to most reactions do not give good results when used with reactions of phenols and anilines; therefore enhanced substituent constant values have been defined for these reactions. Other electron-attracting substituents such as -CN, -COOH and -CHO also require an enhanced value and Jaffe reports that these latter values generally give better correlation in reactions of phenols, phenolic esters, anilines and dimethyl anilines than σ' values although he does quote reactions where the reverse is true.

As yet no satisfactory theoretical explanation for this multiplicity of

values has been put forward and clearly each reaction must be considered separately and the constant which gives the most reasonable correlation should be used. In Table 38 below are listed the substituent constants used in this discussion:

TABLE 38

p-Substituent	Hammett 'sigma' value[113]
t-Butyl	- 0.197
Methyl	- 0.170
Hydrogen	0
Chloro	+ 0.227
Cyano	+ 0.628
Nitro	+ 0.778

The Alumina Surface

The results of the experiments carried out to characterise the alumina used in this work suggest that the sorbent is predominantly χ-alumina, with admixture of γ-alumina, and of pseudo-spinel structure with unit cell edge of 7.95Å.

In the case of the closely related γ-alumina, there is reason to believe that this form may preferentially expose one crystal face.[94] Strong pseudo-morphic relations are known to exist between boehmite and γ-alumina, and electron and X-ray diffraction evidence suggests that dehydration of gelatinous boehmite yields γ-alumina in which a considerable part of the surface is formed by the 100 plane of a spinel lattice.[114]

Arguments for the preferred exposure of the 111 face[50] based on the greater density of packing of oxide ions on this face of dry alumina are unconvincing because actual exposure may still reflect the relative stabilities of hydrated faces (hydroxyl packing) rather than those of dehydrated faces. It is reasonable to suppose, as have past workers[96,115] that chemisorption of water should be closely related to the spacing of oxide ions on exposed faces of a cubic, close-packed oxide lattice. Each oxide ion in a 111 plane occupies $6.74 A^{o2}$ whereas on a 100 face the area per oxide ion is $7.90 Å^2$. The B-points observed in 100° adsorption isotherms suggest exposure of the 100 face.[94]

Assuming that preferential exposure of the 100 face occurs in the alumina used in this work, then calculation shows that each surface ion occupies $7.90 Å^2$ of the hydroxylated surface.

The specific surface area, calculated from low temperature nitrogen sorptions and application of the B.E.T. equation, is reproduced at $131.9 m.^2 g.^{-1}$ Before legitimate use of this value can be made the degree of porosity of the surface must be established. Ibbitson and Vallance[84] examined the hysteresis loop on low temperature nitrogen sorption and desorption isotherms and from the desorption branch were able to calculate a pore size distribution. Micro-porosity was found to be absent, the smallest pores being approximately 20Å in diameter and the great majority were approximately 30Å in diameter. Thus for the purposes of this study it is unlikely that steric effects are important and all the nitrogen area may be assumed available to phenol and dioxan

molecules. Accordingly, the value of 131.9 $m.^2 g.^{-1}$ has been used to evaluate the area requirements of the phenol molecules on the surface of the alumina. These molecular areas, quoted in Table 39 are derived from the equation:-

$$\text{Area per molecule } (\text{Å}^2) = \frac{131.9 \times 10^{20}}{n\,N}$$

where N is the Avogadro Number (6.023×10^{23})

and n is the number of moles sorbed at saturation and determined by application of the Lowett equation[2] to the sorption isotherm.

TABLE 39

Compound	Saturation value (moles x 10^4)	Area per Molecule (Å^2)
Phenol	1.682	130.2
p-cresol	1.567	139.8
p-t-butylphenol	1.452	150.8
p-chlorophenol	1.637	133.8
p-nitrophenol	2.118	103.4
p-cyanophenol	2.247	97.5

Mechanism of Sorption and Orientation at the Solution-Solid Interface

McDonald[116] has shown that the inert gases, nitrogen and oxygen which only physically adsorb on silica surfaces at low temperatures interact with surface hydroxyl groups to cause a broadening and displacement of the associated absorption band to lower frequencies. The interaction indicates the formation of weak hydrogen bonds between surface hydroxyls and adsorbed molecules. The intensity of the free OH

band progressively decreased with increasing adsorption, while a new band associated with these groups interacting with adsorbed molecules grew in intensity at lower frequencies. Frohnsdorff and Kington[117] consider that the relatively large frequency displacement effected by nitrogen, 24 $cm.^{-1}$ (compared with argon 8 $cm.^{-1}$, krypton 16 $cm.^{-1}$, xenon 19 $cm.^{-1}$ and oxygen 12 $cm.^{-1}$) is consistent with the large value for the quadrupole moment of this gas which interacts with the surface hydroxyl groups.

McDonald noted further that all free hydroxyl groups were interacting with adsorbed nitrogen as indicated by the disappearance of the 3749 $cm.^{-1}$ band (a sharp peak with a narrow half width, 15 $cm.^{-1}$, due to the O-H stretching vibration of free hydroxyl groups) when the surface coverage by nitrogen was considerably less than the monolayer capacity determined by gas adsorption isotherms. He concluded that the silica surface was heterogeneous and that OH groups were preferred physical adsorption sites for nitrogen molecules. Kiselev and Khrapova[118] found that the nitrogen adsorption capacity was decreased after the dehydroxylation of silica surfaces, the result being in accord with the view that there is appreciable interaction between the nitrogen adsorbate and the surface hydroxyls.

In their study of the sorption of stearic acid from cyclohexane solution onto activated aluminas Kipling and Wright[99] concluded that hydrogen bonding to the sorbent surface was the essential sorption mechanism; the sorptive being perpendicularly aligned to the surface.

From obvious plateaux in the isotherms these workers estimated limiting sorption values and compared these values with calculated monolayer values based on the two orientations of stearic acid, with molecular areas (expressed in terms of the monomeric molecules) of 114$\mathring{A}^2$ for the parallel orientation and 20.5$\mathring{A}^2$ for the perpendicular orientation. From the ratio of observed to calculated limiting values, it was obvious that the perpendicular orientation is adopted. On the one alumina sample for which this ratio was appreciably less than unity (0.47) the adsorption is too great to correspond to the parallel orientation although much less than for a close-packed monolayer in the perpendicular orientation. Kipling and Wright reasonably suppose that sorption to give less than a close-packed monolayer is unlikely to be due to competition from the solvent if the solute is so strongly attracted to the surface that it adopts the perpendicular orientation. They suggest that in such a case it is more likely that closeness of packing of the sorbed molecules is the dominant factor, and that this is determined by the spacing of the sites, i.e. that sorption is localised.

Again, de Boer et al.[50] suggest that lauric acid is sorbed perpendicularly to an alumina surface from pentane solution, one molecule of lauric acid being sorbed for every four surface oxygen atoms. Kipling represents this localisation of sorption, in the case of stearic acid, more specifically as shown in Fig. 57.

It appears to the author that the conclusions reached by Kipling and Wright regarding the orientation of stearic acid molecules at the

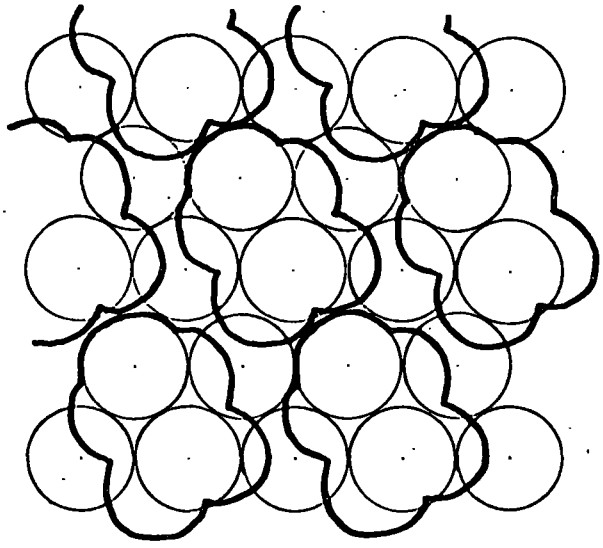

Stearic acid

Fig. 57

Fig. 58

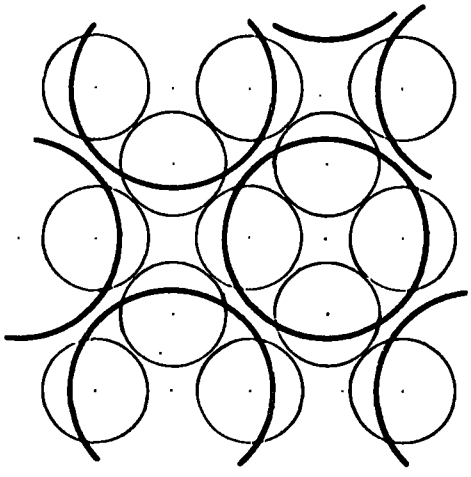

Phenol

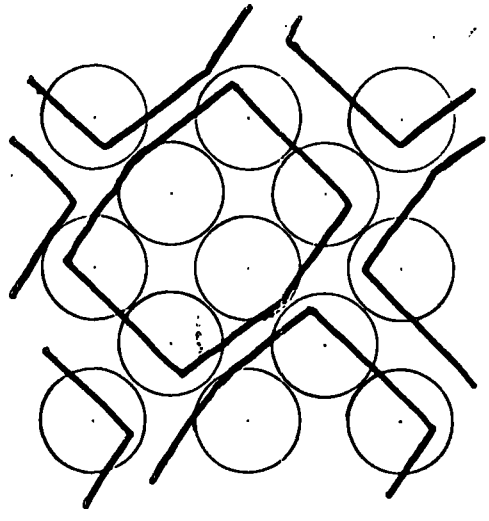

Dioxan

MOLECULES ON AN ALUMINA SURFACE

surface of alumina may, in part, apply to the sorption of phenol from dioxan onto a similar sorbent surface. Whereas cyclohexane is one of the most unreacting solvents, the attraction between dioxan and an hydroxylated surface must be appreciable. Hence in this sorption study it is suggested that two factors are important in explaining the sorption saturation values presented in Table 39, (a) sorption of dioxan and (b) the spacing of sorption sites on the surface.

In support of the first premise it can be seen that the area requirements per sorptive molecule quoted in Column 3 are appreciably greater than the value of 30.9$\mathring{A}^2$ obtained from the sorption of phenol from cyclohexane onto the same alumina, and the implication must be that the solvent, dioxan, competes effectively with the sorptive for sorption sites on the alumina surface. It is not unrealistic to imagine such competition between sorptive and solvent: all the sorptives are substituted phenols and the fundamental OH group is an ideal one for entering into hydrogen bonding with an ionic surface, whether the latter be composed of oxide or hydroxide ions or a mixture of the two. Evidence for hydroxylation of the alumina surface under the conditions pertaining to this work is appreciable (see page 99 et seq.) and dioxan is therefore quite likely to be sorbed parallel to the surface by hydrogen bonding.

The following possible surface arrangements of molecules occurring in the systems studied in this investigation might be proposed:-

(a) phenol and dioxan molecules hydrogen bonded separately to the

alumina surface, the former molecules perpendicularly disposed and the latter parallel to the surface;

(b) phenol molecules hydrogen bonded to dioxan and sorbed as 1 : 1 complex molecules, the complex being hydrogen bonded to the surface via the free oxygen atom of the dioxan molecule.

If sorption were by the latter process a dioxan molecule would be expected to have the same affinity for the surface as a complex molecule since hydrogen bonding in both cases would be through an oxygen atom in the dioxan molecule. Thus one would anticipate the sorption uptake to be directly proportional to the concentration of complex in solution and the sorption isotherm would rise in a linear fashion from the origin. That this is not so in practice points to the existence of arrangement (a).

Applying the second premise, the concept of localisation of sorption, to the present study and assuming cross sectional areas for the phenol and dioxan molecules of 24$\mathring{A}^2$ [119] and 33.6$\mathring{A}^2$* respectively, the diagrams of Fig. 58 illustrate possible packing arrangements of each type of molecule on the 100 plane of the alumina surface.

These packing arrangements involve occupation of four surface ions by one perpendicular phenol molecule and six surface ions by one parallel dioxan molecule. The area requirement of 30.9$\mathring{A}^2$ for the phenol molecule on alumina when sorbed from cyclohexane and calculated from the limiting sorption value and an accessible surface area of 131.9 $m^2 g^{-1}$ is very close to the area occupied by a group of four surface ions (31.6$\mathring{A}^2$) and it is implied therefore that the mode of packing illustrated in Fig. 58

is not unreasonable. Rather more uncertain is the area requirement of the dioxan molecule.

*This value was calculated from the following bond angles and lengths reported in Reference ǂ :- C - H 1.09Å; C - C 1.54Å; C - O 1.42Å; ∠CCO 109°; ∠COC 109.5°.

On the basis of this model, the sorption saturation values given in Table 39 can be explained by a mode of packing of sorptive and solvent molecules such that two molecules of dioxan are sorbed for every phenol molecule (1 unit of sorption). In the instance of phenol itself, the area requirement of a unit of sorption will be (31.6 + 2 x 47.4) $Å^2$ which simplifies to 126.4 $Å^2$. This value is close to the area requirement per molecule of phenol quoted in Table 39, packing defects might be expected to result in the slightly larger experimental area requirement per unit of sorption of 130.2 $Å^2$. The variation in area requirement per unit of sorption for the p-substituted phenols (excepting p-nitro and p-cyano phenol) is in accord with the variation in area requirement of the p-substituent group, the p-t-butyl group having the greatest area requirement.

In the case of p-nitro and p-cyanophenol the interesting possibility of a parallel orientation on the sorbent surface arises. This is more conceivable in the case of p-nitrophenol in which the nitro group could hydrogen-bond with an hydroxylated surface in addition to the hydroxyl group. The area requirement of a unit of sorption for this model, in which an arbitrary unit is, say, one molecule of dioxan and one molecule

ǂ "INTERATOMIC DISTANCES", CHEM. SOC. 1958.

of p-nitrophenol will be of the order of 94.8 $Å^2$, assuming that both types of molecule occupy a surface site comprising six ions. This value approximates to the areas per molecule quoted in Table 39 for p-nitro and p-cyanophenol. Equally reasonable of course would be a perpendicular orientation of these sorptives to the surface in which the unit of sorption is two molecules of the phenol to one molecule of dioxan giving an area requirement per sorption unit of approximately 110.6 $Å^2$.

In attempting to weigh the evidence for an orientation of p-nitrophenol onto the surface of activated alumina, it is noteworthy that a perpendicular orientation seems likely when sorption occurs from benzene solution, the area requirement calculated from the sorption isotherm being 36.2 $Å^2$. A parallel orientation of this sorptive would be expected to yield a larger area requirement per molecule than this value.

The work of Giles and Nakhwa[97] has shown that p-nitrophenol is adsorbed 'end-on' at polar surfaces and they quote the following effective cross sectional areas for an adsorbed p-nitrophenol molecule: 15 $Å^2$ and 25 $Å^2$ for 'end-on' adsorption from benzene and water respectively and 52.5 $Å^2$ for 'flat' adsorption. These values, together with experimentally determined monolayer capacities, are used to calculate specific surface areas which are then compared with results from low temperature nitrogen sorptions. The authors suggest that the much higher areas obtained by the latter technique are due to microporosity of the alumina surfaces, permitting penetration of nitrogen molecules into

the fine capillaries but excluding the larger p-nitrophenol molecules. The Giles' value of 15 $\mathring{A}^2$ for the effective cross sectional area of a p-nitrophenol molecule seems a little unrealistic and when the surface areas are recalculated using the value obtained from the non-porous alumina used in this study (36.2 $\mathring{A}^2$), they show much closer agreement with the results from nitrogen sorptions.

The results discussed above, then, suggest that in the sorption of p-substituted phenols from solution in dioxan onto an activated alumina the forces on the surface seem to be the dominant ones, since the phenols are not sorbed as complexes, but bonds between phenol and dioxan molecules are broken and the phenol molecules sorbed as discreet entities. Interaction with the surface appears to be through the mechanism of hydrogen bonding and the phenol molecules probably assume a vertical orientation on localised sorption sites.

An Index of Sorption and the Effect of Structural Changes

Isotherms are often used for estimating affinities of sorptives for sorbent surfaces when correlation is sought between sorptive behaviour and structural features in sorptive molecules. The determination of an affinity value requires a knowledge of the activities of the solute in the solution and substrate phases, although in practice it is very difficult to arrive at a realistic value for the activity in the substrate. Firstly, the extent of the substrate phase, i.e. the true area of the adsorbing surface layer, is hard to define; and secondly, the adsorbed solute is not present in ideal solution and may even occur

as aggregates or micelles. In spite of these difficulties three proposed methods of affinity measurement might be mentioned:

(a) Assuming no interaction between adsorbed species the term $\theta / (1 - \theta)$ can be used to express activity in the solid where θ is the proportion of available sites occupied. Gilbert and Rideal[120], and Vickerstaff[121] have used this technique to calculate affinities for acids and acid dyes for wool fibres.

(b) The adsorbed solute may be considered as being in solution in a specific volume of solvent more closely associated with the substrate than the rest of the solvent. The volume term, although derived empirically, is of dubious significance, but useful results have been obtained[122, 123] enabling correlations to be made between affinity and solute molecular structure.

(c) Bartell et al.[124] devised a method based on the initial slope of the isotherm: $\Delta\mu^{o} = -RT \ln K$ where K is the equilibrium constant. Again, the layer volume or thickness must be estimated and there is the added drawback that so much emphasis is placed on the initial part of the isotherm which is the least accurate portion. The method cannot be applied to H or S type isotherms and no regard is given to the total amount of solute adsorbed.

The process of sorption from solution onto a solid surface is essentially one of phase change as the accessible surface is at all times completely occupied by molecules of sorptive and solvent. If the total number of molecules in the surface phase remains constant, then this phase change can be represented by

$$(1)^s + (2)^{\ell} \rightleftharpoons (1)^{\ell} + (2)^s$$

where 1 and 2 represent one molecule each of solvent and solute and s and ℓ denote surface and liquid phases respectively.

The Everett relationship derived in the Introduction is based on such an equilibrium together with the further conditions that

(a) sorption is monomolecular,

(b) the sorbed phase consists of identical sorption sites, and

(c) the solution and adsorbed phase behave in an ideal manner.

$$\frac{x_1^{\ell}(1 - x_1^{\ell})}{n^o \Delta x_1^{\ell}/m} = \frac{1}{n^s}\left[x_1^{\ell} + \frac{1}{(K - 1)}\right] \qquad \ldots\ldots\ldots\ldots (9)$$

The left-hand side plotted against x_1^{ℓ} should give a linear graph of slope $1/n^s$ and intercept (when $x_1^{\ell} = 0$) of $1/n^s (K - 1)$, hence this equation, derived from statistical thermodynamic arguments, enables equilibrium constants to be evaluated.

Because of the strong hydrogen bonding interactions in solution between sorptives and solvent used in this study, it is hard to conceive of ideality existing in this phase. From the polar nature of the sorptive and the hydrogen bonding tendency of dioxan to the sorbent surface, it is

considered unlikely that interactions between the sorbed species in the surface layer will be minimal. The suggested orientations of sorptive and solvent molecules at the sorbent surface imply a difference in area requirement, and hence the total number of molecules sorbed will not remain constant. The phase change reaction is unlikely to be so simply represented as

$$(1)^s + (2)^l \rightleftharpoons (1)^l + (2)^s$$

In fact, it is difficult to visualise a system departing so much from the conditions inherent in Everett's treatment of sorption at the solution-solid interface.

However, in spite of this realisation, the plot of $x_1^l (1 - x_1^l) / \frac{n^o \Delta x_1^l}{m}$ against x_1^l is essentially linear in the case of all the sorptives studied (Fig. 59), although linearity of plot, essential as it is, is insufficient justification to apply the Everett equation to the system studied. The constants n^s and K determined from the slope and intercept must also be reasonable values.

Apparent values of n^s and K determined from Fig. 59 are recorded in Table 40 below.

TABLE 40

Compound	Slope	Intercept	$n^s \times 10^4$	K	Av. area per mol. ($Å^2$)
Phenol	5372	2.38	1.862	2258	117.6
p-cresol	6010	2.07	1.664	2904	131.6
p-t-butylphenol	6650	1.44	1.504	4619	145.6
p-chlorophenol	5712	1.21	1.751	4722	125.1
p-nitrophenol	4428	1.60	2.258	2769	97.0
p-cyanophenol	4326	0.83	2.312	5213	94.7

Fig. 59

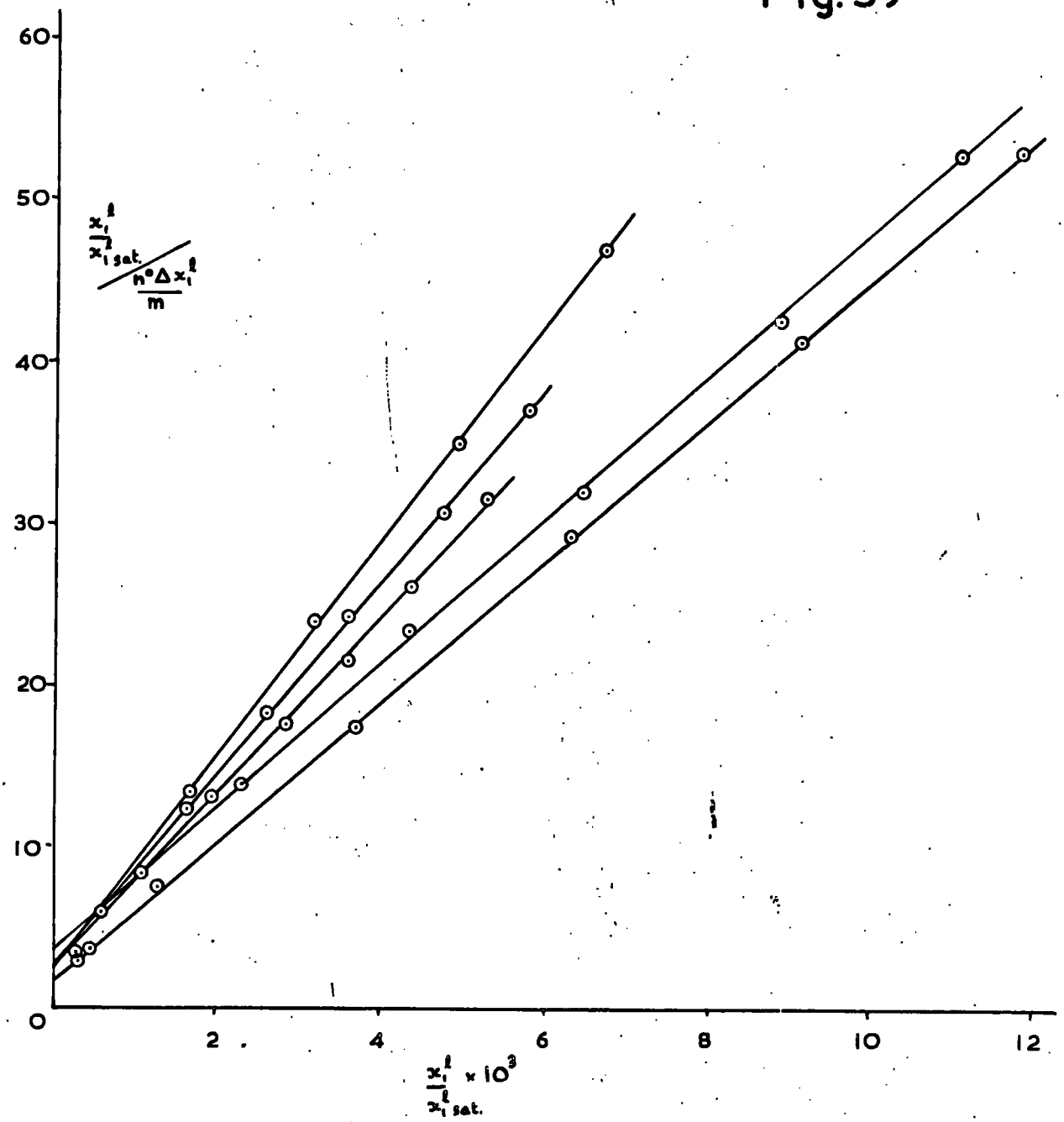
60
50
40
30
20
10
0
2
4
6
8
10
12
$\frac{x_i^l}{x_{i\,sat.}^l} + \frac{n^o \Delta x_i^l}{m}$
$\frac{x_i^l}{x_{i\,sat.}^l} \times 10^3$

The area requirement per sorbed molecule, given in Column 6, is very much greater than the area requirement of either a phenol (31.6 $\mathring{A}^2$) or a dioxan molecule (47.4 $\mathring{A}^2$). From this test alone, it is clear, and not surprising, that the Everett equation does not explain the experimental data. Furthermore, the values of K, the sorption affinity, do not reflect any constitutional property of the sorbed species.

In order to compare the sorptive affinity of the alumina surface for the phenols used in this study, an index of sorption has been defined as "the number of moles of phenol sorbed at constant relative mole fraction of phenol in the mobile phase". The relative mole fraction referred to is the ratio $x_1^{\ell} / x_{1\ sat.}^{\ell}$ in which x_1^{ℓ} is the equilibrium mole fraction of phenol in the mobile phase and $x_{1\ sat.}^{\ell}$ is the mole fraction of phenol in a saturated solution of the phenol in dioxan at the temperature of sorption. By comparing moles sorbed at constant relative mole fraction it is considered that the mobile phases, although not ideal, will be in corresponding states.

Plots of moles sorbed against sigma, the Hammett substituent constant, are shown in Fig. 60 and it is evident that fluctuations occur at low and high relative mole fractions. These fluctuations may be explained, in part, by experimental uncertainty and the possible influence of surface heterogeneity at low relative mole fractions, and by enhanced intermolecular attractions in the sorbed layer at high relative mole fractions. It is not unreasonable to select, for purposes of comparison, an intermediate value of relative mole fraction. Since sigma is a parameter

Fig. 60

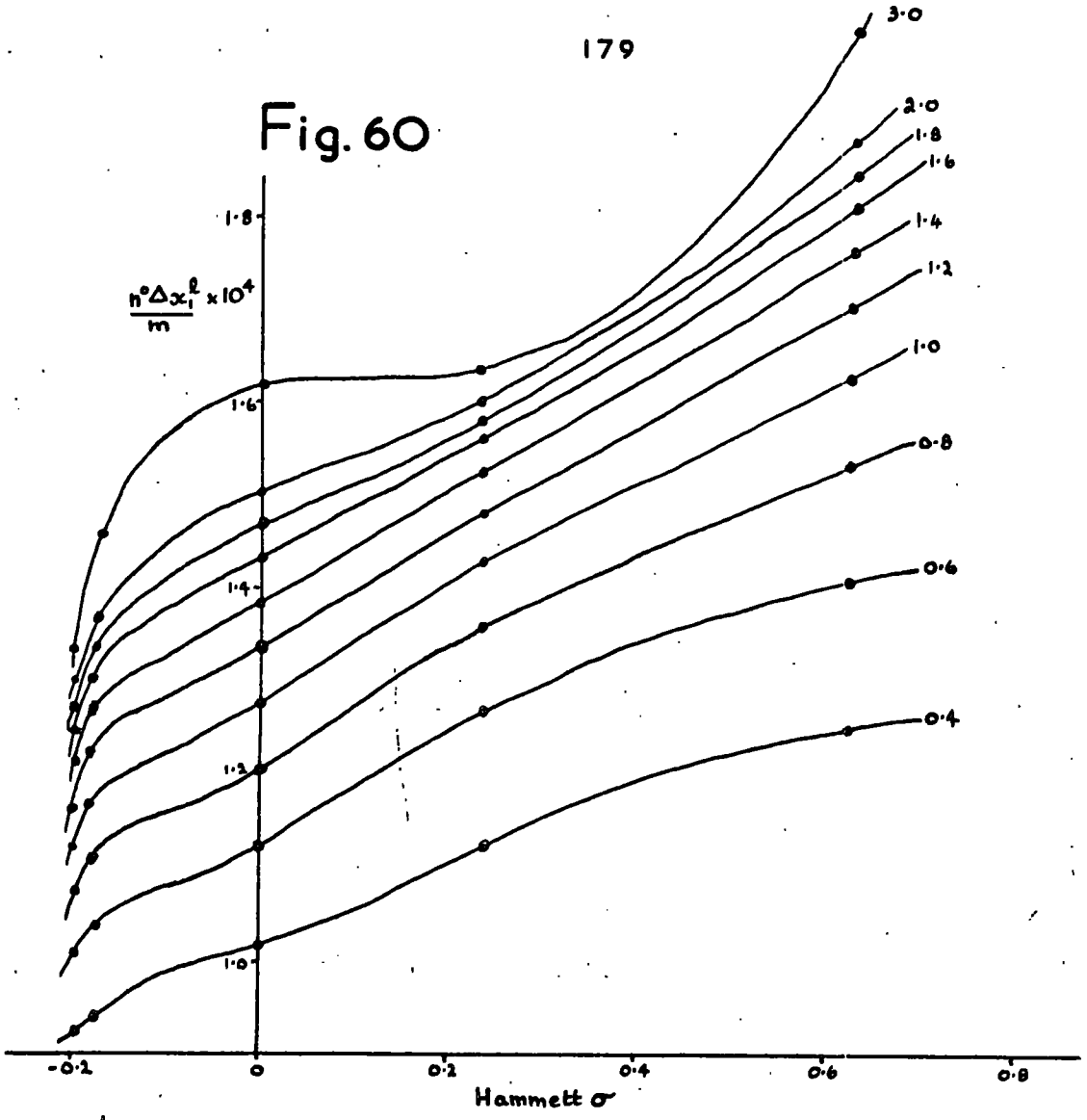
3·0
2·0
1·8
1·6
1·4
1·2
1·0
0·8
0·6
0·4
$\frac{n^{o}\Delta x_1^{l}}{m} \times 10^{4}$
1·8
1·6
1·4
1·2
1·0
-0·2
0
0·2
0·4
0·6
0·8
Hammett σ

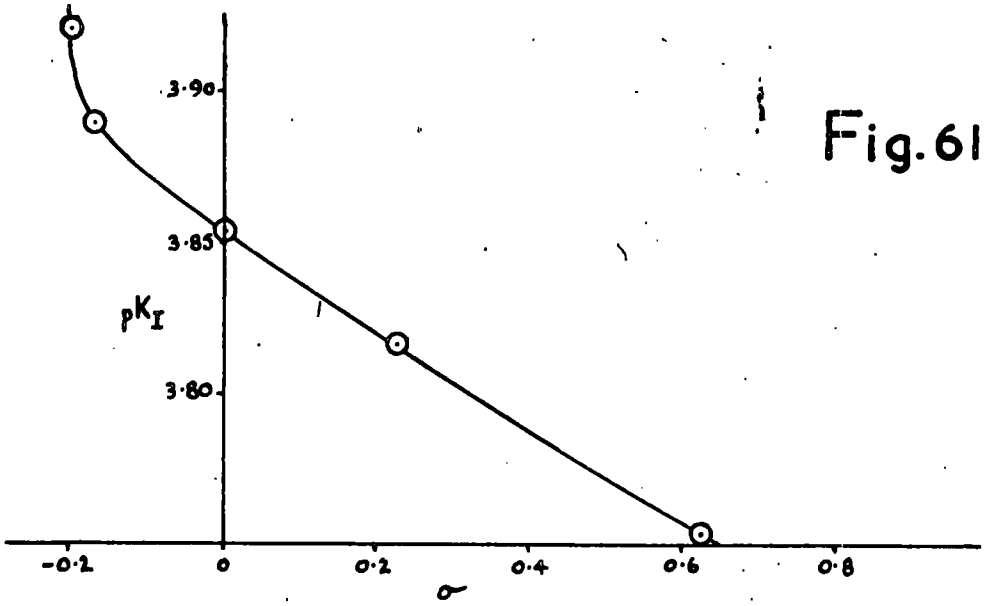
3·90
3·85
3·80
pK_I
-0·2
0
0·2
0·4
0·6
0·8
σ

Fig. 61

in a logarithmic relationship, it seems more appropriate to plot $\log_{10} (n^{o}\Delta x_1^{\ell}/m)$ against σ and, doing so, it is seen from Fig. 61 that a reasonable $x_1^{\ell}/x_1^{\ell}{}_{sat.}$ value for comparison is 1.4×10^{-3} (see Table 41).

TABLE 41

Compound	Hammett σ	$(n^{o}\Delta x_1^{\ell}/m) \times 10^{4}$	pK_I
p-t-butylphenol	- 0.197	1.200	3.921
p-cresol	- 0.170	1.286	3.891
Phenol	0	1.387	3.858
p-chlorophenol	0.227	1.524	3.817
p-cyanophenol	0.628	1.762	3.754
p-nitrophenol	0.778	1.482	3.829

From the pK_I values in Column 4 of Table 41, where pK_I by definition is $-\log_{10} (n^{o}\Delta x_1^{\ell}/m)$, it is seen that excepting the p-nitro compound, the index of sorption reflects the change in electrical character of the OH group brought about by substitution in the para position.

Influence of p-Substitution on other Physical Properties of the OH Bond

Since the OH group is functional in the sorption process and hydrogen bonding to the surface is the proposed mechanism, it is of interest to consider the magnitude of the effect of p-substitution on properties of the OH group which reflect its hydrogen bonding tendency. Acidity, polarity, near-infra red stretching frequency and association to dioxan are all properties of the OH group of significance in this respect.

(1) Acidity

A study of the data presented in Table 42 and Fig. 62, enables a comparison to be made of the effects of p-substitution on the acidities of the substituted phenols. The acidity of the phenol is seen to be related to the substituent constant sigma logarithmically as explained by Hammett, electron attracting substituents causing a decrease in pK_a and electron releasing substituents an increase.

TABLE 42

Compound	σ	pK_a
p-t-Butylphenol	-0.197	
p-Cresol	-0.170	10.19
Phenol	0	9.95
p-Chlorophenol	0.227	9.38
p-Cyanophenol	0.628	7.95
p-Nitrophenol	0.778	7.14

(2) Polarity

As previously mentioned, much evidence is available that hydrogen bonding between the OH group of a phenol molecule and the oxygen atom of a dioxan molecule results in an increase in dipole moment.[75-80] In all cases of sterically unhindered phenols, the dipole moments of these compounds in dioxan are greater than in benzene, cyclohexane and carbon tetrachloride.[12, 125] It is suggested that this increase is due partly to an increase in OH bond moment and partly to increased conjugation between the OH group and the aromatic nucleus. It is, of

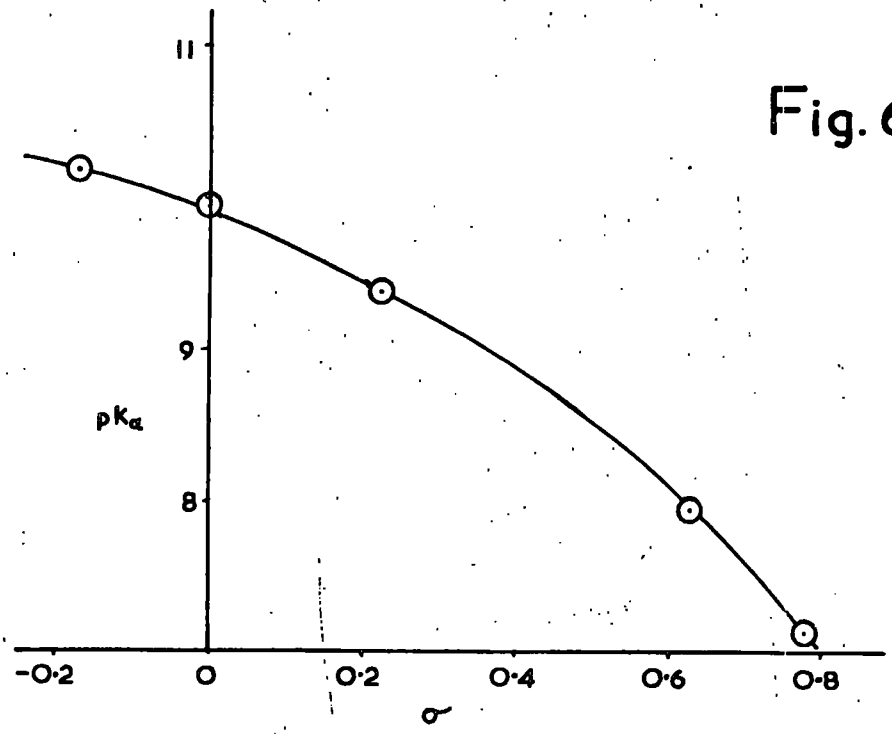

Fig. 62

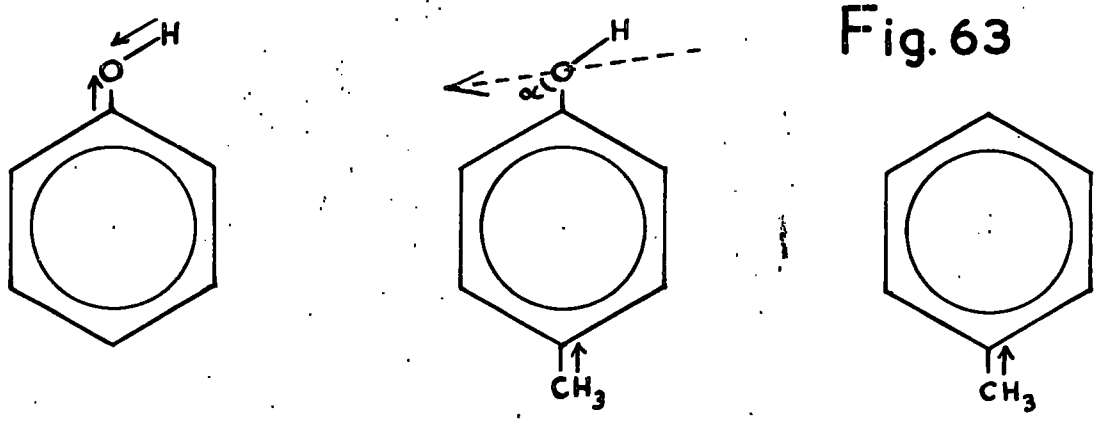

Fig. 63

$\mu_{(cyclohexane)} = 1{\cdot}46$D $\quad \mu_{(cyclohexane)} = 1{\cdot}44$D $\quad \mu = 0{\cdot}37$D

$$\therefore (1{\cdot}44)^2 = (1{\cdot}46)^2 + (0{\cdot}37)^2 + 2(0{\cdot}37).\cos(180-\alpha) \qquad \therefore \alpha = 79°36'$$

course, impossible to assess the magnitudes of these two effects, but it is not unreasonable to imagine that the increase in OH bond moment may be the more important. After all, the hydrogen atoms of the OH groups form the "bridge" in the bonding between the phenol and dioxan molecules.

If all the dipole moment increase on hydrogen bonding to dioxan is assumed to occur in the OH bond, then an assessment of this increase can be made, its variation becomes comparable with the p-substituent constant, sigma.

In order to determine the increase in OH bond moment on hydrogen bonding, it is first necessary to determine the angle which the OH group dipole makes with the major axis of the aromatic ring. This is effected by Marsden and Sutton's method[126] which involves vector addition of group moments, the groups being p-substituted relative to one another, and one of the groups being methyl. From the dipole moments of phenol (1.46 D), p-cresol (1.44 D) and toluene (0.37 D) the angle made by the OH group moment to the major axis of the molecule was calculated to be 79° 36' (Fig. 63).

It is now possible by application of the Sine Rule to evaluate the O - H and $C_{(ring)}$ - O bond moments as illustrated in Fig. 64, assuming $\angle COH = 115^{\circ}$.[127]

Having measured the dipole moment of a p-substituted phenol in dioxan, the new OH bond moment can now be calculated as shown in Fig. 65.

It is seen from Table 43 and Fig. 66 that the OH bond moment is a

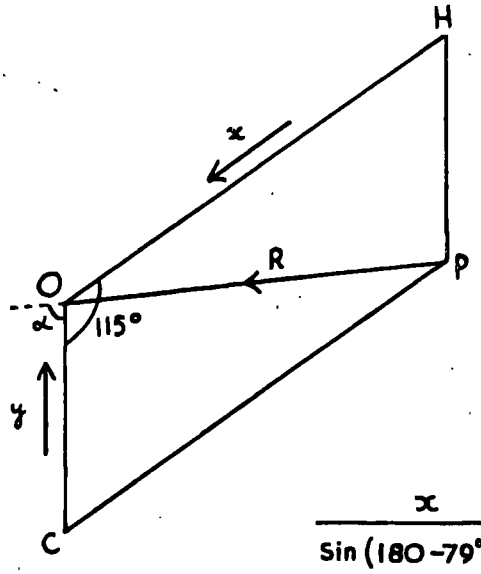

Fig. 64

$\angle COP = 180 - 79°36'$

$\angle POH = 115 - (180 - 79°36')$

$\angle OPH = COP = 180 - 79°36'$

$$\frac{x}{\text{Sin}\,(180-79°36')} = \frac{y}{\text{Sin}\,[115-(180-79°36')]} = \frac{R}{\text{Sin}\,65°}$$

$\therefore x = 1{\cdot}58$ D and $y = 0{\cdot}41$ D

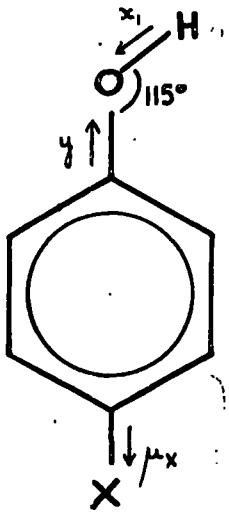

Fig. 65

x_1 : OH bond moment in substituted phenol

μ_X : moment due to substituent X

μ_2 : dipole moment of the phenol in dioxan

$$\mu_2^2 = x_1^2 + (\mu_X - y)^2 + 2x_1(\mu_X - y).\,\text{Cos}\,115°$$

reflection of the electrical character of the p-substituent group as given by sigma:

if x = OH bond moment in cyclohexane for phenol

and x_1 = OH bond moment in dioxan for substituted phenol,

$$p\,\Delta\mu = p\,(x_1 - x)$$

TABLE 43

Compound	σ	$\frac{\Delta\mu^{128}}{(D)}$	$p\,\Delta\mu$
p-t-Butylphenol	-0.197		
p-Cresol	-0.170	0.35	0.456
Phenol	0	0.42	0.377
p-Chlorophenol	0.227	0.54	0.268
p-Cyanophenol	0.628	0.99	0.004
p-Nitrophenol	0.778	1.18	-0.072

(3) Near-Infra red Stretching Frequency

The effect of hydrogen bonding on the vibrational spectrum of a compound containing the OH group is to shift the characteristic group stretching frequency to lower values. Ibbitson and Sandall[68] report that when phenol is dissolved in a dioxan-cyclohexane solvent mixture of dioxan weight fraction 0.0131, the shift produced is 222 $cm.^{-1}$ and this is attributed to hydrogen bonding between the phenol and dioxan molecules.

It becomes of interest to compare the shifts in OH stretching frequencies on hydrogen bonding when the phenol molecule is para-

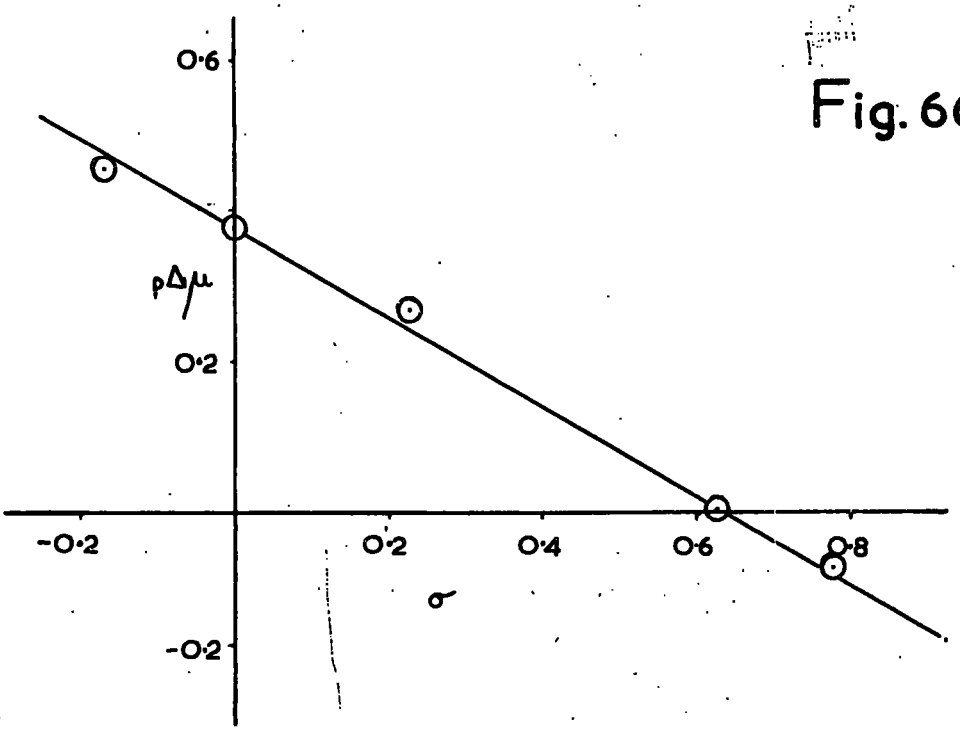

Fig. 66

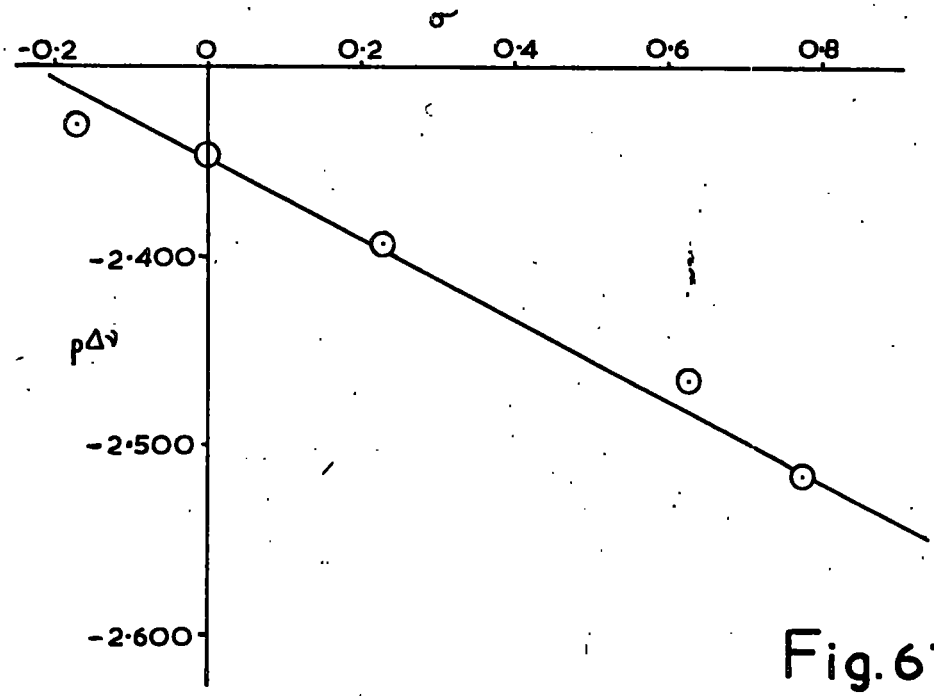

Fig. 67

substituted, results published elsewhere[68] are reported in Table 44, p $\Delta\nu$ is plotted as a function of sigma in Fig. 67.

It is seen, once again, that p $\Delta\nu$ is a reflection of the electrical character of the p-substituent as measured by sigma, electron attracting substituents enhancing and electron releasing substituents diminishing the shift in OH stretching frequency.

TABLE 44

Compound	σ	$\frac{\Delta\nu}{(cm^{-1})}$	p $\Delta\nu$
p-t-Butylphenol	-0.197		
p-Cresol	-0.170	215	-2.332
Phenol	0	222	-2.346
p-Chlorophenol	0.227	247	-2.393
p-Cyanophenol	0.628	292	-2.465
p-Nitrophenol	0.778	328	-2.516

(4) Association to Dioxan

Finally, hydrogen bonding tendency to dioxan is measured by the equilibrium constant of the process

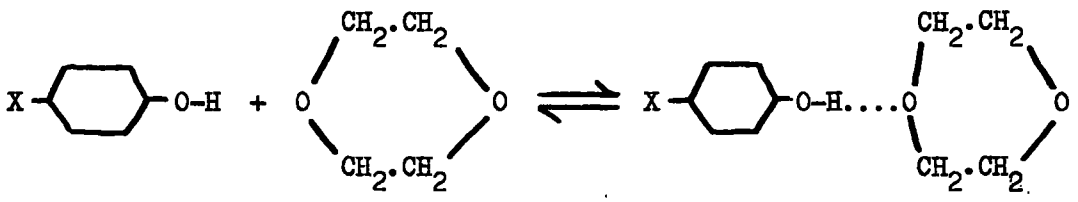

These constants have been determined experimentally at 25°C. and 35°C. in this work and their values reported in Table 37 on Page 159.

The temperature coefficient of complex formation is as anticipated,

values of K decreasing with increase in temperature. At both temperatures the values of K reflect the effect of the p-substituent on the hydrogen bonding tendency of the OH group and when plotted against sigma (Fig. 68) extend the parallelism already observed between acidity, OH bond moment increase, near infrared frequency shift and Hammett's substituent constant.

Fig.68

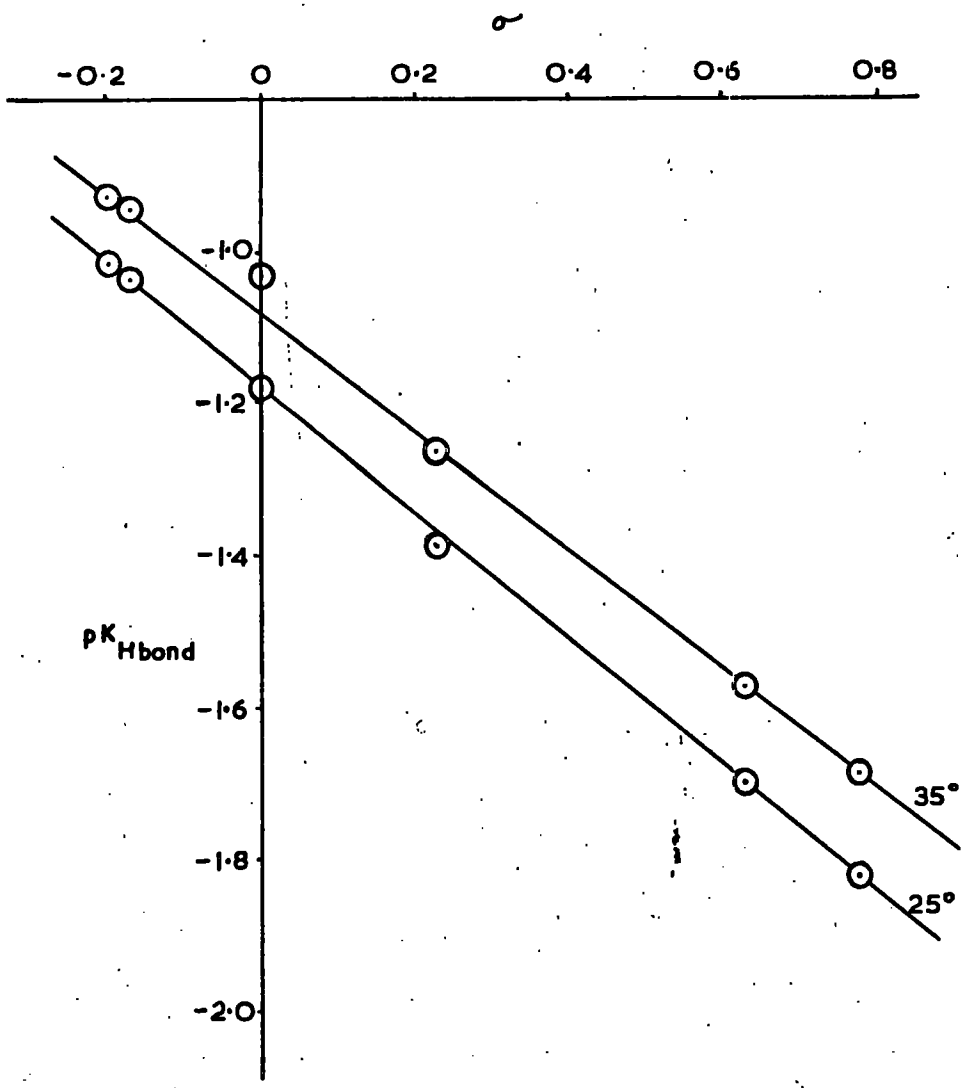

REFERENCES

1. Giles, MacEwan, Nakhwa and Smith, J. Chem. Soc., 1960, 3973.

2. Frangiskos, Harris and Jowett, "Proceedings of the Third International Congress of Surface Activity", Verlag der Universitatsdruckerei, Mainz, 1961, Vol.4, p.404.

3. Everett, Trans. Far. Soc., 1964, 60, 1803.

4. Schuchowitzsky, Acta physio chim., 1944, 19, 176 and 508.

5. Belton and Evans, Trans. Far. Soc., 1945, 41, 1.

6. Elton, J. Chem. Soc., 1954, 3813.

7. Patterson and Delmas, J. Physic. Chem., 1960, 64, 1827.

8. Kipling and Tester, J. Chem. Soc., 1952, 4123.

9. Kipling and Wright, J. Chem. Soc., 1962, 855.

10. Ibbitson and Moore, J. Chem. Soc.(B), 1967, 76 and 80.

11. Cummings, Carven, Giles, Rahman, Sneddon and Stewart, J. Chem. Soc., 1959, 535.

12. Eric, Goode and Ibbitson, J. Chem. Soc., 1960, 55.

13. Freundlich, "Colloid and Capillary Chemistry", 1926 (Methuen, London).

14. Ibbitson, Smith and Stone, Private Communication.

15. Traube, Annalen, 1891, 265, 27.

16. Baum and Broda, Trans. Far. Soc., 1938, 34, 797.

17. Miculicich, Arch. Expt. Path. Pharmak., 1933, 172, 373.

18. Nekrassow, Z. Phys. Chem., 1928, 136, 18.

19. Kipling and Wright, J. Chem. Soc., 1965, 4340.

20. Millard, Caswell, Leger and Mills, J. Phys. Chem., 1955, 59, 976.

21. Blackburn and Kipling, J. Chem. Soc., 1955, 1493.

22. Landt and Knop, Z. Phys. Chem., 1932, A162, 331.

23. Lemieux and Morrison, Canad. J. Res., 1947, B25, 440.

24. Wright, J. Chem. Soc., 1966, 355.

25. Linner and Gortner, J. Phys. Chem., 1935, 39, 35.

26. Sata, Kolloid, Z., 1929, 49, 275.

27. Bartell and Scheffler, J. Am. Chem. Soc., 1931, 53, 2507.

28. Amiot, Compt. Rend., 1936, 202, 1852 and 1939, 208, 1575.

29. Mair and Forziate, J. Res. Nat. Bur. Stand., 1944, 32, 151.

30. Bakr and McBain, J. Am. Chem. Soc., 1924, 46, 2718.

31. Heymann and Boye, Z. Physik. Chem., 1930, A150, 219.

32. Eric, Ph.D. Thesis, University of London, 1963.

33. Heymann and Boye, Kolloid Z., 1932, 59, 153.

34. Arnold, J. Am. Chem. Soc., 1939, 61, 1911.

35. Bhatnager, J. Ind. Chem. Soc., 1941, 17, 361.

36. Giles, Mehta, Stewart and Subramanian, J. Chem. Soc., 1954, 4360.

37. Ibbitson, Jackson, McCarthy and Stone, J. Chem. Soc., 1960, 5127.

38. Sandall, M.Sc. Thesis, University of London, 1963.

39. Bartell and Benner, J. Phys. Chem., 1942, 46, 847.

40. "Proceedings of the Second International Congress of Surface Activity", Butterworths, London, 1957.

41. Kipling and Peakall, J. Chem. Soc., 1956, 4828 and 1957, 4054.

42. Schroeder, J. Am. Chem. Soc., 1951, 73, 1122.

43. Wheeler and Levy, Canad. J. Chem., 1959, 37, 1235.

44. Kipling, Quart. Rev., 1956, 10, 1.

45. Smith, Quart. Rev., 1959, 13, 287.

46. Bartell and Lloyd, J. Am. Chem. Soc., 1938, 60, 2120.

47. Puri, Kumar and Sandle, Ind. J. Chem., 1963, 1, 418.

48. Gregg, "The Surface Chemistry of Solids", 2nd. Edn., 1961 (Chapman and Hall Ltd., London).

49. Goodman and Gregg, J. Chem. Soc., 1959, 694.

50. De Boer, Hauben, Lippens, Mëys and Walrave, J. Catalysis, 1962, 1, 1.

51. Hansen, Hansen and Craig, J. Phys. Chem., 1953, 57, 215.

52. Morrison and Miller, Canad. J. Chem., 1955, 33, 330.

53. Linner and Williams, J. Phys. Chem., 1950, 54, 605.

54. Taylor, J. Phys. Chem., 1926, 30, 145.

55. Roberts, Proc. Roy. Soc., 1935, A152, 445 and 469.

56. Halsey and Taylor, J. Chem. Phys., 1947, 15, 624.

57. Sidorov, Zh. fiz. Khim., 1956, 30, 995.

58. Folman and Yates, Proc. Roy. Soc., 1958, A246, 32.

59. Cant and Little, Canad. J. Chem., 1964, 42, 802.

60. Peri and Hannan, J. Phy.Chem., 1960, 64, 1526.

61. Parry, J. Catalysis, 1963, 2, 371.

62. Yates and Lucchesi, J. Phys. Chem., 1963, 67, 1197.

63. Elder and Springer, J. Phys. Chem., 1940, 44, 943.

64. Gasser and Kipling, J. Phys. Chem., 1960, 64, 710.

65. Gasser and Kipling, "Proceedings of the Fourth Conference on Carbon", 1962 (Pergamon Press, London and New York).

66. Daniel, Trans. Far. Soc., 1951, 47, 1345.

67. Wohler and Wenzel, Kolloid Z., 1930, 53, 273.

68. Ibbitson and Sandall, J. Chem. Soc., 1964, 4547.

69. Badger and Bauer, J. Chem. Phys., 1937, 5, 839.

70. Bellamy, Hallam and Williams, Trans. Far. Soc., 1958, 54, 1120.

71. Cutmore and Hallam, Trans. Far. Soc., 1962, 58, 40.

72. Pimentel and McClellan, "The Hydrogen Bond", 1960 (Freeman and Co., San Francisco and London).

73. Huggins and Pimentel, J. Phys. Chem., 1956, 60, 1615.

74. Nakamoto, Margoshes and Rundle, J. Am. Chem. Soc., 1955, 77, 6480.

75. Rao and Jatkar, J. Indian Inst. Sci., 1942, 5, 98 and 1943, 6, 1.

76. Ehrenberg and Fischer, Acta. Chem. Scand., 1948, 2, 657.

77. Few and Smith, J. Chem. Soc., 1949, 2663.

78. Smith, J. Chem. Soc., 1950, 3522.

79. Smith, J. Chem. Soc., 1953, 109.

80. Smith and Walshaw, J. Chem. Soc., 1957, 3217.

81. Richards and Walker, Trans. Far. Soc., 1961, 57, 399, 406 and 412.

82. Hulett, Pegg and Sutton, J. Chem. Soc., 1955, 3901.

83. Hoyer, Kolloid Z., 1951, 121, 121.

84. Ibbitson and Vallance, Private Communication.

85. Stumpf, Russell, Newsome and Tucker, Ind. and Eng. Chem., 1950, 42, 1398.

86. Brown, Clark andElliott, J. Chem. Soc., 1953, 84.

87. Day and Hill, J. Phys. Chem., 1953, 57, 946.

88. Sato, J. Appl. Chem., 1959, 9, 331.

89. Evans, "An Introduction to Crystal Chemistry", 2nd. Edn., 1964 (Cambridge University Press).

90. Peri, J. Phys. Chem., 1965, 69, 220.

91. Cornelius, Milliken, Mills and Oblad, J. Phys. Chem., 1955, 59, 809.

92. Sheppard, "Hydrogen Bonding", 1957 (Pergamon Press, London).

93. Bersohn, J. Phys. Chem., 1958, 29, 326.

94. Peri, J. Phys. Chem., 1965, 69, 211.

95. Uvarov, Zh. Fiz. Khim., 1962, 36, 1346.

96. Kipling and Peakall, J. Chem. Soc., 1957, 834.

97. Giles and Nakhwa, J. Appl. Chem., 1962, 12, 266.

98. Smith and Stone, Private Communication.

99. Kipling and Wright, J. Chem. Soc., 1964, 683, 3535.

100. Greatorex and Stone, Private Communication.

101. Benesi and Hildebrand, J. Am. Chem. Soc., 1949, 71, 2703.

102. Ketelarr et al., Rec. Trav. Chim., 1952, 71, 1104.

103. Nagakura and Baba, J. Am. Chem. Soc., 1952, 74, 5693.

104. Baba and Nagakura, J. Chem. Phys., 1961, 35, 1118.

105. Nagakura, J. Am. Chem. Soc., 1958, 80, 520.

106. Andrews and Keefer, J. Am. Chem. Soc., 1952, 74, 4500.

107. Keefer and Andrews, J. Am. Chem. Soc., 1953, 75, 543.

108. Rose and Drago, J. Am. Chem. Soc., 1959, 81, 6138.

109. Grunwald and Coburn, J. Am. Chem. Soc., 1958, 80, 1322.

110. Conrow, Johnson and Bowen, J. Am. Chem. Soc., 1964, 86, 1025.

111. Hammett, J. Am. Chem. Soc., 1937, 59, 96.

112. Hammett, Trans. Far. Soc., 1938, 34, 156.

113. Jaffe, Chem. Rev., 1953, 53, 191.

114. Lippens, "Structure and Texture of Aluminas", 1961, Thesis, Technische Hogeschool of Delft, The Netherlands.

115. de Boer, Fortuin, Lippens and Meijs, J. Catalysis, 1963, 2, 1.

116. McDonald, J. Am. Chem. Soc., 1957, 79, 850.

117. Frohnsdorff and Kington, Trans. Far. Soc., 1959, 55, 1173.

118. Kiselev and Khrapova, Kolloid Zh., 1957, 19, 572.

119. Adam, "The Physics and Chemistry of Surfaces", 1930 (Clarendon Press, Oxford).

120. Gilbert and Rideal, Proc. Roy. Soc., 1944, A 182, 335.

121. Vickerstaff, "The Physical Chemistry of Dyeing" 1954, 2nd Edn. (Oliver and Boyd Ltd., Edinburgh).

122. Giles and Hassan, J. Soc. Dyers and Colourists, 1958, 74, 846.

123. Galbraith, Giles, Halliday, Hassan, McAllister, Macaulay and Macmillan, J. Appl. Chem., 1958, 8, 416.

124. Bartell, Thomas and Fu, J. Phys. Colloid Chem., 1951, 55, 1456.

125. Goode and Ibbitson, J. Chem. Soc., 1960, 4265.

126. Marsden and Sutton, J. Chem. Soc., 1936, 599.

127. Anzilotti and Curran, J. Amer. Chem. Soc., 1943, 65, 607.

128. Ibbitson and Stone, Private Communication.